Voltage Induction on Pipelines Caused by Power Line Harmonic Currents

by

Bing Xia

A thesis submitted in partial fulfillment of the requirements for the degree of

Master of Science

in

Energy Systems

Department of Electrical and Computer Engineering
University of Alberta

Abstract

The coordination between pipeline and power line has always been a concern at the fundamental frequency. However, there is limited research on the impact of inductive coupling on pipeline at harmonic frequencies. In recent years, with the rapidly growing application of power electronic-based loads, the harmonic currents are abundant in distribution feeders, especially those supplying residential areas. The increased emphasis on the pipeline safety has resulted in the need to examine the severity of inductive coupling caused by harmonic currents in distribution feeders in greater detail.

The thesis first discusses the impacts of harmonic currents on pipeline to reveal the importance and the severity of harmonic induction impacts by comparing these with the impacts of fundamental currents in power distribution lines. The zero-sequence-dominant harmonic currents have the most significant impact on induced voltage. Based on the field data, the simulation results show that the induced voltages at the 3^{rd} and 9^{th} order harmonic frequencies can be larger than that at the fundamental frequency. Secondly, the main impact factors of harmonic induction are found through sensitivity study. For example, the multi-grounded neutral system, which is the unique characteristics of a distribution system, significantly influences the induced voltage. Finally, the mitigation methods at harmonic frequencies are discussed to analyze the effectiveness of applying these methods to mitigate the induced harmonic voltages on pipeline. The potential mitigation methods, such as islanded multi-grounded neutral and mitigation wire, are effective in voltage reduction at the 3^{rd} and 9^{th} order harmonic frequencies.

Preface

This thesis is an original work by Bing Xia. No part of this thesis has been previously published.

Acknowledgement

First and foremost, I would like to express my most sincere gratitude to my supervisor, Dr. Wilsun Xu for his tireless guidance over the past three years. Studying under his supervision gives me a good opportunity to conduct this research and gain valuable knowledge and experience. Other than that, my learning how to approach a question in a logical and creative manner is the most valuable achievement that I will allow myself to succeed in my future career.

I'd like to show my special appreciation to Dr. Yong Jing, Ricardo and Pooya, whose patient guidance and insightful suggestions have contributed greatly to this thesis. I thank all my colleagues for their friendship, and it's a great pleasure to work with them.

I'd like to express my highest appreciation to my parents, Mr. Wei Xia and Mrs. Lijuan Xu for their unconditional love, and my grandfather, Mr. Deli Xu whose meticulous attitude and genial personality inspire me to make everything in my life possible.

Contents

List of Tables

List of Figures

List of Abbreviations

EMF	Electromotive Force
EMI	Electromagnetic Interference
MGN	Multi-Grounded Neutral
CP	Cathodic Protection
IDD	Individual Demand Distortion
TDD	Total Demand Distortion
FEM	Finite Element Method

Chapter 1

Introduction

Due to the continuous growth of energy consumption and also the tendency to site power lines and pipelines along the same routes, power and gas/oil shared corridors are becoming increasingly restricted in both urban and rural areas. Power transmission lines generally carry high currents, especially under fault conditions, and may run several kilometers parallel to a pipeline. As a result, there has been a great deal of recent attention to the induction coordination between the power transmission line and pipeline at the fundamental frequency. In comparison, distribution feeders carry smaller current and have a lower fault level. There has been only limited attention paid to inductive coordination of distribution lines in the past.

In recent years, with the rapidly growing application of power electronic-based loads, the harmonic currents are abundant in distribution feeders, especially supplying residential areas. The increased emphasises on the pipeline safety has resulted in the need to examine the severity of inductive coupling caused by harmonic currents in distribution feeders in more detail.

The main topic of this thesis is to analyze the impacts of harmonic current induction in power distribution lines for pipeline safety concerns, especially the pipeline corrosion issue. This introductory chapter briefly reviews the background of the coordination between the power line and the pipeline. The chapter also explains the motivation of assessing the impact of harmonic current induction on the pipeline. At the end of this chapter, the scope and outline of this thesis are presented.

1.1 Background of the Coordination between the Power Line and Buried Pipeline

Pipelines are generally buried at low depths and can reach several hundreds of kilometers in length. In order to prevent electrochemical corrosion of the metal, buried pipelines are provided with an outside insulating coating. As a result, the buried pipelines can be considered as conductors relatively insulated from earth depending on the type of pipeline coating. They may, for part of their length, be exposed to the zone of influence caused by the close proximity to the power lines. In this subsection, a literature review is presented about 1) the nature of influences on the buried pipeline caused by the currents in power lines; 2) problems caused by power line induction; 3) criteria suggested by existing electrical coordination standards and 4) methods for evaluating induced voltage on buried pipeline.

1.1.1 Nature of the Influences

When AC current flows in a conductor, such as a power line, a magnetic field is naturally produced circulating the conductor, which consequently induces voltage on the nearby conductors [1][2]. One of the nearby conductors could be the buried pipeline. The induced voltage manifests itself as a series of driving voltage sources with the buried pipeline, as shown in Figure 1.1 [3]. The buried pipelines can be affected by the induced voltages when they are located parallel to, approaching, or crossing a power line. Specifically, the pipe-to-ground voltage varies at different locations along the buried pipeline due to its inherent distributed parameter characteristic. Although the electromagnetic inductions occur under normal and fault conditions, they differ in magnitudes and durations. In normal conditions, because of load current flowing in the power line, the induced voltage exhibits a moderate magnitude but a long duration characteristic. On the other hand, during a fault, when the power line carries a high and unbalanced current, the induced voltage is of high magnitude but of rather short duration.

No matter where the electromagnetic field is generated by, whether the fundamental current or the harmonic current, the voltage induction phenomenon explained earlier is the same on the buried pipeline.

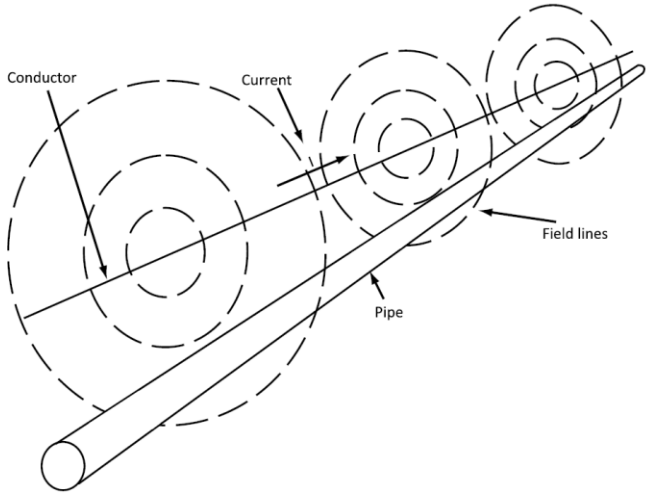

(a) Electromagnetic field from power line

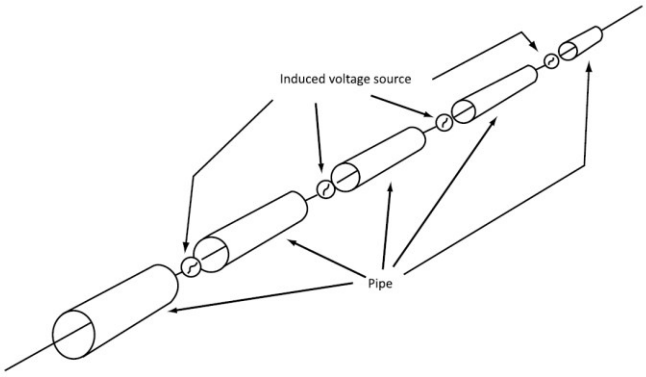

(b) Induced voltage source on buried pipeline

Figure 1.1: Electromagnetically induced voltage on a pipeline [3].

1.1.2 Problems Caused by Power Line Induction

No matter if the system is in normal or fault condition, when the power line is energized, there will be induced voltage on a buried pipeline. Therefore, the pipe-to-ground voltage can be a hazard to pipeline operators, the general public, and the pipeline itself. Three main issues due to electromagnetic induction are considered in the following section:

A. Personnel Safety Issue

According to Figure 1.2, the voltage difference between a pipeline and the ground may exceed the touch voltage criterion for personnel safety [3]-[5]. In addition, the touch voltage criterion is dependent on exposure duration [5]. Therefore, the allowable touch voltage in the normal condition should be much lower than that in fault condition. There should be two touch voltage criteria established for each system operation condition so that the associated potential risk of danger on personnel can be avoided.

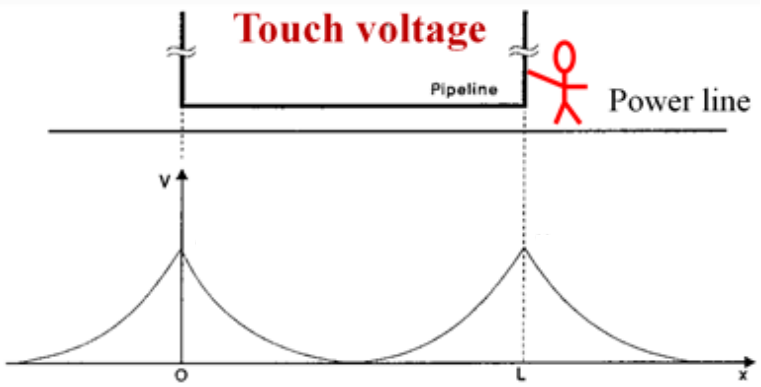

Figure 1.2: Pipeline touch voltage issue.

B. AC Corrosion Issue

In order to prevent electrochemical corrosion of the metal, the buried pipeline is provided with an outside insulating coating and normally connected to a cathodic protection (CP) installation. However, when AC voltage is induced on the buried pipeline, the additional pipe-to-ground AC voltage potential can be established. The holiday on the pipeline coating will provide a path for AC current leakage into soil (Figure 1.3). The leakage current will accelerate the pipeline corrosion with the increasing current density [6]-[33]. Thus, the higher induced voltage results in more severe corrosion. However, the corrosion is an aggregative effect that requires long-term exposure, which is unlikely to be caused by fault conditions where the exposure duration is limited.

There is a professional consensus that the AC corrosion likelihood is linked to the AC current density at the coating holiday and the consequent flowing between the buried pipeline and the soil. Primarily, the cathodic protection is set up to avoid DC corrosion. In fact, if the AC current density is in some lower range, the AC corrosion may be prevented by CP [34][35]. The effectiveness of CP on AC corrosion is still under study.

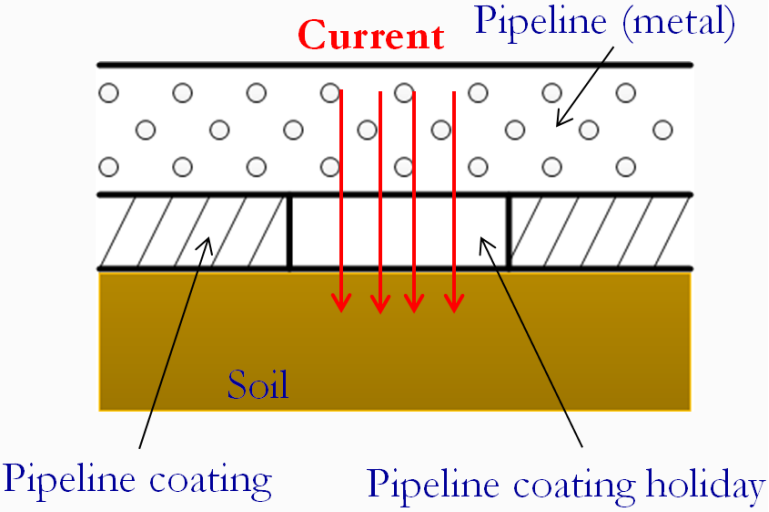

Figure 1.3: Pipeline AC corrosion issue.

C. Pipeline Coating Breakdown Issue

Under fault condition, although the induced voltage is not a threat to corrosion due to its short duration, it produces a great voltage stress on the coating material as shown in Figure 1.4. The amount of stress on the coating material is primarily determined by the breakdown voltage rather than the exposure duration. If the induced voltage exceeds the coating breakdown voltage, the pipeline coating could be potentially damaged immediately. The damaged coating will further contribute to the process of pipeline corrosion after the power system restores to normal conditions.

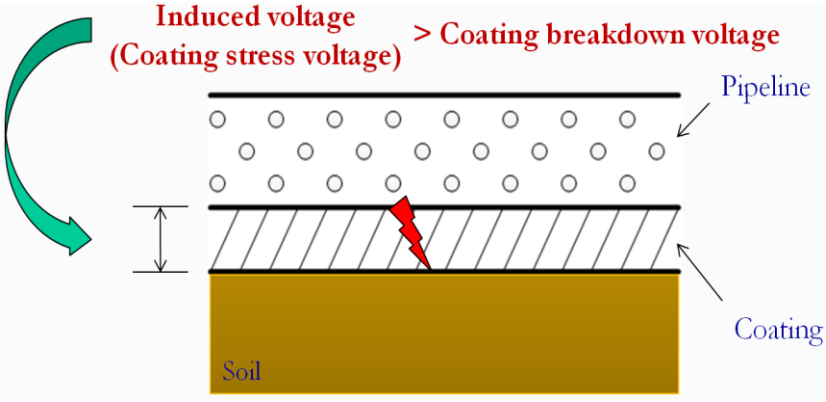

Figure 1.4: Pipeline coating breakdown issue.

1.1.3 Criteria Suggested by Existing Electrical Coordination Standards

In general, CSA C22.3 No.6-2013 [3] specifies the criteria for both personnel safety and AC corrosion issues; NACE SP0177-2014 [4] specifies the criteria for AC corrosion, personnel safety and pipeline coating breakdown issue; ISO 15589 [34] and CEN/TS 15280 [35] specify the criterion for an AC corrosion issue of the pipeline. As can be seen, the criteria for induction effects assessment of the power line on the pipeline at fundamental frequency are already available. However, since research of AC corrosion issue is still under way, the standards have slight variations in their proposed limits. Therefore, the limits are segregated and presented in Table 1.1.

Table 1.1: Criteria for assessing the induction effects of power lines on pipelines.

Issue	**Criteria**			**Standard**
	Index	Condition	Limit	
Personnel safety	Touch voltage V_{touch}	normal	15 V	CSA C22.3 No.6-13 NACE SP0177-2014
		Fault	See IEEE std. 80-2000	CSA C22.3 No.6-13 NACE SP0177-2014

Table 1.1 (continued): Criteria for assessing the induction effects of power lines on pipelines

Issue	Criteria			Standard
	Index	Condition	Limit	
Pipeline AC corrosion	AC current density $J_{corrosion}$	Low risk	<20 A/m^2	CSA C22.3 No.6-13
			<30 A/m^2	NACE SP0177-2014 CEN/TS 15280-2006 ISO 15589-1-2003
		Medium risk	20~100 A/m^2	CSA C22.3 No.6-13
			30~100 A/m^2	NACE SP0177-2014 CEN/TS 15280-2006
		High risk	>100 A/m^2	CSA C22.3 No.6-13 NACE SP0177-2014 CEN/TS 15280-2006
	AC corrosion voltage $V_{corrossion}$	Soil resistivity >25Ωm	10V	CEN/TS 15280-2006
		Soil resistivity <25Ωm	4V	
Pipeline coating breakdown	Coating breakdown voltage $V_{breakdown}$	Bitumen coating	1~1.2 kV	NACE SP0177-2014
		FBE, polyethylene	3~5 kV	

1.1.4 Method for Evaluating Induced Voltage on Buried Pipeline

Based on the analysis of the issues considered, the main cause of different pipeline issues is the induced voltage of the power line on the buried pipeline. The inductive coupling effect between the power line and the pipeline has been widely studied at fundamental frequency. Westinghouse originally presented methods to calculate the induced voltage on above-ground pipeline due to single phase and

three phase AC power lines [36]. The International Telegraph and Telephone Consultative Committee summarize the prediction and mitigation methods for induced voltages on above-ground pipeline. In their analysis of buried pipeline, some papers attempt to apply the above-ground equations directly, which calculate the induced voltage on pipeline in the following general equation [37]:

$$V_{\max} = f(I, d) \times L \tag{1.1}$$

where

V_{max} = the maximum induced voltage;

I = the power line current;

d = the distance between the power line and the pipeline;

L = the parallel length.

As discussed by several researchers, the values of induced voltage on buried pipeline calculated by the above-ground methods are too high [38]. This error of calculating the induced voltage is simply because a buried pipeline, most of time wrapped in an electrically insulated coating, has a larger but finite resistance to earth distributed along its entire length. The resistance of coating electrically differs a buried pipeline from an above-ground pipeline. Buried pipeline and its surrounding earth parameters, such as coating material and soil resistivity, need to be considered in the calculation of induced voltage on buried pipeline.

In order to model the inductive coupling from a power line to a buried pipeline more accurately, researchers have proposed a circuit-based method to consider a buried pipeline as a lossy electrical transmission line with a distributed voltage source along the parallel section of the buried pipeline due to the inductive coupling. This method is successfully applied to analyzing the inductive coupling issues from the power line to the buried pipeline at 60 Hz [38]-[53].

This method is based on the concept of “distributed source”, which means the source of induced voltage that drives the buried pipeline is distributed along the

parallel section of the buried pipeline. The equivalent circuit model of the buried pipeline with a distributed source is, by definition, one that consists of many increments of buried pipeline with each increment of source voltage in series. An element of the equivalent model in *dx* length is illustrated in Figure 1.5. The general two steps to calculate the induced voltage are as follows:

Step A: Determine the electromotive force (EMF) induced along the buried pipeline. EMF is the virtual electric generator inside each buried pipeline increment resulting from the influence of the inductive coupling from the power line.

Step B: Calculate the induced voltage from buried pipeline to earth in response to the EMF. This voltage, produced by EMF, represents the actual voltage stress on the buried pipeline.

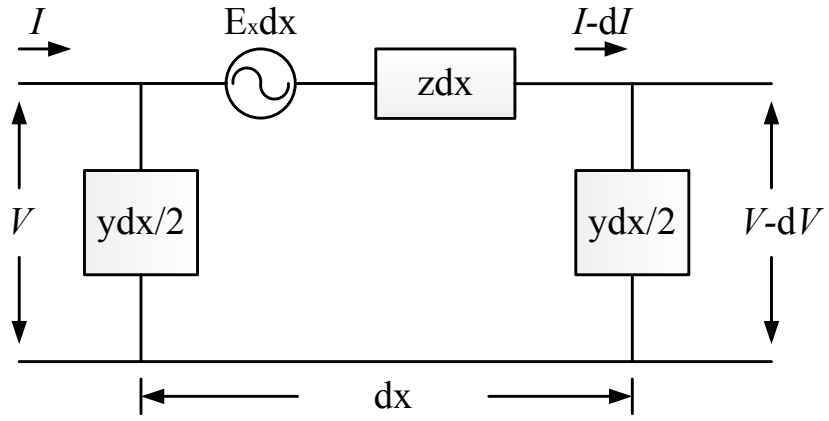

Figure 1.5: The element of the equivalent model in *dx* length.

The limitation of the circuit-based method is that it cannot precisely predict induced voltages near the terminals of buried pipeline or power line since it is a 3D problem. In recent years, simulation tools have been developed and become dominant in the industry. CDEGS is a commercial software package developed by SES for dealing with problems involving grounding, EMF (Electromagnetic Fields), and EMI. CDEGS has two programs suitable for pipeline studies: (a) Right-Of-Way is designed for calculating the effects of inductive coupling under normal and fault conditions using a circuit-based method, which is the same

method as the EPRI guide adopts, and conductive coupling under fault conditions using a hybrid method; (b) MultiFields uses a field-based method to calculate the effects of inductive and conductive coupling in a network with complex grounding structures, especially under fault conditions [54]. It could be used to deal with complex power line-pipeline interference problems.

1.1.5 Summary

To date, there are many papers dealing with AC induction impact on buried pipeline at the fundamental frequency. However, the impact of harmonic current induction in the distribution line on buried pipeline is not fully investigated. Generally, the circuit-based method can be applied to analyze the inductive coupling at the harmonic frequencies between power distribution line and buried pipeline because the inductive coupling mechanisms are the same at different harmonic frequencies. The detailed explanations of the methodology and special discussion for harmonic models are documented in the next several chapters.

1.2 Motivation for Assessing the Harmonic Induction Impact of Power Distribution Feeder

As mentioned in the standard CSA C22.3 No.6-2013, the industry understanding of the induction impact on pipeline caused by harmonic currents is not mature at this time [3]. However, the contribution of the third harmonic to induction on pipelines has been observed in some situations [3]. Therefore, there are strong reasons for assessing the harmonic induction impact on the buried pipeline. This subsection explains the motivation in the following aspects:

1.2.1 Harmonic Situations in Today's Distribution System

The harmonics produced by distribution systems has become a great concern in recent years due to the extensive applications of power electronic-based nonlinear loads [55]. This phenomenon especially exists in power distribution feeders supplying residential areas [55]. Figure 1.6 shows a typical harmonic current

spectrum of a distribution feeder on a weekday [56]. The harmonic currents from today's residential loads clearly indicate that the harmonic currents could become significant sources of AC induction on buried pipeline in addition to the fundamental current.

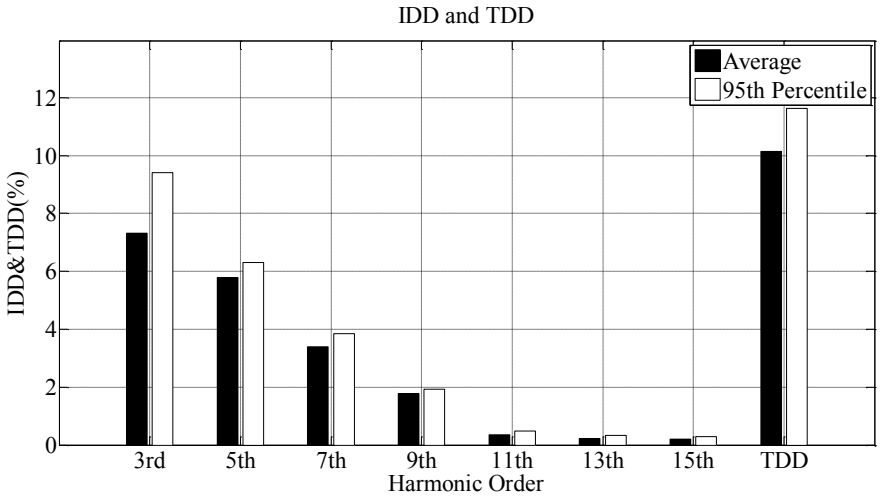

Figure 1.6: Average and the 95th Percentile IDD and TDD [56].

1.2.2 Field Measurements of Harmonics on Pipeline

The contribution of the harmonic currents to induction on a pipeline, which shares a corridor with an AC transmission line, has been observed in North America and Europe [57][58]. The original intention of those studies was to examine the phase relation of the fundamental waveforms from different places along the pipeline. However, the recorded waveforms were found to have much greater harmonic components than expected. Figure 1.7 shows the recorded waveforms and the spectra based on the selected recording in North America [57]. The recorded waveforms are not simple sinusoids but have considerable distortion. Spectral analysis shows that, as well as the fundamental frequency, there are significant components at the 3rd and 9th harmonics, which are even higher than the fundamental frequency. Additionally, the 5th and 7th harmonics are observed.

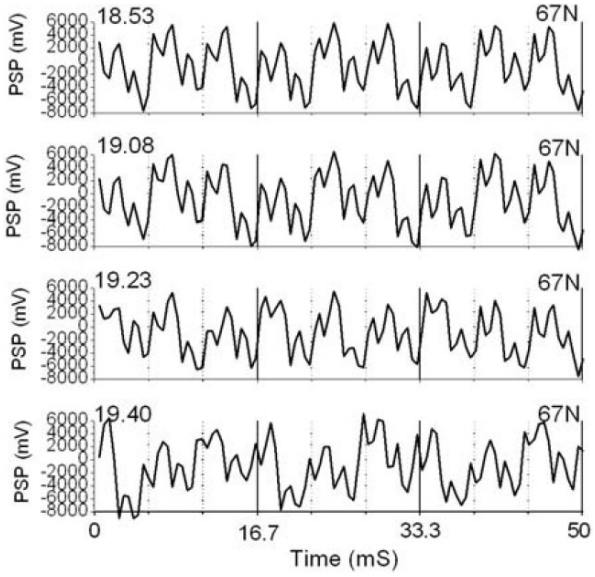

(a) Recording of the induced voltage waveforms

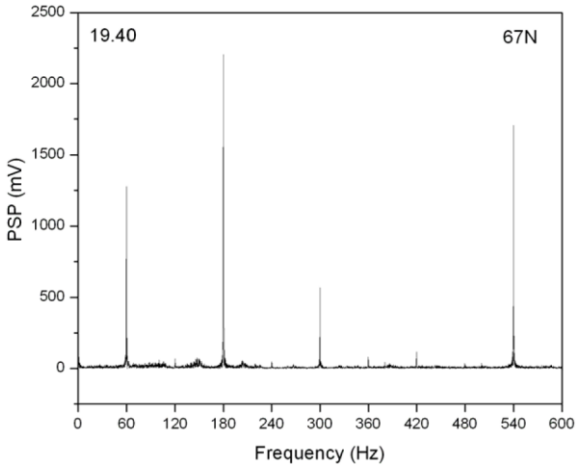

(b) Spectra of the induced voltage waveforms

Figure 1.7: Example of the induced voltage on pipeline in North America [57].

In reality, the scale of harmonic currents in the distribution system is larger than that in the transmission system. In this case, it is worthwhile to investigate the impact of harmonic currents on buried pipeline that shares corridors with the distribution feeder.

1.2.3 Harmonic Impact on Metal Corrosion

So far, the mechanisms of AC corrosion at the harmonic frequency range are still not completely understood. However, this issue has been reported based on

several experiments [32][33]. A paper by Song [32] reports the corrosion rate with a contribution of 180 Hz harmonic, of measured coupons installed next to a buried cathodically protected pipeline for 6 and 12 months. A set of corrosion experiments was conducted by Pagano [33] at various frequencies from 5 to 500 Hz. The relationship between the average corrosion rate and the frequency of the supplied alternating voltage source is shown in Figure 1.8. It is clear to see that there is a sharp drop in the corrosion rate at about 60 Hz with an increasing frequency from 5 to 500 Hz, but the corrosion rate decreases very slowly after 60 Hz. The corrosion rates at fundamental and harmonic frequencies are comparable. Based on the relationship between corrosion rate and frequency, the harmonic impact on pipeline corrosion cannot be ignored as there appears to be an agreement that the corrosion at the fundamental frequency is possible.

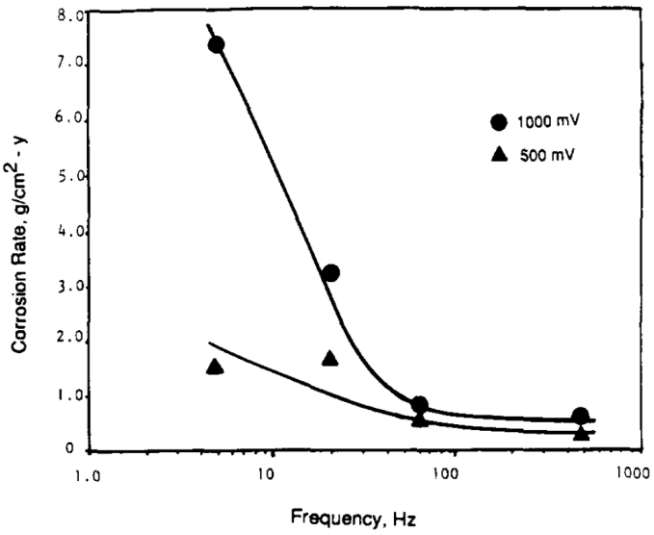

Figure 1.8: The relationship between corrosion rate and frequency [33].

1.2.4 Summary

In summary, the current situation of coordination between the distribution feeder and buried pipeline at harmonic frequencies requires detailed investigation. Unfortunately, this problem has not yet been fully studied. Thus, there are strong reasons for discussing the harmonic induction impact on buried pipeline in as much detail as possible.

1.3 Thesis Scope and Outline

The scope of this thesis addresses the harmonic induction impact of the power distribution line on buried pipeline. Three main topics are investigated in this thesis.

The first topic is to discuss the impacts of harmonic currents on buried pipeline to reveal the importance and the severity of harmonic induction impacts by comparing with the impact of fundament currents in power distribution lines. As the foundation of harmonic induction analysis, the analytical method to calculate the induced voltage at harmonic frequencies is fully investigated.

The second topic is to present the main impact factors of harmonic induction through sensitivity study. As mentioned above, the unique characteristics of distribution system, which have not been discussed in transmission system, may aggravate the inductive coupling effects. Thus, there are many factors that affect the induced voltage on buried pipeline. Hence, it is necessary to find out the main impact factors.

The third topic is the mitigation methods at harmonic frequencies. The objective of this topic is to analyze the effectiveness of applying those methods to mitigate harmonic induced voltages on buried pipeline.

The thesis is organized as follows:

Chapter 2 first presents the analytical methods of calculating the induced voltage on buried pipeline due to power line induction at the fundamental frequency. Then methods of the criteria for assessing the effects of power line induction are also reviewed.

Based on the methods for calculating the induced voltage at the fundamental frequency in Chapter 2, Chapter 3 extends these methods to the harmonic frequency range to analyze the impacts of harmonic currents on the buried pipeline due to inductive coupling. First, the distortion levels of harmonic currents

in power distribution system are organized based on the field measurements in recent years to give support to the calculation of the induced voltage on buried pipeline. Second, a detailed examination is conducted in order to confirm the feasibility of adopting the analytical methods from the fundamental frequency to the harmonic frequency range and to demonstrate the necessity of modification for the mutual impedance calculation. Third, this chapter illustrates the comparison of induced voltages at fundamental and harmonic frequencies. Finally, the potential issue of buried pipeline caused by harmonic current is investigated through the aspect of pipeline AC corrosion perspective.

Chapter 4 conducts the sensitivity study to illustrate the main impact factors at the harmonic frequencies by using the analytical methods discussed above. Pole structure, multi-grounded neutral, soil resistivity, coating material and parallel length will be taken into consideration in the sensitivity study.

Once the severity of induced voltage on buried pipeline due to harmonic currents is demonstrated, it is necessary to discover the proper ways to mitigate it. Chapter 5 first analyzes the islanded multi-grounded neutral configuration in mitigation usage, which is distinct from the existing mitigation methods used in the coordination between power transmission line and pipeline. Methods such as mitigation wire, multi-grounded neutral and pipeline grounding are then discussed at harmonic frequencies.

Chapter 6 concludes this thesis and provides suggestions for future research.

Appendix A presents the simulation results of the current of the multi-grounded neutral.

Appendix B documents the typical pipeline parameters at fundamental and harmonic frequencies.

Appendix C shows the field measurements of harmonic currents in distribution and transmission systems.

Appendix D introduces the setup of pipeline AC corrosion experiments.

Appendix E discusses the transmission line harmonic current induction.

Appendix F explains the impact of pipeline diameter on induced voltage.

Chapter 2

Methods of Inductive Coordination at Fundamental Frequency

The electrical coordination between power transmission line and buried pipeline has been given sufficient attention. In order to estimate the severity of this problem, the methods of calculating the induced voltage on pipeline due to power line have been widely studied at fundamental frequency.

This chapter summarizes the analysis of electromotive force (EMF) and coated pipeline buried in earth at fundamental frequency respectively. The distributed source method is then fully presented for calculating the induced voltage on buried pipeline. In addition, the methods of calculating the criteria for assessing the effects of power line inductive coupling are reviewed as well. Section 2.1 presents the method of calculating induced voltage on buried pipeline at fundamental frequency, which contains the descriptions of the model of EMF, the model of buried pipeline and the distributed source method. In Section 2.2, methods of calculating criteria for pipeline corrosion and personnel safety issues are presented. The criteria of pipeline coating breakdown issue, which may happen in fault condition, are reviewed as well.

2.1 Method of Calculating Induced Voltage on Pipeline at Fundamental Frequency

The zone of influence on buried pipeline generally comprises a succession of parallelisms, approaches and crossings, which is shown in Figure 2.1. The analytical method of calculating induced voltage is given for parallelisms between pipeline and power line. The approaches and crossings should be converted into parallelisms [59][60].

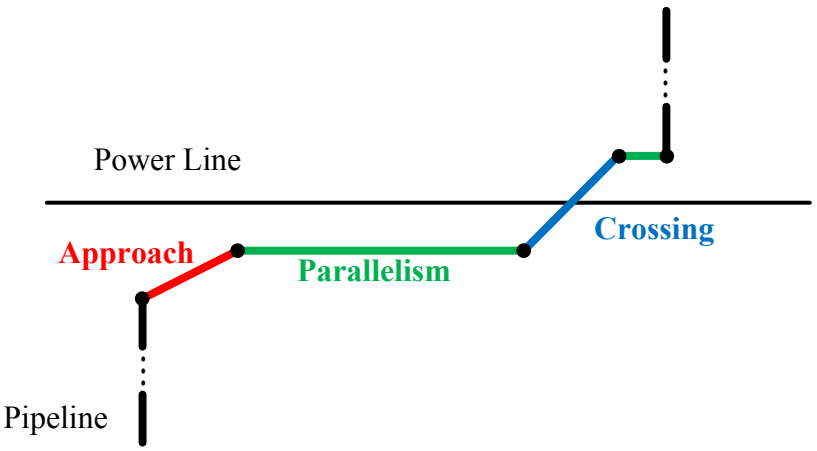

Figure 2.1: The zone of influence of power line on pipeline including parallelisms, approaches and crossings.

Calculation of the induced voltages is normally worked out in two steps:

Step A: Determining the EMF along the buried pipeline;

Step B: Calculating the induced voltage on the buried pipeline in response to the EMF.

A clear distinction has to be made between EMF and voltage appearing on the pipeline. When pipeline is in close proximity to an AC power line, the pipeline is influenced by power line induction. In this situation, the pipeline can be treated as a lossy electrical transmission line with impedance per unit length of z and admittance per unit length of y. Figure 2.2 illustrates one element of the equivalent circuit of pipeline/earth. The EMFs, E_x in this figure, are the virtual voltage sources inside the circuit of pipeline/earth resulting from the influence of the inductive coupling. These EMFs produce voltages V, so called induced voltages, which are distributed along the buried pipeline, corresponding to the longitudinal electromagnetic field of the power line current. Only these voltages represent the actual stresses on the pipeline and its equipment.

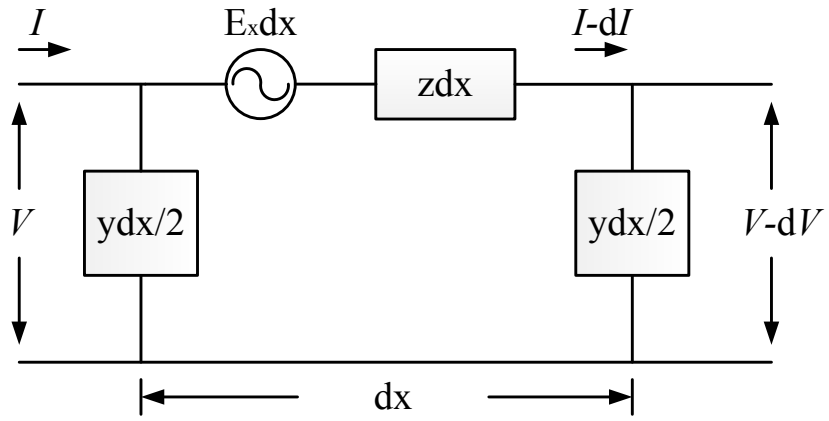

Figure 2.2: The element of the equivalent circuit of pipeline/earth in *dx* length.

2.1.1 Modelling of Electromotive Force

It is well known that the EMF, E, induced by the AC current I on nearby conductor, can be calculated by

$$\vec{E} = \vec{Z}_m \vec{I} \tag{2.1}$$

where Z_m is the mutual impedance between two conductors.

If more than one conductor exists, the total EMF should be the phasor summation of the EMFs induced by each conductor. For a pipeline parallel to a distribution power line, the total EMF effect during normal condition is contributed by the combination of load currents flowing in three phase conductors and also the neutral conductor if existing. Therefore, the total EMF per unit length can be expressed under the form:

$$\vec{E}_{total} = \vec{Z}_{mA}\vec{I}_A + \vec{Z}_{mB}\vec{I}_B + \vec{Z}_{mC}\vec{I}_C + \vec{Z}_{mN}\vec{I}_N \tag{2.2}$$

where Z_{mA}, Z_{mB}, Z_{mC} and Z_{mN} are mutual impedances per unit length of each phase (neutral) conductor/earth and pipeline/earth. I_A, I_B, I_C and I_N are three phase and neutral currents.

A. Determination of Mutual Impedances

The mutual impedance of two earth-return circuits, i.e., phase (neutral) conductor/earth and pipeline/earth, depends mainly on:

- Distance between the conductor and the pipeline *d*;
- Soil resistivity ρ;
- Angular frequency ω.

For the inductive coupling between the loop of an overhead conductor with earth return and the loop of a buried conductor with earth return, many papers can be found through the literature review [61]-[69]. Two of the most well-known methods are the original work of Pollaczek and Carson [61][62], deriving ground earth correction expressions with

$$Z_{m\_Pollaczek} = \frac{\rho m^2}{2\pi}\int_{-\infty}^{\infty}\frac{\exp\left(-h|\alpha| + h_p\sqrt{\alpha^2+m^2}\right)}{|\alpha|+\sqrt{\alpha^2+m^2}}\exp(j\alpha x)\,d\alpha$$
$$m = \sqrt{\frac{j\omega\mu_0}{\rho}} \tag{2.3}$$

$$Z_{m\_Carson} = \frac{\mu_0\omega}{\pi}\int_0^{\infty}\left(\sqrt{\alpha^2+j}-\alpha\right)e^{\left(-(h-h_p)\sqrt{\frac{\mu_0\omega}{\rho}}\alpha\right)}\cos\left(\sqrt{\frac{\mu_0\omega}{\rho}}\alpha x\right)d\alpha \tag{2.4}$$

where

$\mu_0 = 4\pi 10^{-7}$ H/m;

$\omega = 2\pi f$;

ρ = soil resistivity (Ωm);

h = height of the overhead conductor (m);

h_p = depth of the buried conductor (m);

x = horizontal distance between overhead conductor and buried conductor.

Further, Ametani uses an approximation to simplify the above integral into the identical expression with Carson's formula by replacing $y\sqrt{\alpha^2+m^2}$ with $y|\alpha|$ [63]. As a result, Carson and Pollaczek's formulas are generally the same [64].

However, both Carson's and Pollaczek's formulas require the computational support program to calculate the mutual impedance. To simplify the calculation for easy and practical evaluation with enough accuracy, industrial guides recommend the Carson-Clem formula defined in equation (2.5) [37][59][60].

$$Z_m = \frac{\omega\mu_0}{8} + \frac{j\mu_0\omega}{2\pi}\left[\ln\left(\frac{2}{gd\sqrt{\frac{\omega\mu_0}{\rho}}}\right) + \frac{1}{2}\right] \tag{2.5}$$

where

g = 1.7811 Euler's constant;

d = geometrical distance between conductors (m).

The Carson-Clem formula is derived from the Carson's formula by the assumptions that the geometrical term is neglected and the terms considered from the Carson's series expressions are only the first term of real part and two terms from imaginary part. In practical, the Carson-Clem formula can be applied to those cases where the value of the geometrical distance yields the limit according to the soil resistivity and angular frequency as following [60]:

$$d < 90\sqrt{\frac{2\pi\rho}{\omega}} \tag{2.6}$$

The limit of Carson-Clem formula used in harmonic study will be discussed in Chapter 3.

B. Determination of Neutral Current

Multi-grounded neutral (MGN) is a typical configuration at distribution level in North America. The neutral current varies with different locations along a distribution feeder [70]. Besides, it can't be measured directly. Therefore, in order to identify the impact of MGN on the total EMF, a simulation study is conducted at fundamental frequency with the results are shown in Appendix A. Based on the

simulation results, the neutral current is about 30% of the phasor summation of three phase currents $3I_0$, where I_0 indicates the zero sequence current. In fact, neutral current flows in an opposite direction of $3I_0$, which tends to have a cancelling effect of the EMF generated by three phase conductors. The detailed analysis of neutral current at harmonic frequencies will be presented in Chapter 4.

2.1.2 Modelling of Buried Pipeline Self-Impedance and Self-Admittance

For the buried pipeline case, which involves wave propagating and returning mostly within the soil, the expressions of self-impedance and self-admittance are developed by many researchers from fundamentals of electromagnetic theory [61]-[64][71][72][78]. The expressions for self-impedance z and self-admittance y at fundamental frequency have been introduced by industrial guides as following [59][60]:

$$z = z_i + j\frac{\omega\mu_0}{2\pi}\ln\frac{1.85}{\alpha'\sqrt{\gamma^2 + j\omega\mu_0\left(\frac{1}{\rho} + j\omega\varepsilon\right)}} \tag{2.7}$$

$$z_i = R_i + jX_i = \frac{\sqrt{\omega\mu_r\mu_0\rho_p}}{\sqrt{2}\pi D}\left[\frac{\sinh(t_n)+\sin(t_n)}{\cosh(t_n)-\cos(t_n)} + j\frac{\sinh(t_n)+\sin(t_n)}{\cosh(t_n)-\cos(t_n)}\right] \tag{2.8}$$

$$y^{-1} = y_i^{-1} + \frac{\ln\left(\frac{1.12}{a'\gamma}\right)}{\pi\left(\frac{1}{\rho} + j\omega\varepsilon\right)} \tag{2.9}$$

$$y_i = \frac{\pi D}{r_c} + j\omega\frac{\varepsilon_0\varepsilon_r\pi D}{\delta_c} \tag{2.10}$$

where

μ_r = 300 relative permeability of the pipeline;

ρ_p = 1.7*10^{-7} Ωm resistivity of pipeline;

ε_0 = 8.85*10^{-12} F/m electrical permittivity of the air;

ε_r = 5 relative electrical permittivity of the pipeline coating;

$\varepsilon = 3 * \varepsilon_0$ electrical permittivity of the soil;

r_c = $1*10^5$ Ωm^2 polyethylene coating resistance ($1*10^3$ Ωm^2 bituminous coating resistance);

D = 0.6 m diameter of the pipeline;

a = 0.3 m radius of the pipeline;

a' = equivalent radius of burial pipeline (m) $\alpha' = \sqrt{\alpha^2 + 4h_p'^2}$;

h_p' = 1 m depth of buried pipeline;

δ_c = 0.004 m thickness of the coating;

t_n = pipeline wall thickness (m) $t_n = 0.0157 \frac{\sqrt{2\omega\mu_r\mu_0\rho_p}}{\rho_p} D^{0.421}$;

γ = propagation constant of the circuit pipeline/earth (m^{-1}) $\gamma = \sqrt{zy}$.

These expressions are based on Sunde's formulas, which are used for wide frequency range without low frequency approximation [71]. The usage of Sunde's formula in the harmonic frequency range will be discussed in Chapter 3.

2.1.3 Method of Calculating Induced Voltage

This section reviews the calculation of the induced voltage on the pipeline in response of the EMFs [38][59][60]. The voltage calculation method is demonstrated for the simple theoretical case of a parallelism. The calculation presented hereafter is based on the following assumptions:

- the pipeline is parallel to the distribution line;
- the coating resistance per unit length of the pipeline is uniform and independent of the applied voltage;
- the soil resistivity along the parallel route is constant.

Figure 2.3 shows the situation with a parallelism between x=0 and x=L. Z_A is the impedance of the pipeline situated at the left side and seen from point x=0. Z_B is the impedance of the pipeline situated at the right side and seen from x=L.

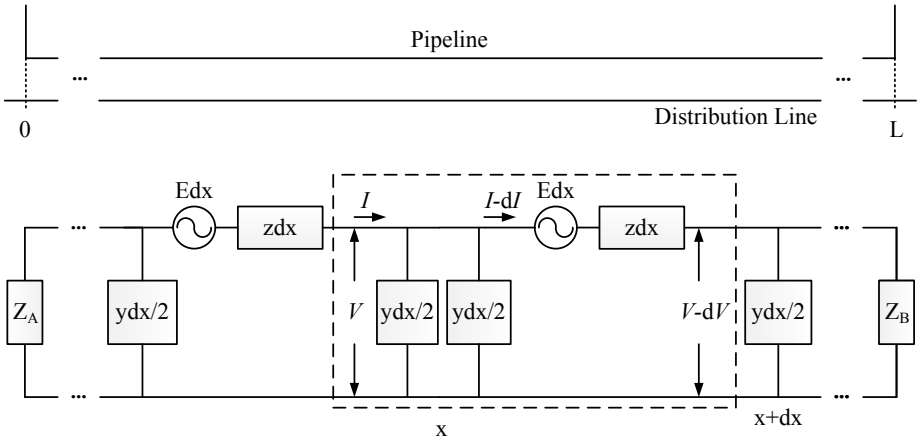

Figure 2.3: Situation of power line and pipeline parallel.

On basis of the above assumptions, the equations of the circuit pipeline/earth are:

$$\frac{dV(x)}{dx} + zI(x) - E = 0 \tag{2.11}$$

$$\frac{dI(x)}{dx} + yV(x) = 0 \tag{2.12}$$

where

z = impedance per unit length of the circuit pipeline/earth;

y = admittance per unit length of the circuit pipeline/earth;

E = EMF induced on the pipeline per unit length.

Combination of equation (2.11) and (2.12) leads to the following expressions:

$$\frac{d^2V(x)}{dx^2} - zyV(x) - \frac{dE(x)}{dx} = 0 \tag{2.13}$$

$$\frac{d^2I(x)}{dx^2} - zyI(x) + yE(x) = 0 \tag{2.14}$$

If we consider the influence in normal condition, the inducing current is constant along the zone of influence and consequently E(x) equals a constant value. Solutions of equation (2.13) and (2.14) can be written under the following forms:

$$V(x) = -\frac{Z_c}{\gamma}\left(Ae^{\gamma x} - Be^{-\gamma x}\right) \tag{2.15}$$

$$I(x) = \frac{1}{\gamma}\left(Ae^{\gamma x} + Be^{-\gamma x}\right) + \frac{E}{z} \tag{2.16}$$

The constants A and B depend on the boundary conditions at the ends:

$$A = \frac{E}{2Z_c}\frac{(1+v_1)v_2 - (1+v_2)e^{\gamma L}}{e^{2\gamma L} - v_1 v_2} \tag{2.17}$$

$$B = \frac{E}{2Z_c}\frac{(1+v_2)v_1 - (1+v_1)e^{\gamma L}}{e^{2\gamma L} - v_1 v_2}e^{\gamma L} \tag{2.18}$$

$$v_1 = \frac{Z_A - Z_c}{Z_A + Z_c} \tag{2.19}$$

$$v_2 = \frac{Z_B - Z_c}{Z_B + Z_c} \tag{2.20}$$

Where

v_1 = reflection factor at the beginning of the pipeline;

v_2 = reflection factor at the end of the pipeline;

$Z_c = \sqrt{z/y}$ characteristic impedance of the circuit pipeline/earth.

In practice, three particular cases are worth analyzing:

A. The pipeline extends for a few kilometers L_e[1] beyond the parallel routing without grounding (Figure 2.4)

$$Z_A = Z_B = Z_c; v_1 = 0; v_2 = 0 \tag{2.21}$$

$$V(x) = \frac{E}{2\gamma}\left[e^{-\gamma(L-x)} - e^{-\gamma x}\right] \tag{2.22}$$

$$I(x) = -\frac{E}{2\gamma Z_c}\left[e^{-\gamma(L-x)} + e^{-\gamma x}\right] + \frac{E}{z} \tag{2.23}$$

Then the maximum pipeline induced voltages occur at the terminals of the parallel section at x=0 and x=L [60]:

$$|V(0)| = |V(L)| = V_{\max} = \frac{E}{2\gamma}(1 - e^{-\gamma L}) \tag{2.24}$$

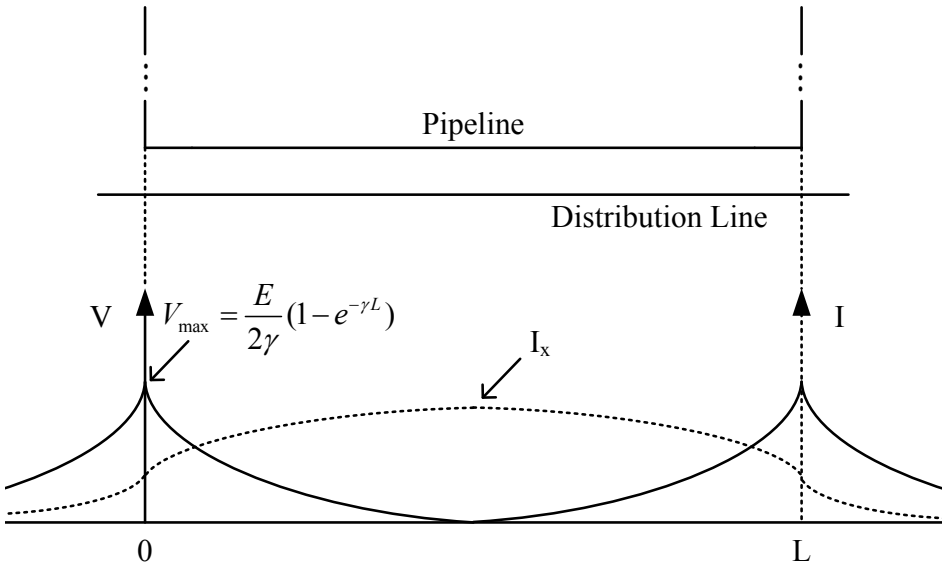

Figure 2.4: Evolution of the voltage along a pipeline extending beyond the zone of influence.

Outside the exposure, if the pipeline extends longer than L_e, the pipeline potential declines according to exponential function [60]:

[1] This distance is discussed in detail in Appendix B.

$$V(x) = V_{\max} e^{-\gamma x} \tag{2.25}$$

with x = co-ordinate outside the parallel section.

If the pipeline extends a few kilometers l, which is shorter than L_e, and then stops with grounding R_g, the new boundary equivalent impedance Z_{eq_g} in the calculation of v_1 is calculated based on the equivalent circuit of pipeline in Figure 2.5:

$$Z_{eq\_g} = \left[\left(R_g \frac{2}{y'l} \middle/ \left(R_g + \frac{2}{y'l}\right) + z'l\right)\frac{2}{y'l}\right] \middle/ \left[\left(R_g \frac{2}{y'l} \middle/ \left(R_g + \frac{2}{y'l}\right) + z'l\right) + \frac{2}{y'l}\right] \tag{2.26}$$

$$z' = z\frac{\sinh(\gamma l)}{\gamma l} \tag{2.27}$$

$$y' = y\frac{\tanh\left(\frac{\gamma l}{2}\right)}{\frac{\gamma l}{2}} \tag{2.28}$$

Eventually, the induced voltage is calculated based on equation (2.15), (2.17) - (2.20), (2.26) – (2.28).

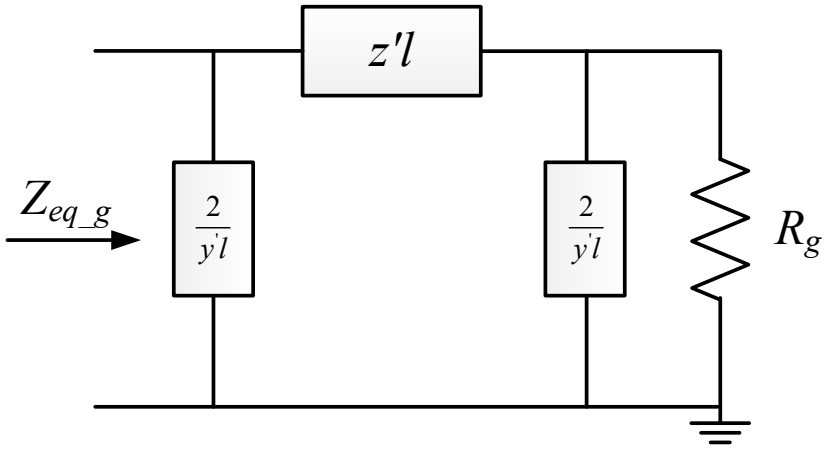

Figure 2.5: Outside the exposure, the pipeline extends a few kilometers and stops with grounding.

If the pipeline extends a few kilometers l, which is shorter than L_e, and then stops without grounding, the pipeline is an open circuit. The new boundary equivalent impedance is calculated based on the equivalent circuit of pipeline in Figure 2.6:

$$Z_{eq\_open} = \left(z'l + \frac{2}{y'l} \right) \frac{2}{y'l} \Bigg/ \left[\left(z'l + \frac{2}{y'l} \right) + \frac{2}{y'l} \right] \tag{2.29}$$

Therefore, the induced voltage is calculated based on equation (2.15), (2.17) - (2.20), (2.27) - (2.29).

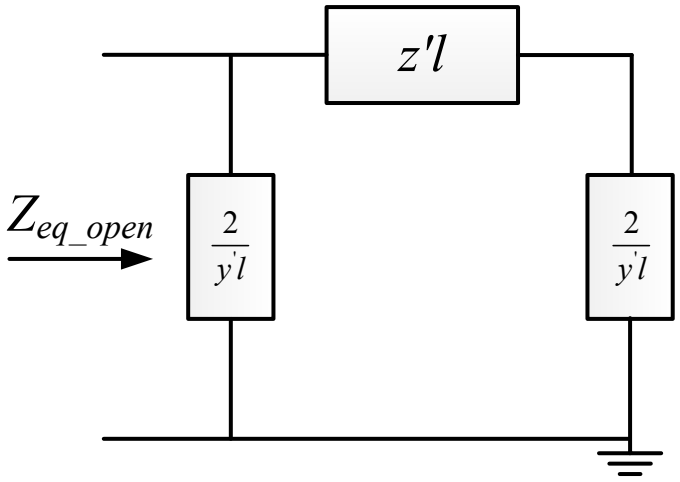

Figure 2.6: Outside the exposure, the pipeline extends a few kilometers and stops without grounding.

B. The pipeline extends beyond the parallel routing at one extremity (A) and stops at the other extremity (B) without grounding (Figure 2.7)

$$Z_A = Z_c; Z_B = \infty; v_1 = 0; v_2 = 1 \tag{2.30}$$

$$V(x) = \frac{E}{2\gamma} \left[e^{\gamma x} \left(2e^{-\gamma L} - e^{-2\gamma L} \right) - e^{-\gamma x} \right] \tag{2.31}$$

$$I(x) = \frac{E}{2\gamma Z_c} \left[\left(e^{-2\gamma L} - 2e^{-\gamma L} \right) e^{\gamma x} - e^{-\gamma x} \right] + \frac{E}{z} \tag{2.32}$$

Then the maximum pipeline induced voltages occur at x=L, where the pipeline stops without grounding [60]:

$$V(L) = \frac{E}{\gamma}\left(1 - e^{-\gamma L}\right) \tag{2.33}$$

The induced voltage at x=0 is [60]:

$$V(0) = \frac{E}{2\gamma}\left(2e^{-\gamma L} - e^{-2\gamma L} - 1\right) \tag{2.34}$$

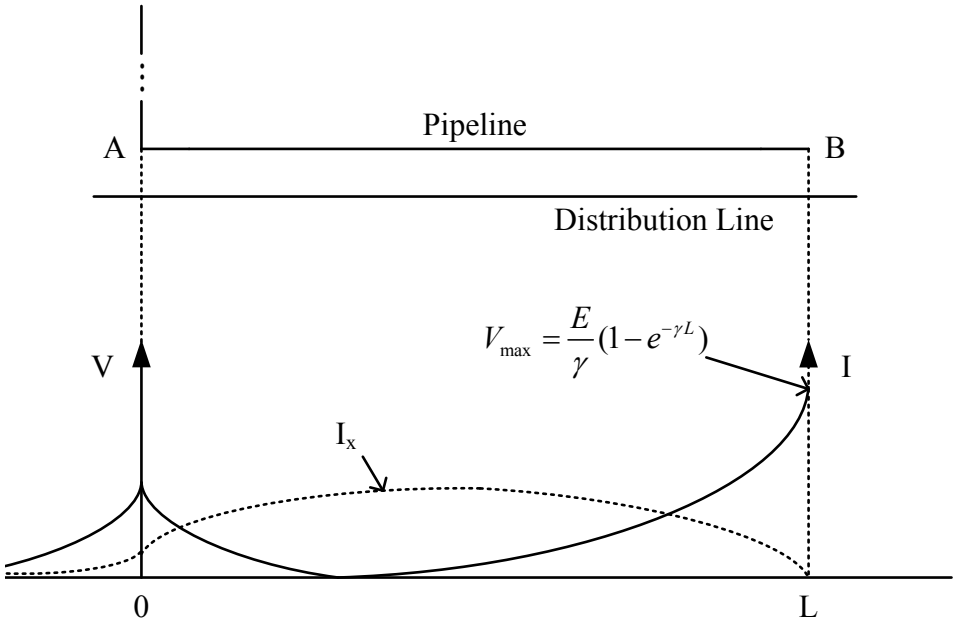

Figure 2.7: Evolution of the voltage when the pipeline extends beyond the zone in one direction.

C. The pipeline is ideally grounded at one extremity of the parallelism (A). It extends at the other extremity (B) (Figure 2.8)

$$Z_A = 0; Z_B = Z_c; v_1 = -1; v_2 = 0 \tag{2.35}$$

$$V(x) = \frac{E}{2\gamma}\left(e^{\gamma x} - e^{-\gamma x}\right)e^{-\gamma L} \tag{2.36}$$

$$I(x) = -\frac{E}{2\gamma Z_c}\left(e^{\gamma x} + e^{-\gamma x}\right)e^{-\gamma L} + \frac{E}{z} \tag{2.37}$$

As the pipeline is ideally grounded at x=0, it is obvious that the induced voltage is equal to the potential of remote earth:

$$V(0) = 0 \tag{2.38}$$

Then the maximum induced voltage appears on the other extremity:

$$V(L) = \frac{E}{2\gamma}\left(1 - e^{-2\gamma L}\right) \tag{2.39}$$

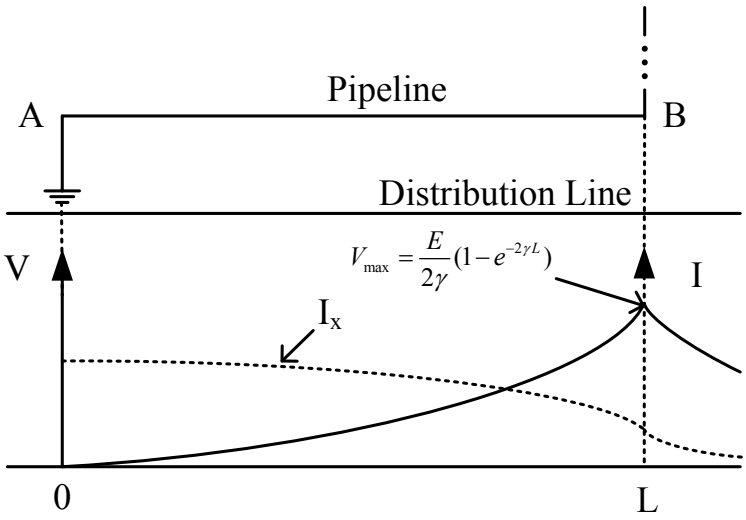

Figure 2.8: Evolution of the voltage when the pipeline is grounded at one extremity.

The typical values of pipeline parameters will be shown in Appendix B.

2.1.4 Non-Parallel Case

The abovementioned expressions and figures concern the parallelism of the power line and the pipeline. In real cases, the zone of influence generally comprises also oblique approaches and crossings.

A. Approach

As shown in Figure 2.9, the calculation is based on the subdivision of the zone of influence into a great number of short sections. If the length of each section is much shorter than the geometrical distance between the power line and the pipeline, the EMF produced on the non-parallel section is roughly equal to that on the parallel section. Therefore, each section can be equivalent to a π network exposed to an EMF. Using the nodal admittance matrix method, the induced voltages $V_1 \sim V_{n+1}$ of each location on the pipeline can be calculated in equation (2.40):

$$\begin{bmatrix} V_1 \\ V_2 \\ \dots \\ V_n \\ V_{n+1} \end{bmatrix} = \begin{bmatrix} Y_{11} & Y_{12} & \dots & Y_{1n} & Y_{1,n+1} \\ Y_{21} & Y_{22} & \dots & Y_{2n} & Y_{2,n+1} \\ \dots & \dots & \dots & \dots & \dots \\ Y_{n1} & Y_{n2} & \dots & Y_{nn} & Y_{n,n+1} \\ Y_{n+1,1} & Y_{n+1,2} & \dots & Y_{n+1,n} & Y_{n+1,n+1} \end{bmatrix}^{-1} \begin{bmatrix} I_1 \\ I_2 \\ \dots \\ I_n \\ I_{n+1} \end{bmatrix} \tag{2.40}$$

where Y_{xx} is the sum of admittances connected to point X, and Y_{xy} is the negative value of admittance connecting point X and Y. $I_1 = E_1 l/zl = E_1/z$, $I_2 = E_2 l/zl - E_1 l/zl = (E_2 - E_1)/z$, $I_n = E_n l/zl - E_{n-1} l/zl = (E_n - E_{n-1})/z$, $I_{n+1} = -E_n l/zl = -E_n l$.

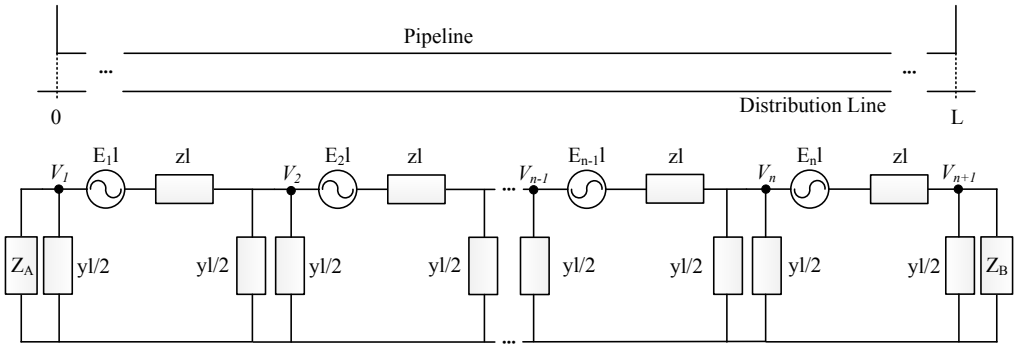

Figure 2.9: Example of subdivision of the zone of influence in sections.

This method requires the computational support to solve the (n+1)*(n+1) matrix equation. CIGRE and EPRI guides propose simplified estimation methods to deal with the non-parallel situations. In CIGRE guides, an oblique approach with distances d_1 and d_2 at the ends can be approximated to a parallelism with a

separation d equals to $\sqrt{d_1 d_2}$ on condition that $1/3 \leq d_1/d_2 \leq 3$ as shown in Figure 2.10 [60]. When the previous condition is not fulfilled, the oblique approach is subdivided in 2 (or more) sections so as to fulfill the requirement in each section. In other words, the length of each section may be limited to $2\sqrt{2}d_2$, where d_2 is the distance between the power line and the pipeline terminal closing to power line.

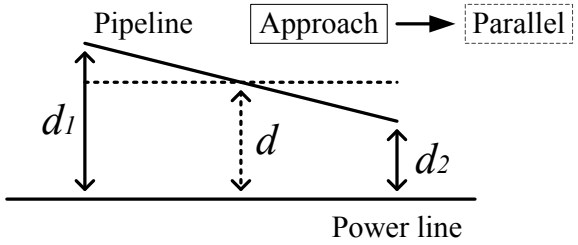

Figure 2.10: CIGRE method for pipeline approach situation [60].

According to EPRI guides, a convenient approximation for the variation of the field is to assume that the magnitude of the electromagnetic field varies inversely with the separation distance from the power line, from S_0 out to d_0 as shown in Figure 2.11. It is assumed that the electromagnetic field is negligible in value at d_0. With this assumption, an approximate evaluation of induced voltage is [59]

$$V_\theta \approx \frac{E(S_0)(d_0 - S_0)}{4\tan\theta} \tag{2.41}$$

Where

θ = the acute angle of the approach.

For situation where $S_0 \geq 300$ m, an approximation of equation (2.41) is $V_\theta \approx 0$.

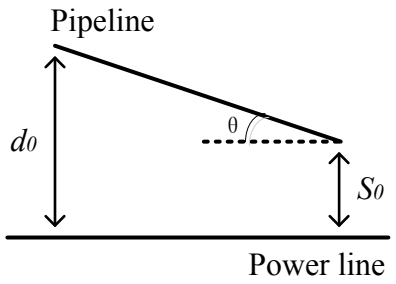

Figure 2.11: EPRI method for pipeline approach situation [59].

B. Crossing

In case of a crossing, CIGRE guide suggests that the zone situated within a distance of 10 m on both sides of the line is considered as a special section. If the acute angle between line and pipeline is larger than 45°, the section can be neglected. If the angle is lower, the section is considered as a parallelism with a horizontal separation of about 6 m. Figure 2.12 explains the previous considerations.

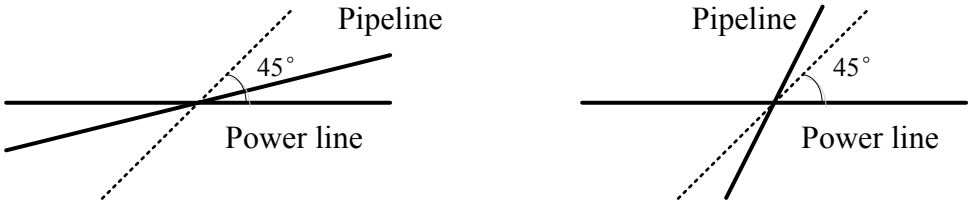

Coupling considered Coupling not considered

Figure 2.12: CIGRE method for pipeline crossing situation [60].

On the other hand, EPRI recommends that the crossing situations can be analyzed by the nodal analysis [59]. That is, for any point along the pipeline section, a Thevenin equivalent circuit is derived for each direction to either side of the point and then combined by a node voltage analysis as shown in Figure 2.13. Evaluation of voltage at a determined point P can be obtained by replacing the left side and the right side by equivalent source voltages V_l, V_r and impedance Z_l, Z_r:

$$V_p = \frac{Z_r V_l - Z_l V_r}{Z_l + Z_r} \tag{2.42}$$

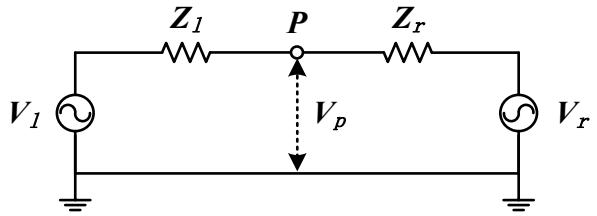

Figure 2.13: The equivalent circuit of the node analysis.

Generally, the pipeline is composed of sections of parallel, crossing and approach with different lengths. The crossing and approach cases can be equivalent to the parallel cases as mentioned before. Therefore, the pipeline becomes multi-section pipeline connected one by one with different circuit parameters for each section.

2.1.5 Equivalent Circuit of Multi-section Pipeline

The EPRI guide also states that the induced voltage calculation method can be further specialized by grouping pipeline sections into electrically long/lossy case, normal case and electrically short case according to electrical length, which allow simplifications of the analysis [59].

A. Electrically Long/Lossy Case

The criterion for an electrically long/lossy pipeline is defined as

$$L > \frac{2}{real(\gamma)} \tag{2.43}$$

Subject to this condition, it can be stated that

$$\left| e^{-\gamma L} \right| << 1 \tag{2.44}$$

Using the inequality (2.44), the general solution can be reduced to obtain the following simple result for the induced voltage on a parallel electrically long/lossy pipeline:

$$V(x) = \frac{E_0}{\gamma}\left[-\frac{Z_A}{Z_A + Z_c} e^{-\gamma x} + \frac{Z_B}{Z_B + Z_c} e^{\gamma (x-L)} \right] \tag{2.45}$$

The terminal values of *V(x)* are given by

$$V(0) = -\frac{E_0}{\gamma}\frac{Z_A}{Z_A + Z_c} \tag{2.46}$$

$$V(L) = \frac{E_0}{\gamma}\frac{Z_B}{Z_B + Z_c} \tag{2.47}$$

V(0) and *V(L)* are seen to be the maximum induced voltages which are independent of pipeline parallel length, assuming that the long/lossy criterion is met. Further, the magnitude of each terminal voltage is fixed by the local terminal impedance and is independent of the remote terminal impedance. The dependence of *V(0)* and *V(L)* upon the values of Z_A and Z_B is modeled by the Thevenin equivalent circuit in Figure 2.14. The Thevenin source impedance Z_θ, is equal to Z_c, the characteristic impedance of the pipeline. The magnitude of the Thevenin voltage source, V_θ, is independent of the pipeline parallel length. V_θ assumes the "-" sign at x=0, and the "+" sign at x=L.

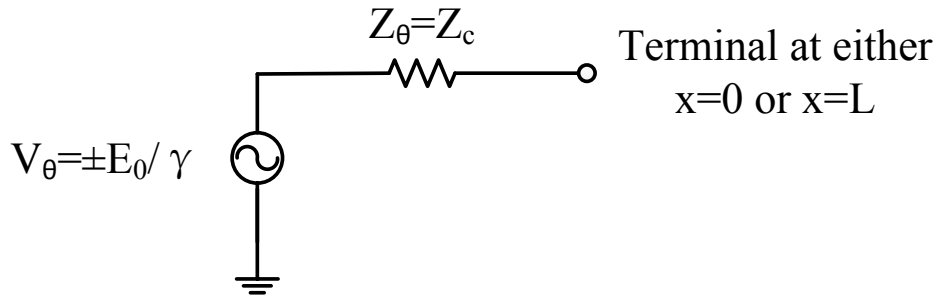

Figure 2.14: Thevenin equivalent circuit for the electrically long/lossy case.

B. Electrically Short Case

For this analysis, the parallel length of an electrically short pipeline satisfies the inequality:

$$L < \frac{0.1}{|\gamma|} \tag{2.48}$$

Normally, this limit of L is 1.3 km for polyethylene coated pipelines and 0.13 km for bituminous coated pipelines. Subject to the inequality (2.48), the first-order-correct approximations

$$e^{\pm\Delta} \approx 1 \pm \Delta \quad for \quad \Delta = \begin{Bmatrix} \gamma L \\ \gamma x \end{Bmatrix} \tag{2.49}$$

can be substituting into the general solution to get the following expression for the induced voltage on a parallel, electrically short pipeline:

$$V(x) = E\left(x - \frac{Z_A}{Z_A + Z_B} L \right) \tag{2.50}$$

From equation (2.50) we can see that induced voltage along the electrically short pipeline is determined only by terminal impedances and location, no impedance z and admittance y of pipeline appearing in equation (2.50). Therefore, the Thevenin equivalent circuit of electrically short pipeline, as shown in Figure 2.15, can be considered as a voltage source with neglect of z and y. The magnitude of the Thevenin voltage source, V_θ, is proportional to the length of the pipeline section.

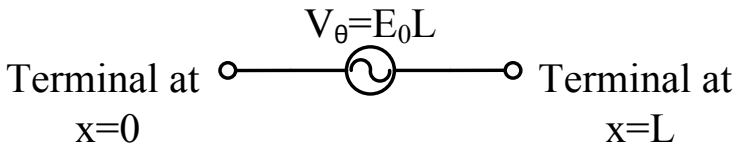

Figure 2.15: Thevenin equivalent circuit for the electrically short case.

C. Normal Case

Under the condition that the parallel length of pipeline section cannot be considered as either electrically short or long/lossy case, this section is represented by the π model shown in Figure 2.16.

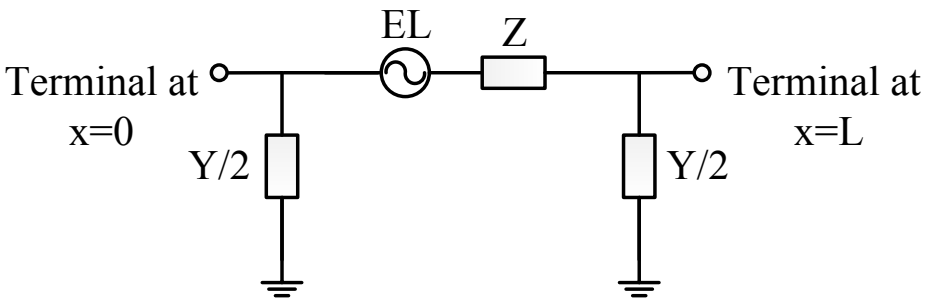

Figure 2.16: The π equivalent circuit for the normal case.

The longitudinal impedance *Z* is the sum of the internal impedance of the pipeline and of the external impedance of the circuit with earth return. The admittance *Y* comprises two terms, the first one corresponds to the stray resistance and the second one to the capacitance between pipeline and earth. The expressions of *Z* and *Y* are shown in the following equations:

$$Z = zL \tag{2.51}$$

$$Y = yL \tag{2.52}$$

where *z* and *y* are impedance and admittance per unit length of the circuit pipeline/earth; *L* is the parallel length of the pipeline section.

D. Equivalent Circuit of Multi-section Pipeline

The zone of influence generally comprises a succession of parallelisms, approaches and crossings of electrically long, short and normal sections such as presented in Figure 2.17. Determination of induced voltages at extremities requires a subdivision of the pipeline in sections with different orientations with respect to an adjacent distribution line. The computation method for the peak induced voltage will be applied based on the equivalent circuit according to the length of each section. Figure 2.18, the circuits between P1 ~P2 and P3 ~ P4 can be treated as cascaded connection of several π circuits with the same z and y, but driven by different EMFs, or converted into parallel sections based on the rules recommended by CIGRE and EPRI.

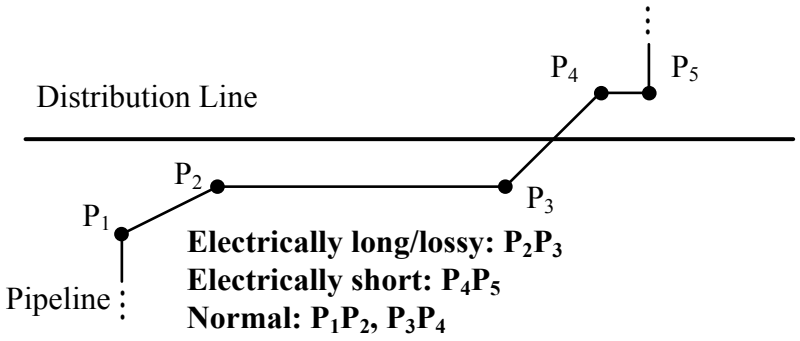

Figure 2.17: Example of multi-section pipeline.

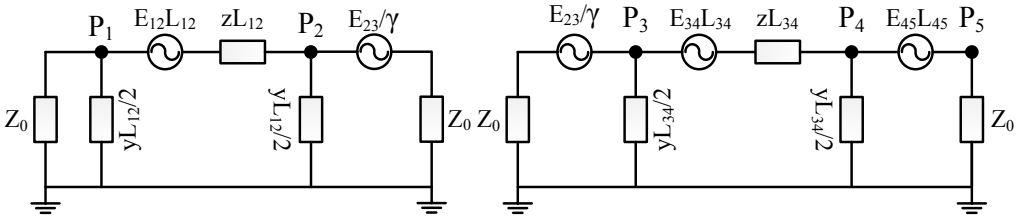

Figure 2.18: Equivalent circuit of the example.

The electrically long/lossy section will spilt the entire pipeline in the zone of influence into two equivalent circuits according to its model discussed above. The electrically short section is modeled as voltage source and the normal sections are modeled as π model. The resolution of the equivalent circuit enables determination of induced voltage at each point P1 ~ P5.

2.2 Calculation Methods for Criteria of Assessing the Effects of Power Line Induction

2.2.1 Pipeline AC Corrosion Criteria

The mechanism of pipeline AC corrosion is still under research and not clearly understood. All the available results are empirical. ISO 15589-1-2003, CSA C22.3 No.6-13 and many other literatures suggest using the equation (2.53) to determine the AC current density incurred by induced voltage [3][4][6][34][35]:

$$J_{ind} = \frac{8V_{ind}}{\pi\rho d} \tag{2.53}$$

where:

J_{ind} = AC current density, A/m^2;

V_{ind} = AC induced voltage, V;

ρ = soil resistivity, Ωm;

d = diameter of holiday, m.

According to equation, decreasing the holiday size increases the AC current density. As concluded in [4], the highest corrosion rates were found on steel samples with a coating holiday in the range of 1 to 3 cm^2. Since the investigation of AC corrosion is beyond the scope of this project, in this thesis, a conservative holiday size of 1 cm^2 is adopted to calculate the AC current density. Given the AC current density (Criterion of AC corrosion), $J_{corrosion}$, and the holiday size of 1 cm^2, limit of AC corrosion voltage can be calculated by equation (2.54):

$$V_{corrosion} = \frac{\pi \rho d J_{corrosion}}{8} \tag{2.54}$$

2.2.2 Personnel Safety Criteria

For personnel safety issue, the danger to human body depends on the magnitude and duration of the current going through. Therefore, the touch voltage limit is determined by the body impedance and admissible current through the body as a function of time.

A. Personnel Safety in Normal Condition

As been reviewed in Section 1.4, the touch voltage limit of 15 V in normal condition is selected as a practical mitigation level that falls within generally accepted guidelines for exposure of the general public to continuous 60Hz rms voltage. This value is selected to limit currents to 10 mA through an assumed hand-to-hand or hand-to-foot resistance of 1500 ohms for an adult male [73]. The 10 mA is the maximum safe let-go current [74].

B. Personnel Safety in Fault Condition

Risks due to faults are limited because of the low incidence of faults and the low probability that somebody will be in contact with the pipeline at the very moment when the danger level is exceeded. The most dangerous consequence of such an exposure is a heart condition known as ventricular fibrillation, resulting in immediate arrest of blood circulation. Due to the occasionality of fault conditions, the current limit for evaluating risks in fault conditions is based on the threshold of ventricular fibrillation other than let-go, which has much higher value than that of let-go [74]. Because the touch voltage that human being can withstand is dependent of exposure duration, there is no certain value recommended by the standards for this criterion.

2.2.3 Pipeline Coating breakdown Criteria

The pipeline coatings can be exposure to extremely large induced voltage acting on the metallic pipeline potentials due to inductive coupling in fault condition. Generally, the pipeline coating breakdown criteria differ with types of coating materials.

As recommended by NACE standard, there are several expected threshold values for different coating materials as shown in Table 2.1.

Table 2.1: Pipeline coating breakdown criteria for different coating materials [4].

Coating Material	Breakdown Criteria [kV]
Bitumen	1 to 1.2
Polyethylene; Fusion-bonded Epoxy	3 to 5

2.3 Summary

In this chapter, the methods of inductive coordination between power line and buried pipeline at fundamental frequency have been reviewed. The main achievements of this chapter are summarized as below:

1. The modelling of electromotive force has been discussed at fundamental frequency. The mutual impedance between the power line and the pipeline is firstly derived from Pollaczek and Carson's formula and then simplified into Carson-Clem formula for practical usage in industry.

2. The modelling of pipeline buried in earth has been reviewed at fundamental frequency. The formulas of self-impedance and self-admittance, recommended by the industrial guides, are based on Sunde's formulas, which are used for wide frequency range without low frequency approximation.

3. The distributed source analysis approach is introduced for the calculation of the induced voltage on the buried pipeline. Three particular parallel cases are firstly analyzed using the induced voltage formula. Thereafter, the approximations of non-parallel cases, recommended by the industrial guides, are reviewed. Finally, the equivalent circuits of multi-section pipeline are documented based on the industrial guides.

4. The calculation methods of pipeline AC corrosion and personnel safety criteria are reviewed. The voltage criterion of pipeline AC corrosion is a function of the soil resistivity, holiday size and AC current density. The touch voltage limit is 15 V for normal condition and absent in fault condition due to the variation of fault duration. The pipeline coating breakdown criteria are also reviewed to fulfill the analysis of potential issues at fundamental frequency.

Chapter 3

Impacts of Harmonic Currents on Pipeline

Chapter 2 has reviewed and investigated the power line and buried pipeline inductive coordination issues at fundamental frequency. Generally, the zero sequence currents play an important role in contributing the EMF. As discussed earlier, the residential loads are significant sources of zero sequence harmonics. Therefore, it is quite essential to assess the severity of inductive coupling between power lines and buried pipelines due to harmonic currents, especially zero sequence harmonics.

The chapter is organized as follows: First, a review of the harmonic current distortions in the power distribution system is presented in Section 3.1. Next, Section 3.2 describes the methods of calculating induced voltage on buried pipeline due to harmonic currents and analyzes the impacts of the harmonic order and its dominant sequence. Based on the findings in Section 3.1 and 3.2, Section 3.3 compares the induced voltages at the fundament and harmonic frequencies in the power distribution system. Section 3.4 discusses the potential pipeline AC corrosion issue caused by the 3^{rd} and 9^{th} harmonic currents, based on the experiment results.

3.1 Harmonic Currents in Power Distribution System

As been reviewed in Section 1.2.1, the substantial increase of nonlinear residential loads, which create harmonic currents resulting from the extensive applications of power electronic-based technologies throughout the system, has become a great concern in recent years. In recent years, with the efforts of the researchers at the University of Alberta, a large volume of field measurements has been collected and analyzed. Therefore, it is possible to provide a whole picture of the harmonic condition in the distribution system. In this section, the observations of harmonic

currents in distribution feeders are analyzed to reveal the harmonic current situations which the pipeline inductive coupling study potentially faces. The detailed measurements are presented in Appendix C.

This section presents the results of the field measurements for 9 residential feeders and 1 mixed-load feeder owned by different utilities [56].

These 10 feeders are numbered as Feeder 1 ~ Feeder 10 in this subsection. Feeder 1 indicates the mixed load feeder. The measurement of Feeder 10 is taken as an example to show the harmonic characteristics of residential feeders. Then the comparison of 10 feeder measurements is provided in this subsection to reveal their behaviour differences.

Figure 3.1, Figure 3.2, and Figure 3.3 present the 24-hour variation pattern of individual harmonic magnitudes, the 24-hour variation pattern of individual harmonic phase angles, and the average and the 95th percentile *IDD* and *TDD*, respectively. The sequence characteristics are demonstrated in Table 3.1. The observation suggests that

- the harmonic magnitudes, except the 3rd one, are almost independent of load and time;
- the phase angles of the most harmonic components, especially the 3rd, 5th, 7th and 9th, are almost time/load independent and concentrated in a very narrow phase-angle range;
- the 3rd harmonic component, IDD_3, is the main contributor to the *TDD*;
- the fundamental and 7th harmonics are dominant in positive sequence. The 3rd and 9th order harmonics are dominant in zero sequence as well as 5th order harmonic is dominant in negative sequence. 11th and 13th order harmonics do not have dominant sequence in this case.

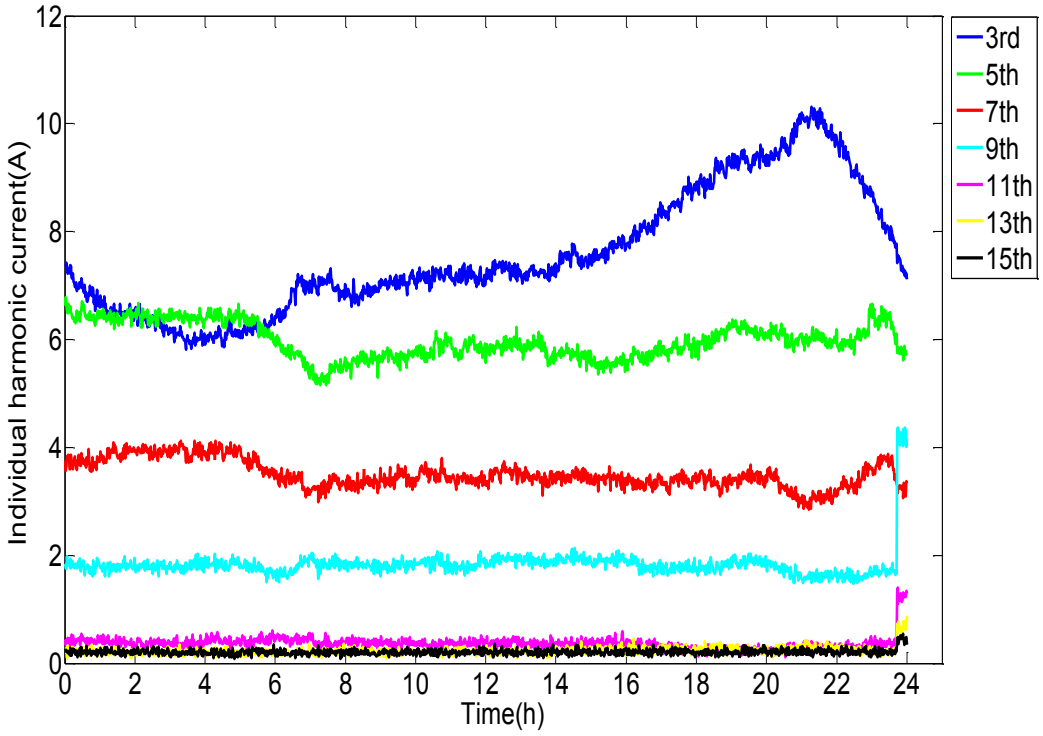

Figure 3.1: Individual harmonic current 24-hour pattern [56].

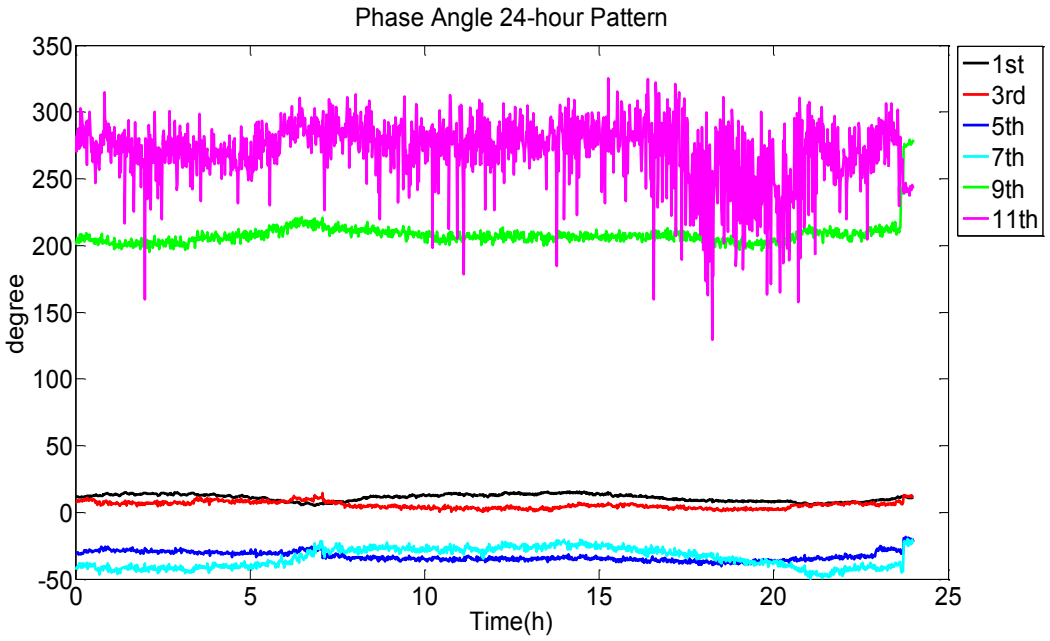

Figure 3.2: Harmonic current phase angle 24-hour pattern [56].

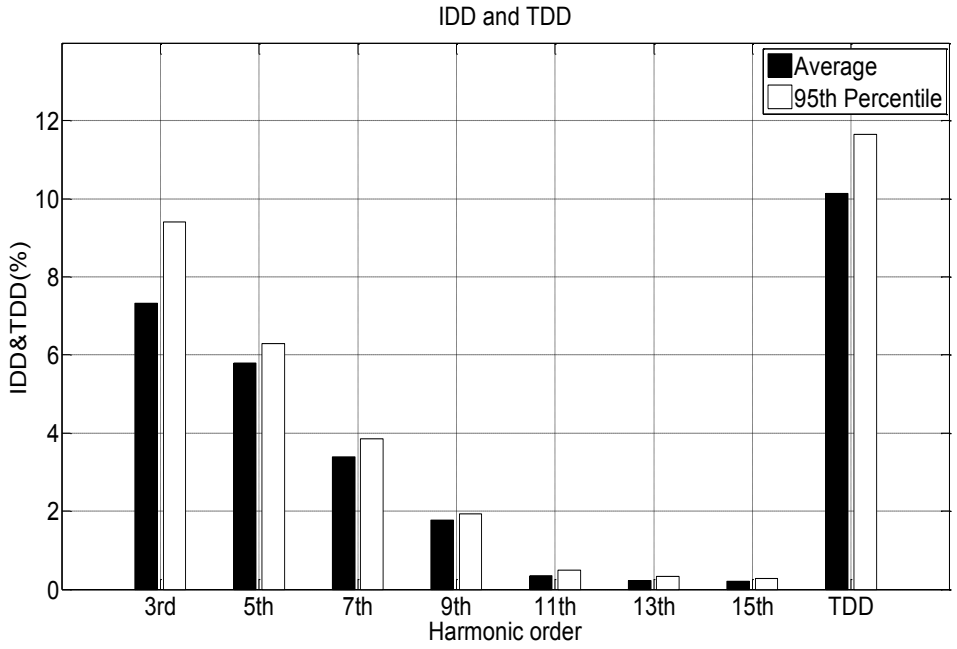

Figure 3.3: Average and the 95th Percentile IDD and TDD [56].

Table 3.1: Sequence characteristics of harmonics [56].

	Sequence Actual Value (A)			Sequence Normalized Value (%)			Dominant Sequence
	Zero	**Positive**	**Negative**	**Zero**	**Positive**	**Negative**	
1st	6.28	59.37	7.96	10.58	100.00	13.41	Positive
3rd	6.22	0.72	0.74	100.00	11.58	11.90	Zero
5th	0.44	0.57	5.01	8.78	11.38	100.00	Negative
7th	0.42	3.22	0.21	13.04	100.00	6.52	Positive
9th	1.81	0.25	0.24	100.00	13.81	13.26	Zero
11th	0.18	0.15	0.33	54.55	45.46	100.00	None
13th	0.17	0.21	0.16	80.95	100.00	76.19	None

The harmonic characteristics of 10 feeders are compared by the 95th percentile *IDD* and *TDD* as presented in Figure 2.4. The average harmonic sequence characteristics of residential feeders (Feeder 2 ~ Feeder 10) are shown in Table 3.2. It can be seen that

- the *IDD* and *TDD* vary in a large range from one feeder to the other;

- the 3rd and 5th harmonics are the main contributors to the *TDD*. For the residential feeders (Feeder 2 ~ Feeder 10), the 3rd harmonic is the most significant one, whereas for the mixed load feeder (Feeder 1), the 5th harmonic is the most significant one;
- the harmonic magnitude decreases with the increase of harmonic order and still follows the exponential trend, except Feeder 1, which supplies mixed loads;
- the residential feeders are of higher harmonic current distortion level than the mixed load feeder.

To provide a more reasonable induced voltage estimation, the following analysis will use the average harmonic current data in Table 3.2.

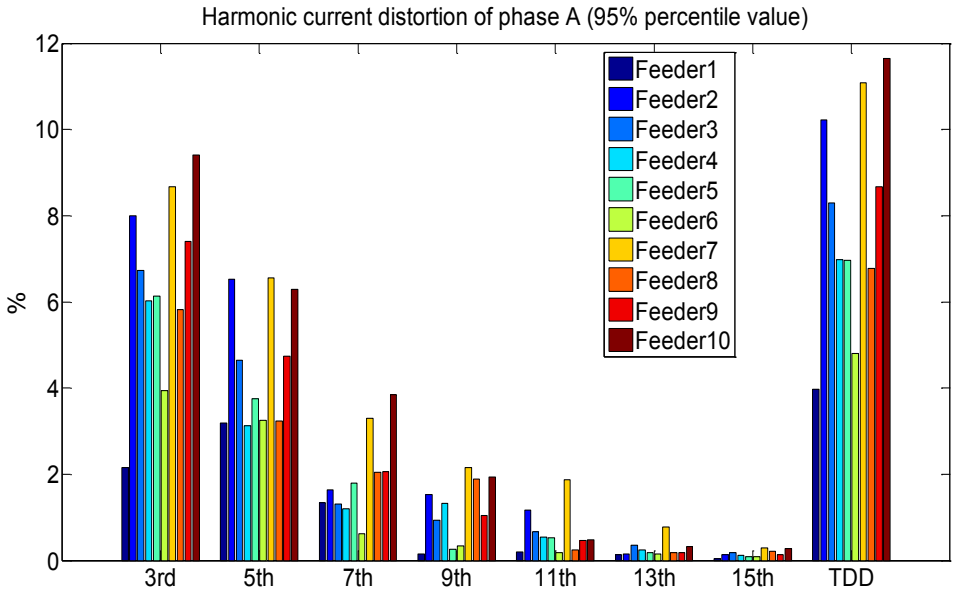

Figure 3.4: Harmonic IDD and TDD of all feeders [56].

Table 3.2: Average harmonic sequence characteristics of residential feeder.

	Sequence Actual Value (A)			Sequence Normalized Value (%)			Dominant Sequence
	Zero	**Positive**	**Negative**	**Zero**	**Positive**	**Negative**	
1st	12.68	291.24	13.57	4.35	100.00	4.66	Positive
3rd	20.45	1.84	1.68	100.00	9.00	8.22	Zero
5th	1.34	1.44	15.28	8.77	9.42	100.00	Negative
7th	0.71	6.56	0.84	10.82	100.00	12.80	Positive
9th	4.68	0.62	0.49	100.00	13.25	10.47	Zero
11th	0.3	0.41	1.96	15.31	20.92	100.00	Negative
13th	0.27	0.85	0.27	31.76	100.00	31.76	Positive
15th	0.49	0.29	0.28	100.00	59.18	57.14	Zero

3.2 Voltage Induced by Harmonic Current on Buried Pipeline

Based on the analytical methods for inductive coupling calculation at the fundamental frequency, this section will first discuss the feasibility of extending the usage of those mutual and self-impedance formulas into the harmonic frequency range. Then, the impacts of harmonic order and dominant sequence on induced voltage will be analyzed by adopting the analytical methods discussed above.

3.2.1 Calculation of Induced Voltage on Buried Pipeline at Harmonic Frequency

As the mechanism of inductive coupling is the same no matter which frequency is worked on, the calculation of the induced voltages appearing on the pipelines is worked out in two steps, determining the total EMF and calculating the induced voltage in response to the total EMF. In this subsection, the calculation methods of both mutual impedance and self-impedance will be verified in the harmonic frequency range and modified if the existing methods are not satisfactory. Finally, the induced voltage can be calculated at harmonic frequency. The typical parameters in industry are shown in Table 3.3 for the further calculations.

Table 3.3: The typical parameters in industry [59][60].

Parameter	Value	Parameter	Value
Pipeline Diameter [m]	0.3	Power Line Height [m]	10
Pipeline Buried Depth [m]	1	Soil Resistivity [Ωm]	100
Horizontal Distance [m]	10	Parallel Length [m]	1000
Coating Type	Polyethylene	Frequency [Hz]	60 ~ 540

3.2.1.1 Mutual Impedance at Harmonic Frequency

The mutual impedance between buried pipeline and power line, provided by Pollaczek, is shown in equation (3.1) [61]:

$$Z_m = \frac{\rho m^2}{2\pi}\int_{-\infty}^{\infty}\frac{\exp\left(-h|\alpha| + h_p\sqrt{\alpha^2+m^2}\right)}{|\alpha|+\sqrt{\alpha^2+m^2}}\exp(j\alpha x)\,d\alpha$$
$$m = \sqrt{\frac{j\omega\mu_0}{\rho}} \tag{3.1}$$

where

$\mu_0 = 4\pi 10^{-7}$ H/m;

$\omega = 2\pi f$;

ρ = soil resistivity (Ωm);

h = height of the overhead conductor (m);

h_p = depth of the buried pipeline (m);

x = horizontal distance between overhead conductor and buried conductor.

However, it has been claimed that this mutual impedance formula, as well as the Carson's formula, cannot be applied to a high frequency region, because the formulas neglect the displacement currents [64]. As suggested by Sunde and Wise [65][71], this problem can be handled by taking the earth permittivity ε_e into consideration:

$$m' = \sqrt{j\omega\mu_0\left[\frac{1}{\rho} + j\omega\left(\varepsilon_e - \varepsilon_0\right)\right]} = \sqrt{j\omega\mu_0\left[\frac{1}{\rho} + j\omega\varepsilon_0\left(\varepsilon_{rs} - 1\right)\right]} \qquad (3.2)$$

where

ε_e: the permittivity of soil;

ε_{rs}: the relative permittivity of soil;

ε_0: the permittivity of free space.

The Carson and Pollaczek formulas are only accurate when the permittivity of soil is the same as it of the air. The relative permittivity of soil is normally from 3 to 30 as shown in Table 3.4 [75].

Table 3.4: The relative permittivity of soil ε_{rs} [75].

Soil Type	Relative Permittivity ε_{rs}
Dry, sandy and flat	10.0
Pastoral hills, rich soil	14.0 ~ 20.0
Pastoral medium hills and forestation	13.0
Fertile land	10.0
Rich agricultural land	15.0
Rocky land, steep hills	10.0 ~ 15.0
Marshy land, densely wooded	12.0
Marshy, forested, flat	12.0
Mountainous/hilly	5.0
Highly moist ground	30.0
City Industrial area of average attenuation	5.0
City industrial area of maximal attenuation	3.0

However, as illustrated by the measurement results, the harmonic frequencies with potential damage magnitudes appear to be lower than 1 kHz. With a conservative estimation of soil resistivity (30 ~ 1000 Ωm), the values of the two terms $1/\rho$ and $\omega\varepsilon_{rs}(\varepsilon_0 - 1)$ are equal to

$$\frac{1}{\rho} = (1 \sim 33) \times 10^{-3} \qquad \omega\varepsilon_0 (\varepsilon_{rs} - 1) = (1 \sim 16) \times 10^{-7}$$
$$\frac{\omega\varepsilon_0 (\varepsilon_{rs} - 1)}{1/\rho} \leq 0.16\% \tag{3.3}$$

As we can see, the term related to the soil resistivity is much large than the permittivity term. Therefore, at interested harmonic frequency range, it is reasonable to neglect the displacement current term in the mutual impedance formula.

Furthermore, the mutual impedance between overhead and underground conductors in multilayered soils is derived and verified with the electromagnetic field equation with the frequency from 50 Hz to 1 MHz using finite-element method (FEM) software [76]. The differences in magnitude of mutual impedance between the analytical method and FEM simulation are shown in Figure 3.5 [77]. As explained in [77], the formula of the analytical method is equivalent to Carson's formula with the assumption that the electromagnetic properties of all earth layers are equal. Therefore, it is reasonable to claim that Carson's formula is valid to use for the mutual impedance in harmonic study.

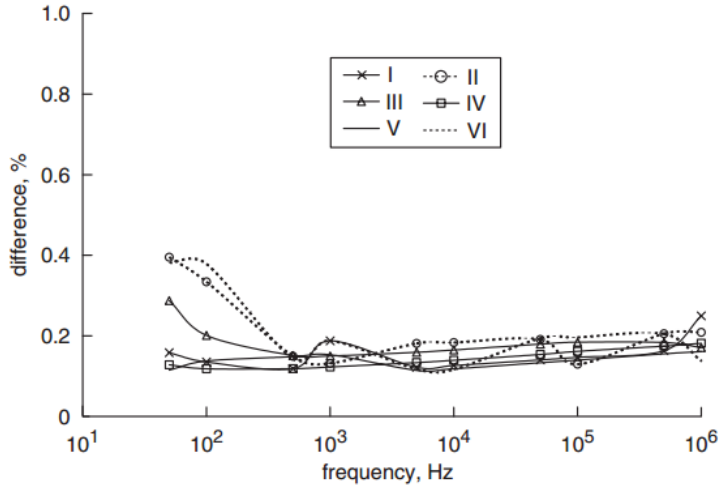

Figure 3.5: Differences in magnitude of mutual impedance between analytical method and FEM simulation (legends "I, II, III, IV, V, VI" represent 6 different cases of soil conditions respectively) [77].

The requirement of computational support restricts the usage of Carson's formula. The Carson-Clem equation is developed to simplify the calculation with the assumptions that the terms considered from the Carson series expressions are only the first term of the real part and two terms from the imaginary part, as shown in equation (3.4) [37][59][60]:

$$Z_m = \frac{\omega\mu_0}{8} + \frac{j\mu_0\omega}{2\pi}\left[\ln\left(\frac{2}{gd\sqrt{\frac{\omega\mu_0}{\rho}}}\right) + \frac{1}{2}\right] \tag{3.4}$$

where

$\mu_0 = 4\pi 10^{-7}$ H/m;

$\omega = 2\pi f$;

d = geometrical distance between conductors (m);

g = 1.7811 Euler's constant;

ρ = soil resistivity (Ωm).

In practical terms, the Carson-Clem formula can be applied to those cases where the value of the geometrical distance yields the limit according to the soil resistivity and frequency as following [60]:

$$d < 90\sqrt{\frac{2\pi\rho}{\omega}} \tag{3.5}$$

For harmonic study, this inequality will limit the range of geometrical distance and soil resistivity which are influenced by the frequency. For the purpose of harmonic study in abundant geometric distance and soil resistivity ranges, the

Carson series expression is analyzed to select enough terms to meet this requirement with acceptable error.

As described in [62], the Carson formula can be extended in equation (3.6):

$$Z_{m\_Carson} = \frac{\mu_0\omega}{\pi}\int_0^{\infty}\left(\sqrt{\alpha^2 + j} - \alpha\right)e^{\left(-(h-h_p)\sqrt{\frac{\mu_0\omega}{\rho}}\alpha\right)}\cos\left(\sqrt{\frac{\mu_0\omega}{\rho}}\alpha x\right)d\alpha = \frac{\mu_0\omega}{\pi}(P + jQ)$$

$$P = \frac{\pi}{8} - r\frac{\cos\theta}{3\sqrt{2}} + r^2\frac{\left[0.6728 + \log\left(\frac{2}{r}\right)\right]\cos 2\theta + \theta\sin 2\theta}{16} + r^3\frac{\cos(3\theta)}{45\sqrt{2}} - r^4\frac{\pi\cos(4\theta)}{1536}\ldots$$

$$Q = \frac{1}{4} + \frac{1}{2}\log\left(\frac{2}{1.7811r}\right) + r\frac{\cos\theta}{3\sqrt{2}} - r^2\frac{\pi\cos 2\theta}{64} + r^3\frac{\cos 3\theta}{45\sqrt{2}} - \frac{\left[1.0895 + \log\left(\frac{2}{r}\right)\right]\cos 4\theta + \sin 4\theta}{384}\ldots \quad (3.6)$$

$$r = \sqrt{\frac{\mu_0\omega}{\rho}} \times \sqrt{(h - h\_p)^2 + x^2} \quad (3.7)$$

$$\theta = \frac{x}{h - h\_p} \quad (3.8)$$

where

x = horizontal distance between overhead conductor and buried pipeline;

h = height of overhead conductor;

h_p = pipeline buried depth.

The mutual impedance is a function of frequency, soil resistivity and separation distance:

- Frequency: 60 ~ 540 Hz;
- Soil Resistivity: 30 ~ 200 Ωm;
- Separation Distance: 0 ~ 100 m.

Studies have been conducted to show the effect of each parameter on the error of simplified expressions (listed in Table 3.5) compared with Caron's formula. The error is defined as follows:

$$error = \frac{Z_{m\_simplified} - Z_{m\_Carson}}{Z_{m\_Carson}} \times 100\% \tag{3.9}$$

The base parameters used in this study are those shown in Table 3.3. The results are shown in Figure 3.6 to Figure 3.8. Based on the simulation results, the following conclusions can be drawn:

- the error of mutual impedance increases with higher frequency;
- the error of mutual impedance decreases with higher soil resistivity;
- the error of mutual impedance increases with higher separation distance;
- the error of mutual impedance can be controlled within 5% using Equation 3, 4, 5 under the extreme condition: 540Hz, 30 Ωm and 100 m.

Table 3.5: Real and imaginary parts of simplified equations.

	Real Part
Equation 1	$P_1 = \frac{\pi}{8}$
Equation 2	$P_2 = \frac{\pi}{8} - r\frac{\cos\theta}{3\sqrt{2}}$
Equation 3	$P_3 = \frac{\pi}{8} - r\frac{\cos\theta}{3\sqrt{2}} + r^2\frac{\left[0.6728 + \log\left(\frac{2}{r}\right)\right]\cos 2\theta + \theta\sin 2\theta}{16}$
Equation 4	$P_4 = P_3 + r^3\frac{\cos(3\theta)}{45\sqrt{2}}$
Equation 5	$P_5 = P_4 - r^4\frac{\pi\cos(4\theta)}{1536}$
	Imaginary Part
Equation 1	$Q_1 = \frac{1}{4} + \frac{1}{2}\log\left(\frac{2}{1.7811r}\right)$

Equation 2	$Q_2 = \frac{1}{4} + \frac{1}{2}\log\left(\frac{2}{1.7811r}\right) + r\frac{\cos\theta}{3\sqrt{2}}$
Equation 3	$Q_3 = Q_2 - r^2\frac{\pi\cos 2\theta}{64}$
Equation 4	$Q_4 = Q_3 + r^3\frac{\cos 3\theta}{45\sqrt{2}}$
Equation 5	$Q_5 = Q_4 - \frac{\left[1.0895 + \log\left(\frac{2}{r}\right)\right]\cos 4\theta + \sin 4\theta}{384}$

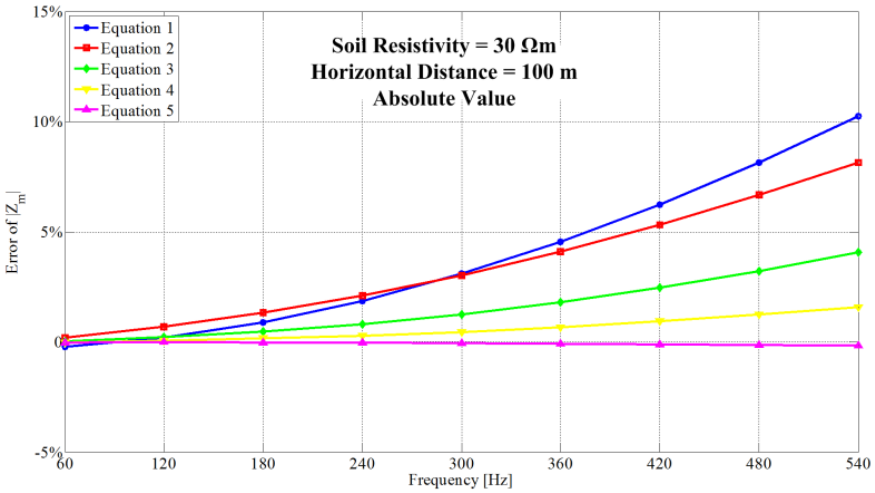

(a) Error of mutual impedance absolute value

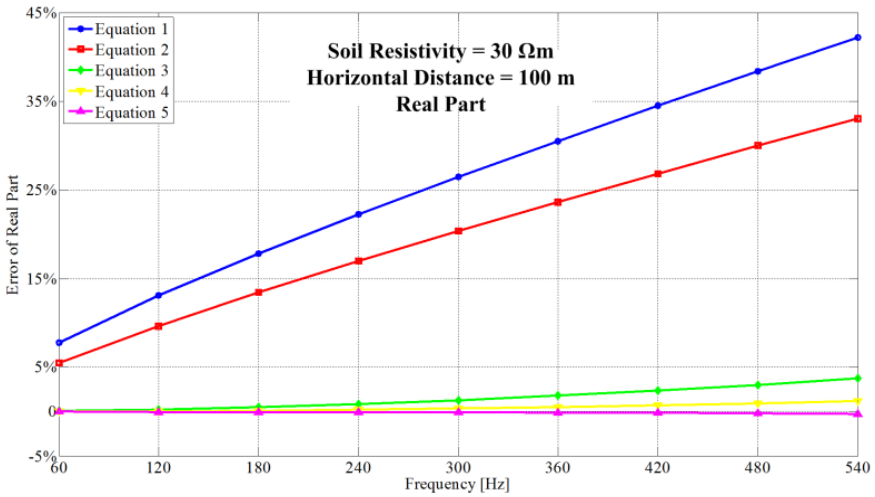

(b) Error of mutual impedance real part

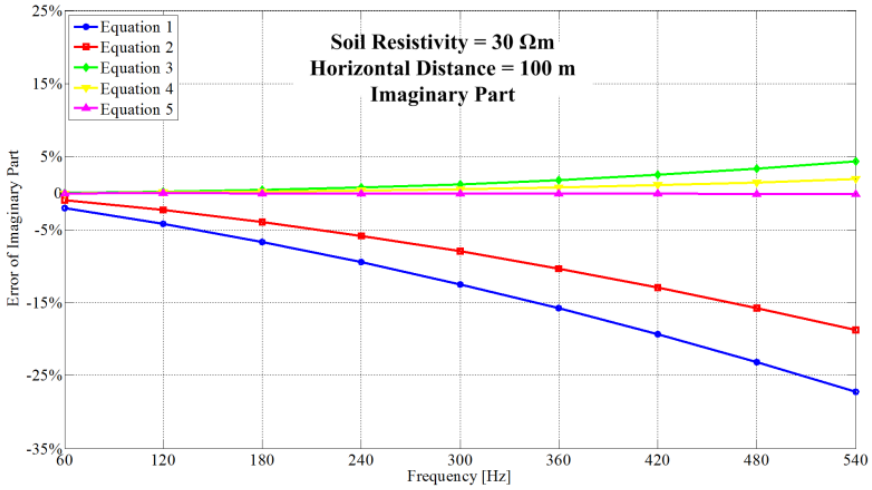

(c) Error of mutual impedance imaginary part

Figure 3.6: Error of mutual impedance due to frequency.

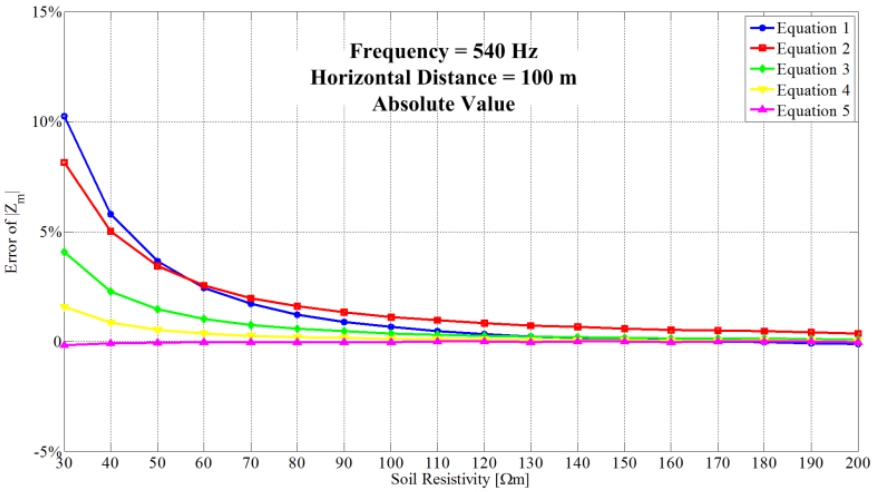

(a) Error of mutual impedance absolute value

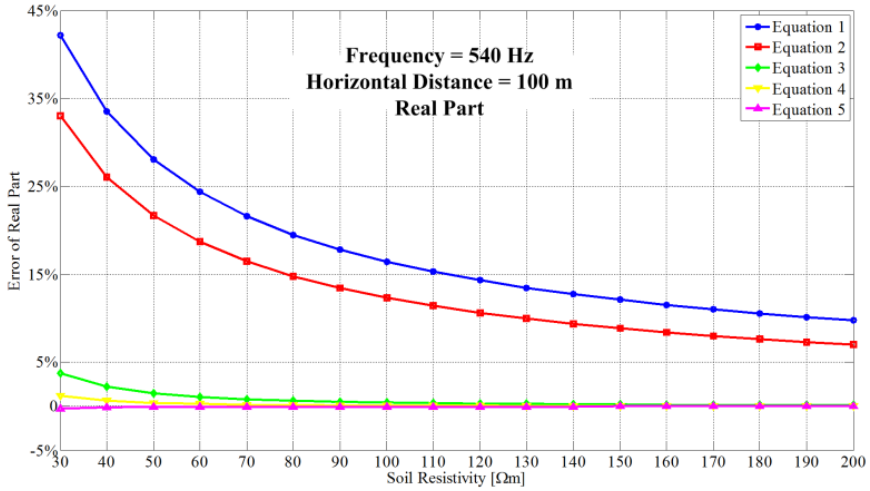

(b) Error of mutual impedance real part

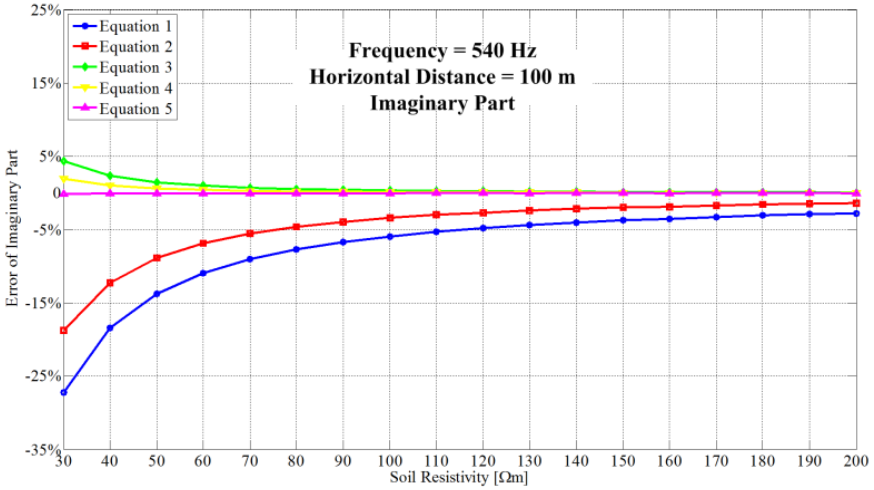

(c) Error of mutual impedance imaginary part

Figure 3.7: Error of mutual impedance due to soil resistivity.

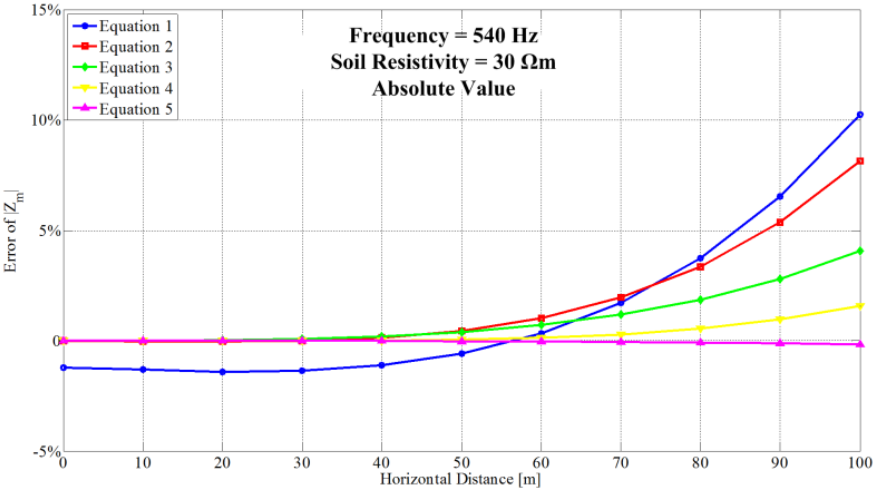

(a) Error of mutual impedance absolute value

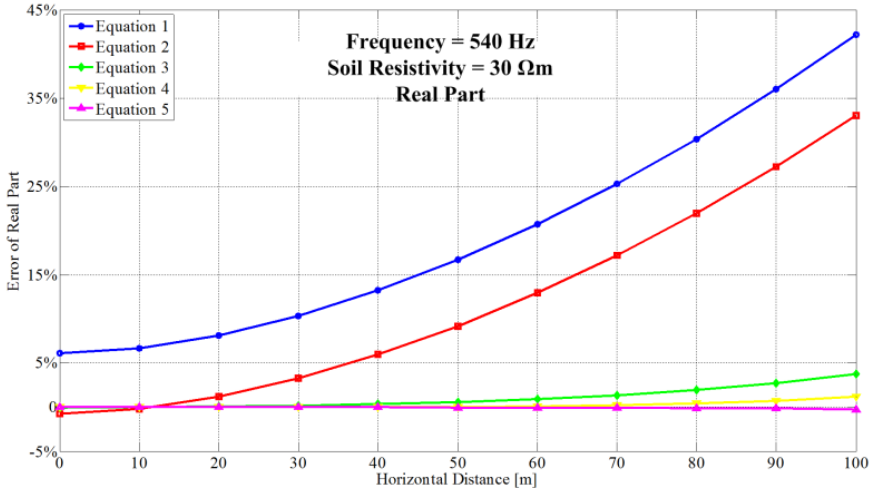

(b) Error of mutual impedance real part

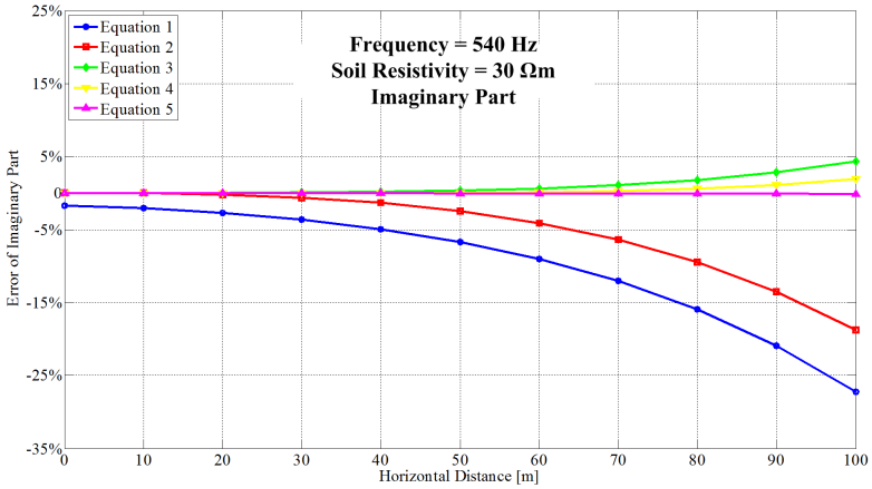

(c) Error of mutual impedance imaginary part

Figure 3.8: Error of mutual impedance due to horizontal distance.

Based on the above analysis, the proposed equations for the mutual impedance calculation are as follows:

$$Z_{m\_proposed} = \frac{\mu_0 \omega}{\pi}\left(P_3 + jQ_3\right) \tag{3.10}$$

$$P_3 = \frac{\pi}{8} - r\frac{\cos\theta}{3\sqrt{2}} + r^2\frac{\left[0.6728 + \log\left(\frac{2}{r}\right)\right]\cos 2\theta + \theta\sin 2\theta}{16} \tag{3.11}$$

$$Q_3 = \frac{1}{4} + \frac{1}{2}\log\left(\frac{2}{1.7811r}\right) + r\frac{\cos\theta}{3\sqrt{2}} - r^2\frac{\pi\cos 2\theta}{64} \tag{3.12}$$

where r and θ can be calculated based equation (3.7) and (3.8) respectively.

3.2.1.2 Comparison of Mutual Impedance Calculation between Proposed Method and Frequency Scaling Method

It is a common practice that the mutual impedance at harmonic frequency can be estimated by the frequency scaling equation:

$$Z_{mutual}(h) = R_{mutual\_60} + jX_{mutual\_60} \times h \tag{3.13}$$

where R_{mutual_60} and X_{mutual_60} are the real and imaginary parts of mutual impedance calculated at 60 Hz.

The comparison between the proposed equation and the frequency scaling equation is shown in Figure 3.9. Compared with the proposed equation, the frequency scaling equation will overestimate the imaginary part of mutual impedance and under estimate the real part of the mutual impedance. On the other hand, the real part of the mutual impedance, calculated by the proposed equation, increases with a higher frequency. As a result, the proposed equation should be used to calculate the mutual impedance at harmonic frequencies.

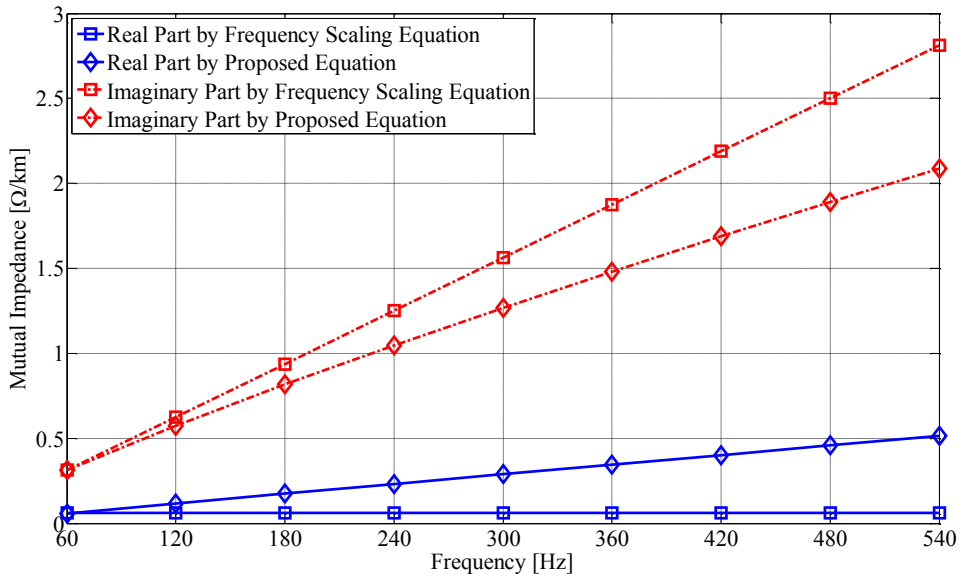

Figure 3.9: The comparison between the proposed equation and the frequency scaling equation.

3.2.1.3 Summary of the Mutual Impedance Calculation Method

In summary, a mutual impedance calculation method is proposed based on the Carson series expression to support the harmonic calculation in abundant geometric distance and soil resistivity ranges. The proposed method is summarized as follows:

$$Z_{m\_proposed} = \frac{\mu_0 \omega}{\pi}(P + jQ) \tag{3.14}$$

$$P = \frac{\pi}{8} - r\frac{\cos\theta}{3\sqrt{2}} + r^2\frac{\left[0.6728 + \log\left(\frac{2}{r}\right)\right]\cos 2\theta + \theta\sin 2\theta}{16} \tag{3.15}$$

$$Q = \frac{1}{4} + \frac{1}{2}\log\left(\frac{2}{1.7811r}\right) + r\frac{\cos\theta}{3\sqrt{2}} - r^2\frac{\pi\cos 2\theta}{64} \tag{3.16}$$

$$r = \sqrt{\frac{\mu_0\omega}{\rho}} \times \sqrt{(h - h\_p)^2 + x^2} \tag{3.17}$$

$$\theta = \frac{x}{h - h\_p} \tag{3.18}$$

where

$\mu_0 = 4\pi 10^{-7}$ H/m magnetic permeability of the air;

$\omega = 2\pi f$;

ρ = soil resistivity (Ωm);

h = height of the overhead conductor (m);

h_p = depth of the buried pipeline (m);

x = horizontal distance between overhead conductor and buried conductor.

3.2.1.4 Self-Impedance and Self-Admittance of Buried Pipeline at Harmonic Frequency

The expressions of pipeline self-impedance and admittance is based on Sunde's formula [71] as shown in equation (3.19) and equation (3.20), respectively, which are used for wide frequency range without low frequency approximation.

$$z(\gamma) = z_i + \frac{j\omega\mu_0}{\pi\alpha' m'^2}\left[\gamma K_1(\alpha'\gamma) - \sqrt{m'^2+\gamma^2}\,K_1\left(\alpha'\sqrt{m'^2+\gamma^2}\right)\right]$$
$$\cong z_i + j\frac{\omega\mu_0}{2\pi}\ln\frac{1.85}{\alpha'\sqrt{m'^2+\gamma^2}} \tag{3.19}$$
$$= z_i + j\frac{\omega\mu_0}{2\pi}\ln\frac{1.85}{\alpha'\sqrt{j\omega\mu_0\left(\frac{1}{\rho}+j\omega\varepsilon\right)+\gamma^2}}$$

$$y(\gamma) = \frac{1}{\pi\left(\frac{1}{\rho}+j\omega\varepsilon\right)}K_0(a'\gamma) \cong \left(y_i^{-1} + \frac{\ln\frac{1.12}{a'\gamma}}{\pi\left(\frac{1}{\rho}+j\omega\varepsilon\right)}\right)^{-1} \tag{3.20}$$

where

$$m'^2 = j\omega\mu_0\left(\frac{1}{\rho}+j\omega\varepsilon\right);$$

K_0 and K_1 are Bessel functions;

z_i and y_i are internal impedance and admittance respectively.

The equation for the propagation constant then becomes

$$\gamma^2\left(y_i^{-1} + \frac{\ln\frac{1.12}{a'\gamma}}{\pi\left(\frac{1}{\rho}+j\omega\varepsilon\right)}\right) = z_i + j\frac{\omega\mu_0}{2\pi}\ln\frac{1.85}{\alpha'\sqrt{\gamma^2+m'^2}} \tag{3.21}$$

Sunde claims that the approximations used in equation (3.19) and equation (3.20) are valid as long as a′γ and a′$\sqrt{m'^2+\gamma^2}$ are less than 0.01. Based on the typical parameters in the industry, the values of a′$\sqrt{m'^2+\gamma^2}$ related to the harmonic order and soil resistivity are shown in Table 3.6. As we can see, only at 7th and 9th harmonic order in very good soil condition, the factors will exceed the limit for

the approximation. Normally, the soil resistivity is selected to be 100 Ωm. Therefore, this approximation for harmonic analysis is acceptable.

Table 3.6: Values of term $a'\sqrt{m'^2+\gamma'^2}$ (the limit is 0.01).

Soil Resistivity [Ωm]	Harmonic Order				
	1st	3rd	5th	7th	9th
30	0.004	0.007	0.009	0.011	0.012
50	0.003	0.005	0.007	0.008	0.009
100	0.002	0.004	0.005	0.006	0.007

On the other hand, the self-impedance of underground conductors in a two-layer earth case has been discussed and verified with the electromagnetic field equation from 50 Hz to 1 MHz using FEM software [76]. The differences in magnitude of self-impedance between analytical method and FEM simulation are shown in Figure 3.10. As explained in [78], the formula of the analytical method is derived by a rigorous and general solution of the EM field equations, using a methodology based on Sunde's approach. The formula of self-impedance in the homogeneous earth case, can be reproduced simply by equalizing the electromagnetic properties of all earth layers [78]. As a result, the adopted method for self-impedance calculation can be used in harmonic study.

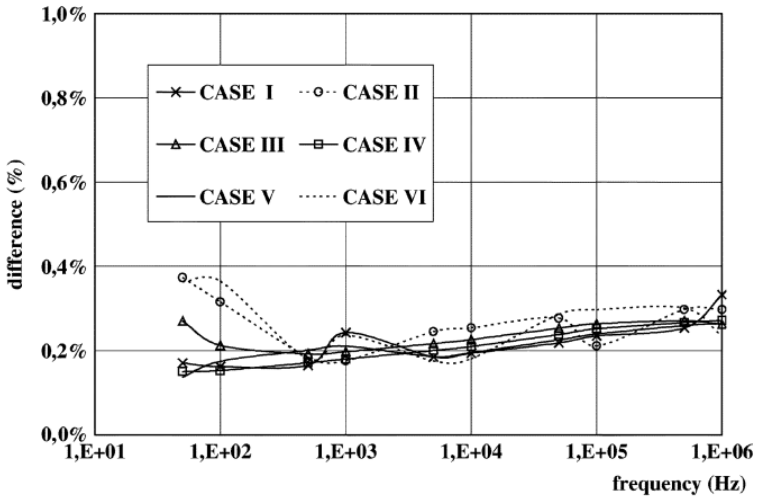

Figure 3.10: Differences in magnitude of self-impedance between analytical method and FEM simulation (legends "Case I, II, III, IV, V, VI" represent 6 different cases of soil conditions respectively) [78].

3.2.1.5 Comparison of Self-Impedance and Self-Admittance Calculation between Sunde's Method and Frequency Scaling Method

Similarly to the mutual impedance, the self-impedance and self-admittance at harmonic frequency can be estimated by the frequency scaling equations:

$$Z_{self}(h) = R_{self\_60} + jX_{self\_60} * h \tag{3.22}$$

$$Y_{self}(h) = G_{self\_60} + jB_{self\_60} * h \tag{3.23}$$

where R_{self_60} and X_{self_60} are the real and imaginary parts of self-impedance calculated at 60 Hz; G_{self_60} and B_{self_60} are the real and imaginary parts of self-admittance calculated at 60 Hz.

Figure 3.11 shows the comparison of self-impedance between Sunde's equation and the frequency scaling equation. Compared with Sunde's equation, the frequency scaling equation will overestimate the imaginary part of the self-impedance and under estimate the real part of the self-impedance. On the other hand, Figure 3.12 shows the comparison of self-admittance between Sunde's equation and the frequency scaling equation. The results show that Sunde's

equation and the frequency scaling equation have the same estimation of self-admittance. As a result, the calculation of self-impedance at harmonic frequencies should use Sunde's equation, but the self-admittance can be estimated based on both equations.

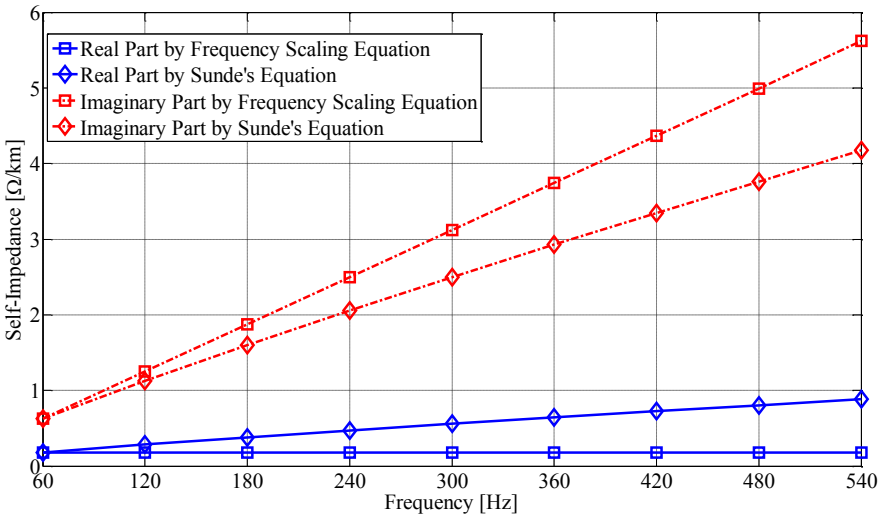

Figure 3.11: The relationship between self-impedance and frequency.

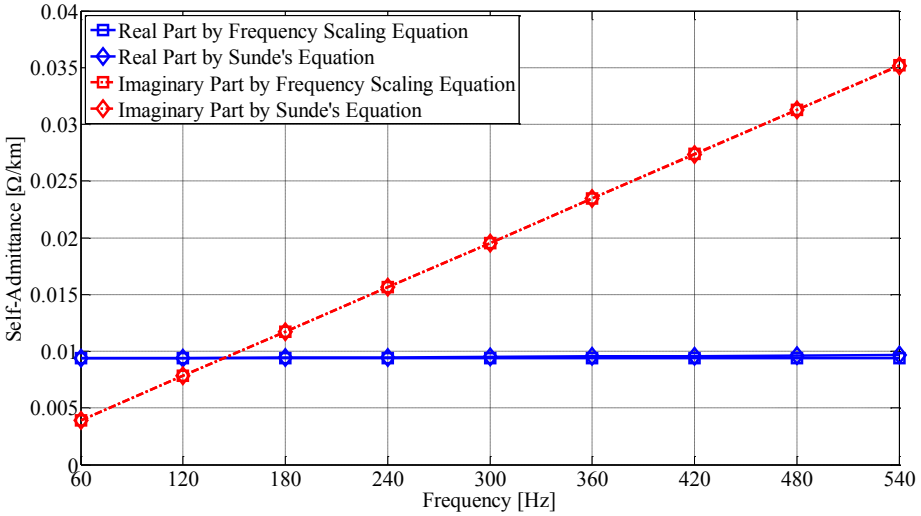

Figure 3.12: The relationship between self-admittance and frequency.

3.2.1.6 Summary of the Self-Impedance and Self-Admittance Calculation Methods

In summary, the calculation of self-impedance and self-admittance calculation at each harmonic frequency is based on the Sunde's equations as follows:

$$z = z_i + j\frac{\omega\mu_0}{2\pi}\ln\frac{1.85}{\alpha'\sqrt{\gamma^2 + j\omega\mu_0\left(\frac{1}{\rho} + j\omega\varepsilon\right)}} \tag{3.24}$$

$$z_i = \frac{\sqrt{\omega\mu_r\mu_0\rho_p}}{\sqrt{2}\pi D}\left[\frac{\sinh(t_n)+\sin(t_n)}{\cosh(t_n)-\cos(t_n)} + j\frac{\sinh(t_n)+\sin(t_n)}{\cosh(t_n)-\cos(t_n)}\right] \tag{3.25}$$

$$y^{-1} = y_i^{-1} + \frac{\ln\left(\frac{1.12}{a'\gamma}\right)}{\pi\left(\frac{1}{\rho} + j\omega\varepsilon\right)} \tag{3.26}$$

$$y_i = \frac{\pi D}{r_c} + j\omega\frac{\varepsilon_0\varepsilon_r\pi D}{\delta_c} \tag{3.27}$$

where

$\mu_0 = 4\pi 10^{-7}$ H/m magnetic permeability of the air;

$\mu_r = 300$ relative permeability of the pipeline;

$\rho_p = 1.7*10^{-7}$ Ωm resistivity of pipeline;

$\varepsilon_0 = 8.85*10^{-12}$ F/m electrical permittivity of the air;

$\varepsilon_r = 5$ relative electrical permittivity of the pipeline coating;

$\varepsilon = 3*\varepsilon_0$ electrical permittivity of the soil;

$r_c = 1*10^5$ Ωm^2 polyethylene coating resistance ($1*10^3$ Ωm^2 bituminous coating resistance);

$D = 0.6$ m diameter of the pipeline;

$a = 0.3$ m radius of the pipeline;

a' = equivalent radius of burial pipeline (m) $\alpha' = \sqrt{\alpha^2 + 4h_p'^2}$;

$h_p' = 1$ m depth of buried pipeline;

$\delta_c = 0.004$ m thickness of the coating;

t_n = pipeline wall thickness (m) $t_n = 0.0157\dfrac{\sqrt{2\omega\mu_r\mu_0\rho_p}}{\rho_p}D^{0.421}$;

γ = propagation constant of the circuit pipeline/earth (m^{-1}) $\gamma = \sqrt{zy}$.

3.2.1.7 Calculation of Induced Voltage at Harmonic Frequency

Based on the above conclusions, the induced voltage can be calculated at harmonic frequency. The method for the up-coming harmonic study is demonstrated for the simple theoretical case of parallelism based on the following assumptions:

- the pipeline is parallel to the distribution line and extends for a few kilometers beyond the parallel routing without grounding;
- the coating resistance per unit length of the pipeline is uniform and independent of the applied voltage;
- the soil resistivity along the parallel route is constant.

On basis of the above assumptions, the equation of the induced voltage is:

$$V(x) = -\frac{E}{2\gamma}\left(e^{-\gamma(L-x)} - e^{-\gamma x}\right) \tag{3.28}$$

The induced voltages at terminals of the parallel section are as in equation (3.29)

$$\left|V(0)\right| = \left|V(L)\right| = \frac{E}{2\gamma}\left(1 - e^{-\gamma L}\right) \tag{3.29}$$

where

γ = propagation constant;

L = total parallel length;

E = EMF induced on the pipeline per unit length.

The typical parameters of pipeline at fundamental and harmonic frequencies, such as self-impedance, self-admittance, propagation constant, effective length and etc., are shown in Appendix B.

3.2.2 Impacts of Harmonic Order and Dominant Sequence on Induced Voltage

Based on the method discussed early in this section, one can analyze the impact of harmonic order and dominant sequence on induced voltage.

Figure 3.13 shows a typical inductive coordination case between the distribution line and buried pipeline [79].

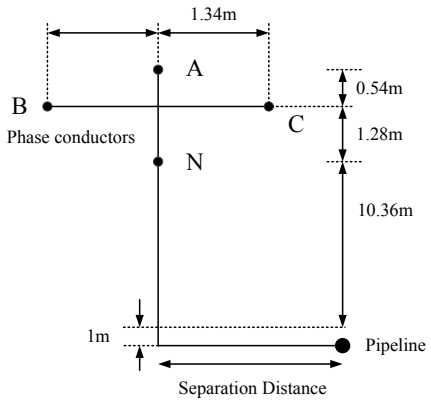

Figure 3.13: Typical inductive coordination case.

The total induced voltage at the end of parallel section can be expressed by the inductive coupling of phase A, B, and C currents, as in equation (3.30):

$$V = \frac{Z_{ma}I_a + Z_{mb}I_b + Z_{mc}I_c}{2\gamma}\left(1 - e^{-\gamma L}\right) \tag{3.30}$$

Considering the current sequence impact, the equation (3.30) will be spread as equation (3.31), equation (3.32) and equation (3.33) for positive, negative and zero sequence, respectively.

$$V_{positive} = \frac{Z_{ma} I_{positive} + \alpha^2 Z_{mb} I_{positive} + \alpha Z_{mc} I_{positive}}{2\gamma}\left(1 - e^{-\gamma L}\right)$$
$$\frac{V_{positive}}{I_{positive}} = \frac{Z_{ma} + \alpha^2 Z_{mb} + \alpha Z_{mc}}{2\gamma}\left(1 - e^{-\gamma L}\right) \quad (3.31)$$

$$V_{negative} = \frac{Z_{ma} I_{negative} + \alpha Z_{mb} I_{negative} + \alpha^2 Z_{mc} I_{negative}}{2\gamma}\left(1 - e^{-\gamma L}\right)$$
$$\frac{V_{negative}}{I_{negative}} = \frac{Z_{ma} + \alpha Z_{mb} + \alpha^2 Z_{mc}}{2\gamma}\left(1 - e^{-\gamma L}\right) \quad (3.32)$$

$$V_{zero} = \frac{Z_{ma} I_{zero} + Z_{mb} I_{zero} + Z_{mc} I_{zero}}{2\gamma}\left(1 - e^{-\gamma L}\right)$$
$$\frac{V_{zero}}{I_{zero}} = \frac{Z_{ma} + Z_{mb} + Z_{mc}}{2\gamma}\left(1 - e^{-\gamma L}\right) \quad (3.33)$$

Equations (3.21), (3.22), and (3.23) present the influences of mutual impedance and propagation constant on the per-unit-current induced voltage in different sequences, which can be used to analyze the impact of harmonic order and dominant sequence on the induced voltage. The comparisons of the induced voltage per-unit-current at different harmonic orders in positive, negative and zero sequences are shown in Figure 3.14, based on the typical parameters used in industry as listed in Table 3.3. The neutral conductor is neglected in this analysis. It can be concluded that:

- the induced voltage per unit current increases with high harmonic order;
- the voltage induced by zero sequence currents is much larger than those in positive and negative sequences.

The reason for the first conclusion is that the mutual impedance has positive correlation with harmonic order and the term $(1 - e^{\gamma L})/\gamma$ decreases very slowly when γ is small. The add-up effect is to increase the induced voltage. For the second conclusion, the reason can be easily achieved from the three equations illustrated above that the voltages induced by positive or negative currents in three phase conductors almost cancel each other because of the similarity of their

mutual impedances with the buried pipeline. Therefore, the zero-sequence dominant harmonics, such as the 3rd and 9th order harmonics, are essential to the induced voltage on buried pipeline.

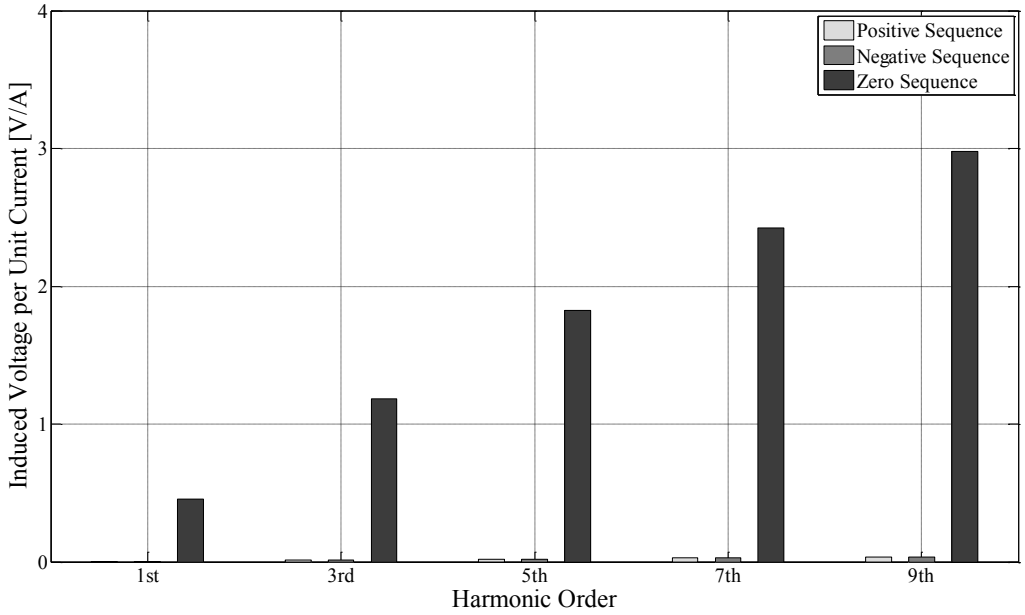

Figure 3.14: Impact of harmonic order in different sequences.

Table 3.7 shows the induced voltages of different sequences at each harmonic frequency calculated by the realistic data from Table 3.2 based on the typical parameters. It is obvious to see that the induced voltage in zero sequence is much larger than those in positive and negative sequence at any harmonic frequency. The positive-sequence induced voltage is 20.77% of the zero-sequence induced voltage at the fundamental frequency. The actual value of the positive-sequence induced voltage at the fundamental frequency is comparable with zero-sequence induced voltages, such as the 5th and 7th order harmonics. For the 5th and 7th order harmonics, the voltages induced by their dominant sequence currents are only 12.50% and 10.83% of their own zero-sequence induced voltages, respectively. Moreover, the actual values of the dominant-sequence induced voltages at the 5th and 7th order harmonics are much smaller than the zero-sequence induced voltages at other harmonic frequencies. Therefore, for the following induced voltage analysis, the positive sequence current at fundamental frequency is still considered. On the other hand, the positive and negative sequence currents at each

harmonic frequency, as well as the negative sequence current at fundamental frequency, are neglected.

Table 3.7: Induced Voltages of different sequences at each frequency based on realistic current data.

Harmonic Order	Induced Voltage [V]			Normalized Value		
	Zero Sequence	Positive Sequence	Negative Sequence	Zero Sequence	Positive Sequence	Negative Sequence
1st	5.78	1.20	0.06	100%	20.77%	0.96%
3rd	24.17	0.02	0.02	100%	0.09%	0.08%
5th	2.45	0.03	0.31	100%	1.20%	12.50%
7th	1.72	0.19	0.02	100%	10.83%	1.36%
9th	13.94	0.02	0.02	100%	0.16%	0.12%

3.3 Comparison between Fundamental and Harmonic Impacts on Pipeline

In this section, the impacts on buried pipeline will be compared between fundamental and harmonic currents based on the data of residential feeders in distribution systems. First, the induced voltage at the fundamental frequency is analyzed. Based on the field data provided from Section 3.1, the induced voltages of fundamental and harmonic frequencies are compared.

3.3.1 Voltage Induced by Fundamental Current

The induced voltage at the terminal of the parallel section is calculated in the following equation (3.34):

$$V = \frac{\left(Z_{ma}I_a + Z_{mb}I_b + Z_{mc}I_c\right)}{2\gamma}\left(1 - e^{-\gamma L}\right) \tag{3.34}$$

where Z_{ma}, Z_{mb}, Z_{mc} and γ are defined at fundamental frequency.

The fundamental phase current I_a, I_b and I_c contain positive, negative and zero sequence components. As analyzed in Section 3.2, the positive and negative

sequence currents have limited impact on the induced voltage per unit current. Based on the magnitude scales of each component at the fundamental frequency, the positive sequence component still needs to be considered, but the negative sequence component is neglected.

Summarized from Table 3.2, the average positive sequence component of fundamental current is 291.24∠0° A and the average zero sequence component is 12.68∠-7.7° A, respectively. The phase angle difference between positive component and zero sequence component currents is obtained by averaging the phase angle difference between those sequence currents of each residential feeder.

The induced voltages caused by combined sequence, positive sequence and zero sequence currents are shown in Figure 3.15, in accordance with the separation distance from 0 to 100 m. It is obvious to see that the zero sequence curve is much closer to the sequence combined curve than the positive sequence curve. This positioning means that the zero sequence current contributes most of the induced voltage. In this case, due to the phase angle difference, the positive sequence current partially cancels the effect of the zero sequence current, so the total induced voltage is slightly smaller than the zero-sequence induced voltage.

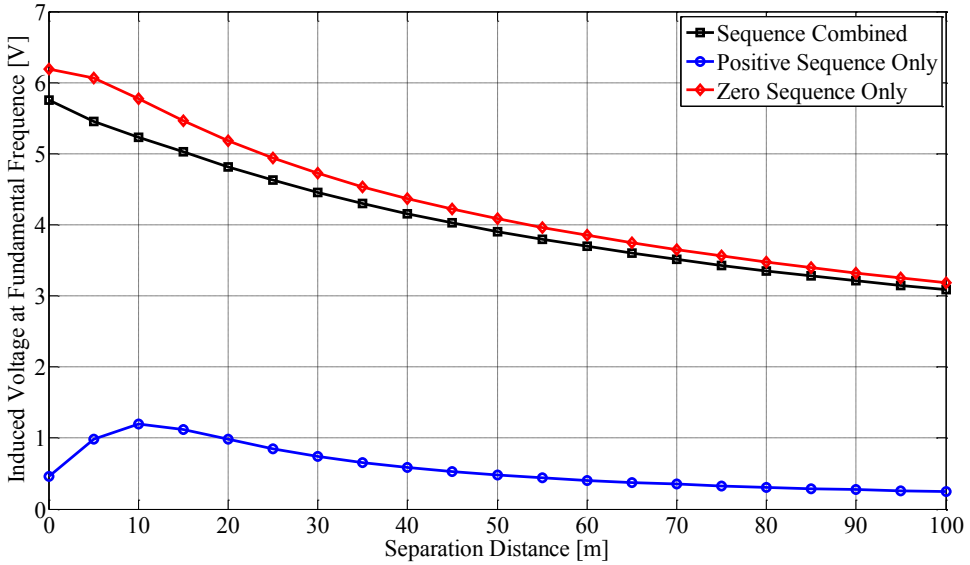

Figure 3.15: Induced voltage in according with the separation distance.

3.3.2 Comparison of Voltages Induced by Fundamental and Harmonic Currents in Distribution System

In this subsection, the induced voltages at fundamental and harmonic frequencies will be compared based on the zero sequence current data summarized in Table 3.8. This comparison mainly analyzes the voltages induced by zero sequence currents. The positive and negative sequence components are neglected due to their limited impact on induced voltage as discussed in the previous sections.

Table 3.8: Zero sequence current data at fundamental and harmonic frequencies.

Harmonic Order	Zero Sequence Current [A]
1st	12.68
3rd	20.45
5th	1.34
7th	0.71
9th	4.68

The comparisons of the induced voltages are shown in Figure 3.16 and Figure 3.17, with respect to the separation distance from 0 to 100 m and the fixed separation distance of 10 m, respectively. The total induced voltage curve shows the rms value that can be calculated by equation (3.35):

$$V_{total} = \sqrt{V_{1^{st}}^2 + V_{3^{rd}}^2 + V_{5^{th}}^2 + V_{7^{th}}^2 + V_{9^{th}}^2} \tag{3.35}$$

where V_{total} is the rms value of the total induced voltage, V_{1}^{st}, V_{3}^{rd}, V_{5}^{th}, V_{7}^{th} and V_{9}^{th} are each induced harmonic voltage.

The results lead to the conclusions that: 1) the 3rd order harmonic induced voltage is the main contributor to the total induced voltage; 2) the 3rd and 9th order harmonic currents in the residential feeder induce significant voltages on the buried pipeline, and are larger than the induced voltage at the fundamental frequency; 3) the 5th order harmonic, one of the main contributors to the TDD, induces relatively small voltage on buried pipeline due to the fact that the zero

sequence current at 5th order harmonic frequency is smaller than those at zero-sequence dominant harmonic frequencies. This reason can also explain the induced voltage at the 7th order harmonic.

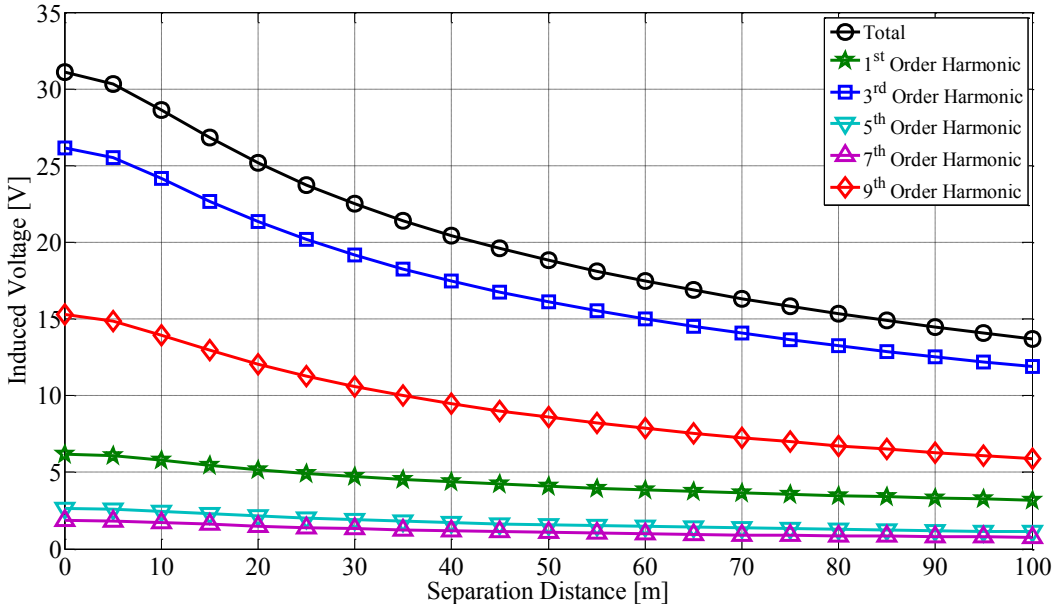

Figure 3.16: The comparison of induced voltages at different frequencies.

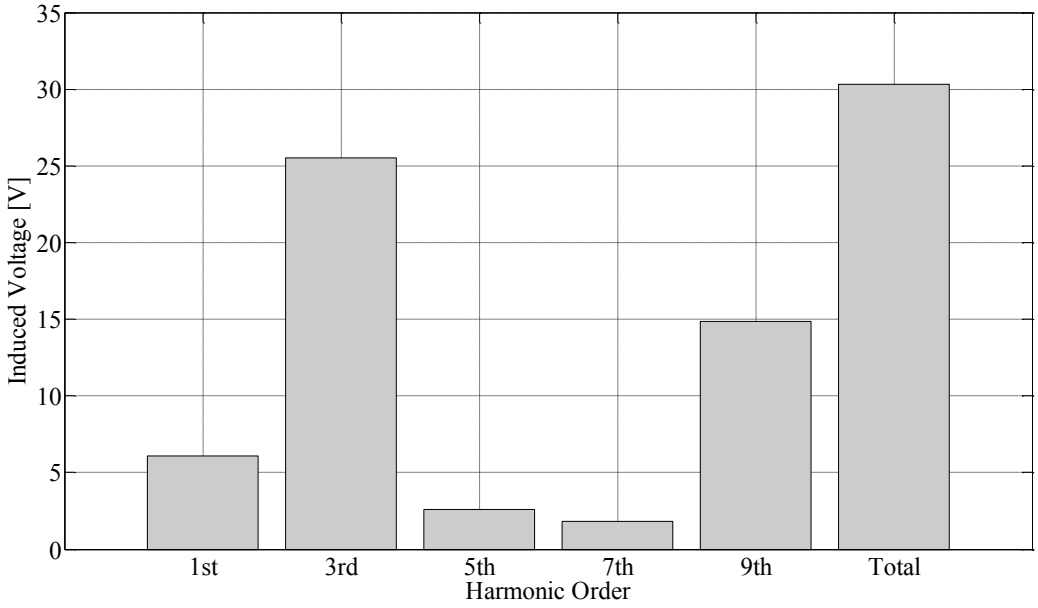

Figure 3.17: The comparison of induced voltages at different frequencies with separation distance of 10 m.

The induced voltage measurements were also taken by the researchers at the University of Alberta. The probe wires were installed along some investigated feeders. The spectra of measured induced voltages on those probe wires are presented in Figure 3.18 [56]. Figure 3.19 shows the comparison of measured induced voltages on probe wires and the simulated induced voltages on buried pipeline, normalized by the total induced voltage of each case. The results lead to the conclusions that 1) the induced voltages on buried pipeline are consistent; 2) the residential feeders induce significant and comparable 3rd and 9th harmonic voltages on the nearby conductors. As a consequence, the potential issues can be introduced into the buried pipeline due to significant 3rd and 9th order harmonic currents.

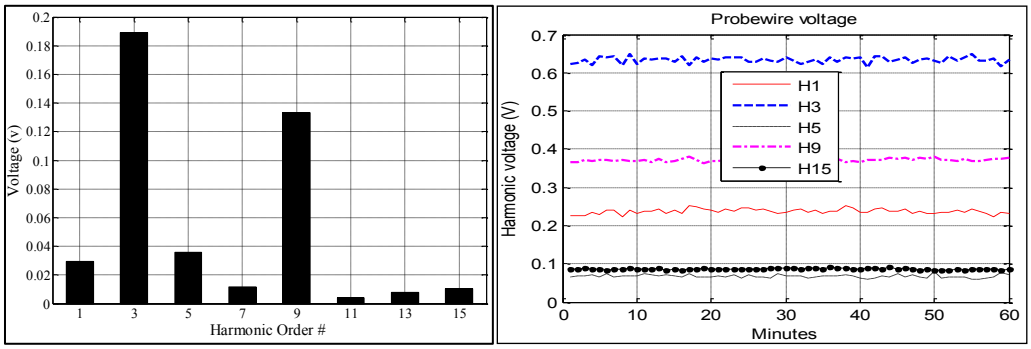

(a) "Location 1" (b) "Location 2"

Figure 3.18: Harmonic spectrum of the induced voltages on the probe wires [78].

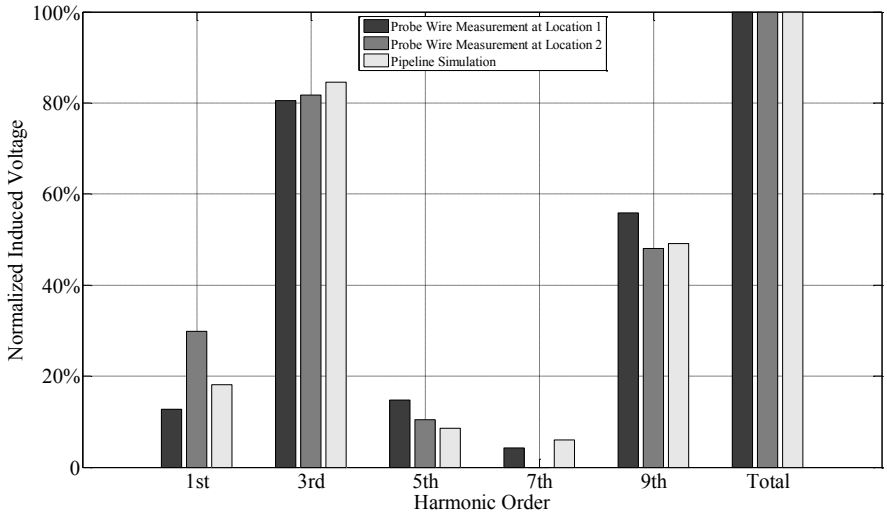

Figure 3.19: The comparison of measured induced voltages on probe wires and the simulated induced voltages on buried pipeline (normalized by the total induced voltage).

3.4 Pipeline AC Corrosion Issue Caused by Harmonic Induction

The three potential issues in inductive coordination between overhead conduct and buried pipeline are pipeline AC corrosion, personnel safety, and pipeline coating breakdown, as discussed before. From the harmonic perspective, the pipeline AC corrosion issue needs to be considered.

A series of experiments have recently been conducted by researchers from the University of Alberta. In this subsection, the results are discussed to reveal the potential pipeline AC corrosion issues affected by harmonic-induced voltage. The details of the experiment setup are presented in Appendix D.

The corrosion experiments are conducted to achieve two aims:

- to show the impact of each individual frequency current on pipeline corrosion rate;
- to reveal the impact of multiple frequency current on pipeline corrosion rate.

Four experiments have been conducted at the fundamental, 3rd order harmonic, 9th order harmonic and multiple frequencies (fundamental, 3rd order harmonic, and 9th order harmonic combined). The currents are controlled to be the same current 1 mA (rms) in the four experiments. Table 3.9 summarizes the voltage source outputs of the four experiments. The magnitude ratios and phase angle differences between each frequency are determined by the field measurements.

Table 3.9: The values of voltage source supplies.

Experiment	Harmonic Order	Voltage Magnitude [V]	Phase Angle [°]
# 1	1st	6.6	0
	3rd	0	0
	9th	0	0
# 2	1st	0	0
	3rd	11.8	0
	9th	0	0
# 3	1st	0	0
	3rd	0	0

	9th	4.3	0
# 4	1st	1.3	0
	3rd	3.9	80
	9th	0.6	130

Figure 3.20 shows the average corrosion rates at different frequencies. The corrosion rates of each sample are presented in Figure 3.21. The following conclusions can be drawn based on the experiment results:

- the corrosion rates at different individual frequencies are comparable. The corrosion rate is 1.34 mil/year at 60 Hz, 0.95 mil/year at 180 Hz, and 1.24 mil/year at 540 Hz based on the average corrosion rate results;
- the corrosion rate at multiple frequencies is slightly larger than the other three of every single sample result. The impact of multiple-frequency current could be severe on pipeline AC corrosion but more research is needed to confirm this finding.

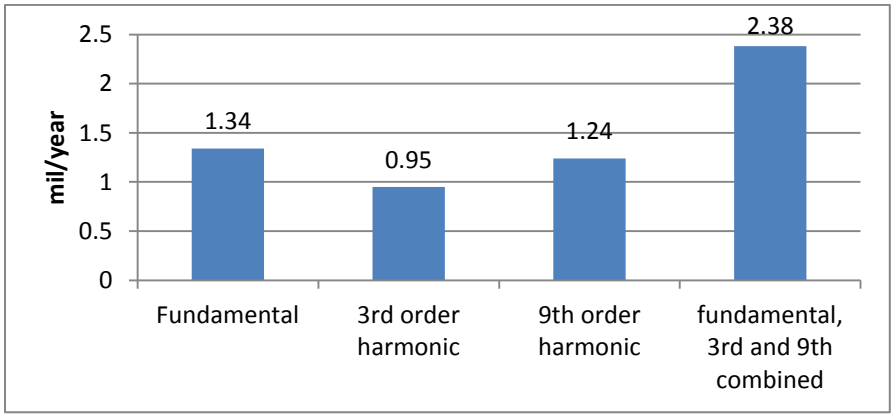

Figure 3.20: Average corrosion rates at different frequencies.

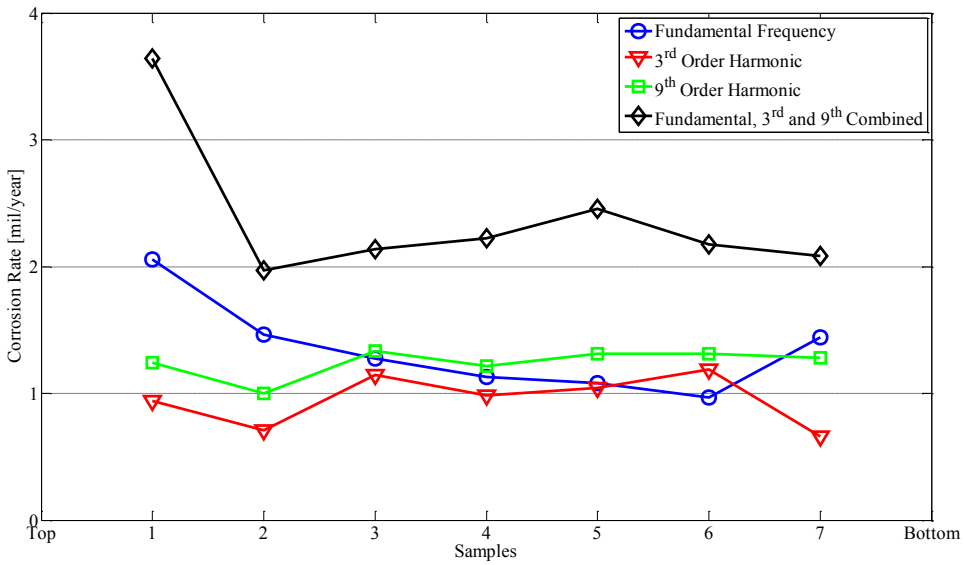

Figure 3.21: Corrosion rates of each sample at different frequencies.

Assuming the corrosion rates at different frequencies are the same, the voltage limit to avoid pipeline AC corrosion issue can be calculated using equation (2.53) in Section 2.2.1. For example, the criterion for avoiding low corrosion risk is 30A/m^2 as recommended by the standards [4][35]. Based on the typical parameter of soil resistivity 100 Ωm and coating holiday diameter 0.01 m (coating holiday area 1cm^2), the voltage limit for low corrosion risk is:

$$V_{corrosion} = \frac{\pi \rho d J_{corrosion}}{8} = 13.2V \tag{3.36}$$

The clearance distances for avoiding low corrosion risk at different frequencies can be achieved from Figure 3.22. The induced voltage calculations are based on Figure 3.16. In this case, the induced voltage at fundamental frequency does not exceed the voltage limit at any separation distance, so the clearance distance is 0 m at fundamental frequency. The induced voltages at 3rd and 9th order harmonic frequencies, as well as the total induced voltage, all exceed the voltage limit when the separation distances are not long enough.

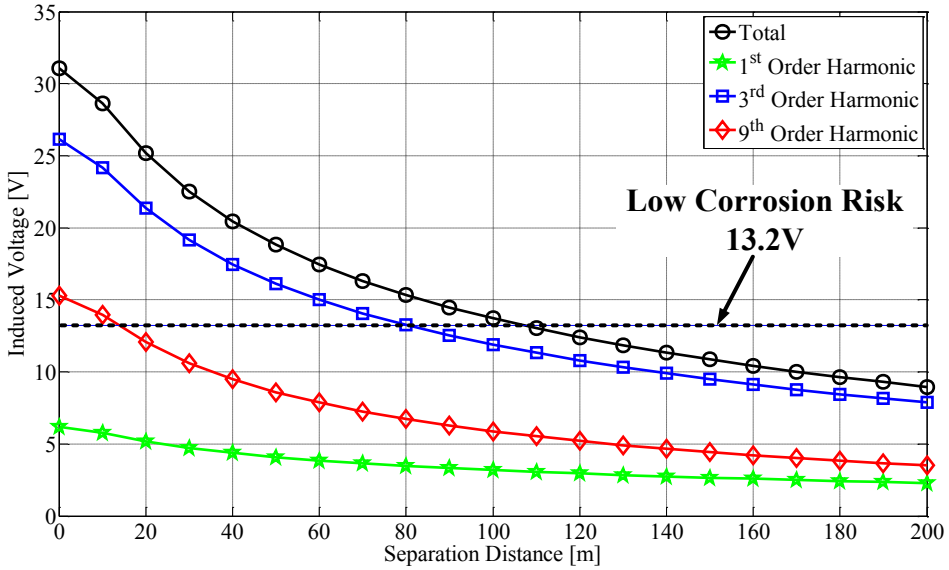

Figure 3.22: The clearance distances between distribution line and pipeline to avoid low corrosion risk at different frequencies.

The clearance distances at different frequencies are concluded in Table 3.10. The third column in Table 3.10 and Figure 3.23 show the equivalent fundamental I_0/I_1 ratios which cause the same clearance distances at different harmonic frequency. Longer clearance distance is needed to avoid corrosion risk at higher I_0/I_1 level. What's more, the increasing speed of clearance distance is faster at higher I_0/I_1 level. If the clearance distance is set only based on the fundamental induced voltage, the potential pipeline corrosion issue may be introduced into pipeline due to significant 3rd and 9th order harmonic induced voltages. The discussion of transmission line harmonic current induction is presented in Appendix E.

Table 3.10: The clearance distances for avoiding low corrosion risk at different frequencies.

Harmonic Order	**Clearance Distance [m]**	**I_0/I_1 of 300 A Fundamental Current**
1st	0	4%
9th	14	10%
3rd	80	16%
Total	108	18%

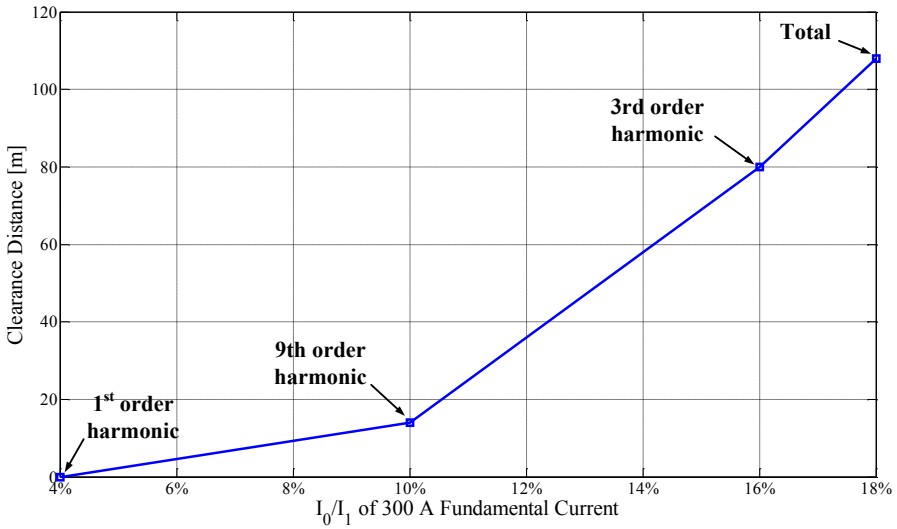

Figure 3.23: The relationship between clearance distance and harmonic order.

3.5 Summary

In this chapter, the harmonic current distortions are firstly reviewed in distribution system. Next, the analytical methods of calculating induced voltage on buried pipeline at harmonic frequencies are presented. Based on the analytical theory, the impacts of harmonic order and its dominant sequence are analyzed. Followed by that, the comparison of induced voltages at fundamental, 3rd and 9th order harmonics is conducted. Finally, the potential pipeline AC corrosion issue caused by the 3rd and 9th harmonic currents is discussed based on the experiment results. The main achievements of this chapter are summarized as below:

1. Currents measured in residential feeders contain much stronger harmonics (3rd ~9th) in the distribution system. The values of IDD for each harmonic decrease from low order to high order harmonics.

2. The adopted methods for mutual and self-impedance calculation at harmonic frequencies have already been discussed and verified by many papers through analytical study and finite-element method simulation.

3. The usage of the Caron-Clem equation for the mutual impedance calculation is restricted by frequency, soil resistivity, and separation distance. A simplified equation from Carson's formula is developed to support the calculation up to 540 Hz and 100 m separation distance under 30 Ωm soil resistivity. The error produced in using this equation can be controlled within 5% based on the simulation results.

4. The induced voltage per-unit-current increases with higher frequency. The zero sequence current is the most significant source of induced voltage on buried pipeline, than the positive and negative sequence currents. Considered the realistic value of each sequence current magnitude, the zero sequence induced voltage is still dominant the total induced voltage at any frequency. The induced voltages at 3^{rd} and 9^{th} order harmonic frequencies, based on the measurements from residential feeders, are larger than those at fundamental frequency.

5. The corrosion rate of the fundamental, 3^{rd} and 9^{th} order harmonic frequencies are comparable, and it is slightly larger when three frequency currents combined together. As a result, if the clearance distance is set only based on the fundamental induced voltage, the potential pipeline corrosion issue may be introduced into pipeline due to significant 3^{rd} and 9^{th} order harmonic induced voltages. Therefore, the potential pipeline AC corrosion at high frequencies needs to be considered.

Chapter 4

Sensitivity Study and Main Impact Factors

As concluded in Chapter 3, the zero sequence current is the most significant source of induced voltage on buried pipeline compared to positive and negative sequence currents, especially at the fundamental, 3rd and 9th order harmonic frequencies. The impact of each factor on the induced voltage needs to be investigated at harmonic frequencies. Therefore, several sensitivity studies are conducted to analyze and compare the impact of the power distribution line and pipeline parameters on the induced voltage at the fundamental, 3rd and 9th order harmonic frequencies based on the unit zero sequence currents as shown in Table 4.1. As a result, the induced voltages are provided with the per-unit-current values, which can also eliminate the influence of current magnitude in the analysis. To compare the realistic induced voltage values, one can multiply the analysis results with the current magnitude at each frequency, for example, by using the sample values of Table 4.2.

Table 4.1: Unit zero sequence current data used in the sensitivity study.

Harmonic Order	**Zero Sequence Current [A]**		
	Phase A Conductor	**Phase B Conductor**	**Phase C Conductor**
1st	1	1	1
3rd	1	1	1
9th	1	1	1

Table 4.2: Realistic current magnitude at each frequency.

Harmonic Order	**Zero Sequence Current [A]**
1st	12.68
3rd	20.45
9th	4.68

Section 4.1 will focus on the analysis of pole structure and MGN from power distribution line perspective. Section 4.2 will discuss about the impacts of soil resistivity, coating type, and parallel length, which represent the pipeline perspective[2]. Section 4.3 will conclude the main findings from the sensitivity study. The representative values of each parameter for the sensitivity study are shown in Table 4.3. The sensitivity studies are based on the following assumptions to produce conservative and reasonable results:

- the pipeline is parallel to the distribution line and extends for a few kilometers L_e[3] beyond the parallel routing without grounding;
- the coating resistance per unit length of the pipeline is uniform and independent of the applied voltage;
- the soil resistivity along the parallel route is constant;
- the separation distance between the distribution line and buried pipeline is 10 m.

Table 4.3: Representative values of parameters [59][60][79].

Parameter	Range	Default Value
Pole Structure	N12_35,40,45FT N12Y_35,40,45FT	N12Y_45FT
Multi-Grounded Neutral	with (out) MGN	without MGN
Soil Resistivity [Ωm]	30 ~ 1000	100
Coating Material	Bitumen; Polyethylene	Polyethylene
Parallel Length [m]	0 ~ 5000	1000

4.1 Effect of Distribution Line Parameters

The factors, pole structure, and MGN from the distribution line perspective will influence the induced voltage mainly by the EMF. Different configurations of

[2] The pipeline diameter does not influence the induced voltage significantly, the detailed analysis is shown in Appendix F

[3] The typical values at fundamental and harmonic frequencies are shown in Appendix B.

pole structure lead to various geometrical distances between phase conductors and buried pipeline, further influencing the mutual impedances. The MGN can partially cancel the EMF with the help of zero sequence current in the neutral conductor. Therefore, the pole structure and the MGN need to be analyzed.

4.1.1 Effect of Pole Structure

In this sensitivity study, six pole structures with two different arm lengths and three different heights have been reviewed and implemented to analyze the effect of pole structure on the induced voltages at the fundamental, 3^{rd},and 9^{th} order harmonic frequencies. Table 4.4 lists the geometry sizes of each pole structure [79].

Table 4.4: Geometry sizes of each pole structure.

Structure type	Arm size [m]	Phase A Height [m]	Phase B,C Height [m]	Neutral Height [m]
N12_35FT	0.94	9.30	8.75	7.47
N12_40FT	0.94	10.83	10.27	8.99
N12_45FT	0.94	12.20	11.64	10.36
N12Y_35FT	1.34	9.30	8.75	7.47
N12Y_40FT	1.34	10.83	10.27	8.99
N12Y_45FT	1.34	12.20	11.64	10.36

Figure 4.1 illustrates the induced voltage according to different pole structures. The difference of induced voltage due to pole height becomes slightly bigger with higher frequency. On the other hand, the arm size influence on the induced voltage can hardly be recognized at each frequency. It is because the differences of pole height and arm size are much smaller than the geometrical distances between phase conductors and buried pipeline. As a result, it can be concluded that both pole height and arm size of pole structure cannot influence the induced voltage on buried pipeline significantly at each harmonic frequency.

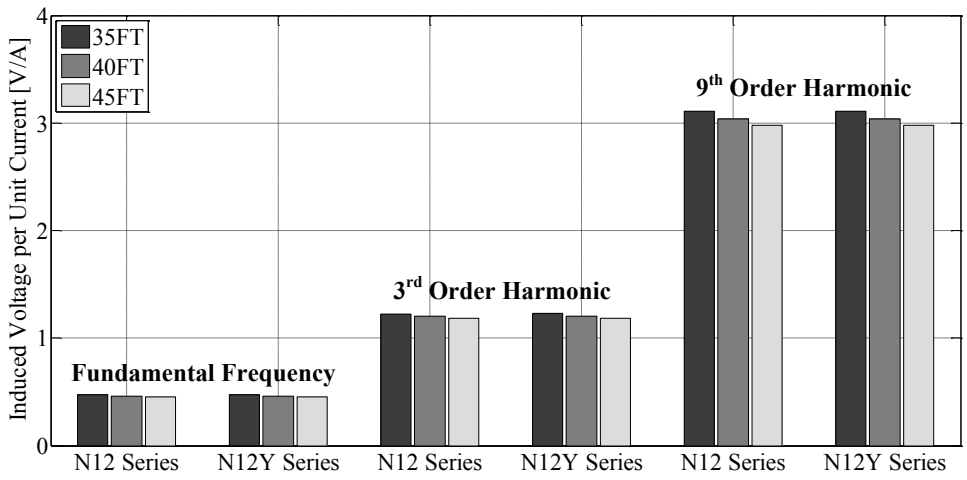

Figure 4.1: The influence of distribution line pole structure on the induced voltage.

4.1.2 Effect of Multi-Grounded Neutral

The neutral conductor in the MGN system contains zero sequence current which has a shielding effect on the pipeline induction. Simulation study has been conducted using MHLF software [80] to show the characteristics of neutral current at the fundamental, 3rd, and 9th order harmonic frequencies. In this simulation, a system (Figure 4.2) with a 12 km feeder is used. Table 4.5 lists the MGN system parameters.

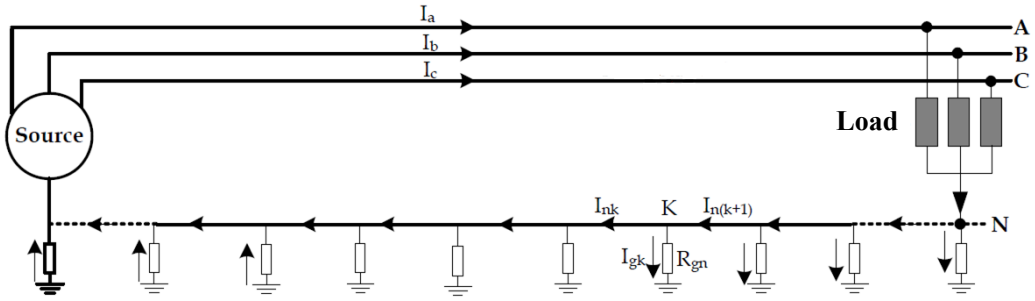

Figure 4.2: Typical MGN distribution system.

Table 4.5: MGN system impedance parameters.

Source and Conductor Parameters		
	Self-Impedance	**Mutual Impedance**
Substation Source [Ω]	0.0721+j2.8858	-0.0018+j0.666
Phase Conductor [Ω/km]	0.396+j0.912	0.058+j0.57 (phase-to-phase)
Neutral Conductor [Ω/km]	0.911+j0.946	0.059+j0.55 (phase-to-neutral)
MGN Parameters		

Substation Grounding [Ω]	0.15
Neutral Grounding [Ω]	15
Neutral Grounding Span [m]	100

The neutral current magnitude ratio, showing the relationship between neutral current and zero sequence phase current, is defined by the following equation (4.1):

$$Ratio_h = I_{n,h} / \left(3 \times I_{0,h}\right) \times 100\% \tag{4.1}$$

where

$Ratio_h$ is the neutral current magnitude ratio at h harmonic order;

$I_{n,h}$ is the neutral current at h harmonic order;

$I_{0,h}$ is the zero sequence phase current at h harmonic order.

As we can observe from the simulation results in Figure 4.3, the neutral current ratios increase with higher frequency within the steady-state range for most portions of the neutral wire due to the inductive coupling. The reason will be explained in detail in the following section. The only exception is that the neutral current ratios of different frequencies increase to almost 100% at the feeder end due to the phase current flowing into the neutral conductor. Therefore, it is reasonable to claim that the steady-state value is the average neutral current ratio as shown in Table 4.6. As a result, the neutral conductor will contain more current to reduce the induced voltage from the zero sequence phase current at a higher frequency.

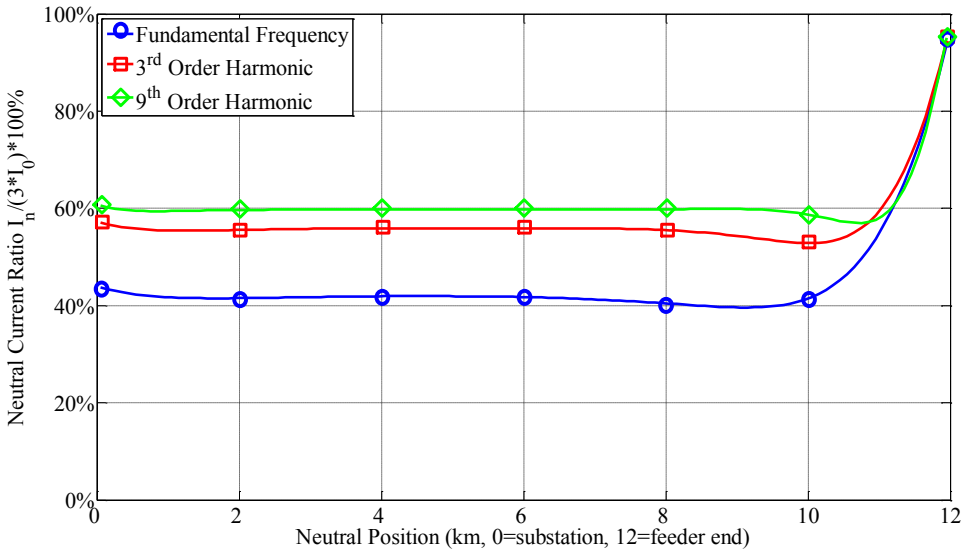

Figure 4.3: Neutral current ratios of MGN system at different frequencies.

Table 4.6: Average neutral current ratios of MGN system at different frequencies.

	Fundamental	**3rd Order Harmonic**	**9th Order Harmonic**
Ratio	42%	56%	60%

The mechanism of inductive coupling in the MGN system can be explained in Figure 4.4. The EMFs, produced by the phase currents ($e_{nk} = \sum Z_m I_0$), will create circling current in each grounding segment.

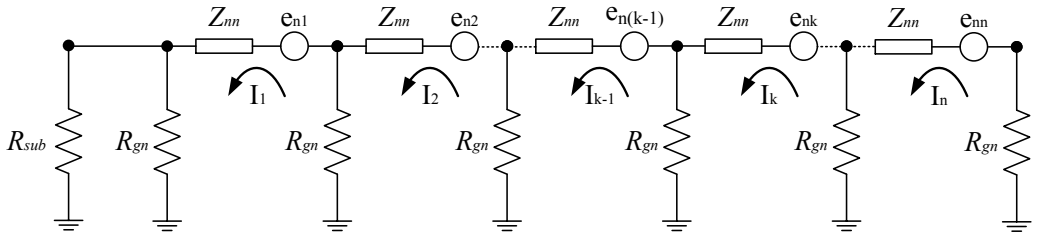

Figure 4.4: Mechanism of inductive coupling in MGN system.

With enough segments in MGN system, the current I_{k-1} and I_k will be nearly the same. Therefore, there will be no current going through the grounding resistance. The current through Z_{nn} in kth segment will be determined by the following equation (4.2):

$$I_k Z_{nn} + e_{nk} = 0$$
$$I_k = -\frac{Z_{na} + Z_{nb} + Z_{nc}}{3Z_{nn}} \times 3I_0 \tag{4.2}$$

where

Z_{na}, Z_{nb} and Z_{nc} are the mutual impedance between neutral conductor and each phase conductor;

Z_{nn} is the self-impedance of the neutral conductor.

The self-impedance and mutual-impedance are defined in equation (4.3):

$$Z_{nn} = R_{nn} + jX_{nn} \times h$$
$$Z_m = R_m + jX_m \times h \tag{4.3}$$

where R_{nn}, X_{nn}, R_m and X_m are the parameters at fundamental frequency.

The neutral currents $I_{k,h}$ at the fundamental, 3rd and 9th order harmonic frequencies are calculated in the following equations:

$$I_{k,1} = -\frac{Z_{na,1} + Z_{nb,1} + Z_{nc,1}}{3Z_{nn,1}} \times 3I_{0,1} = 0.42\angle -142° \times 3I_{0,1} \tag{4.4}$$

$$I_{k,3} = -\frac{Z_{na,3} + Z_{nb,3} + Z_{nc,3}}{3Z_{nn,3}} \times 3I_{0,3} = 0.56\angle -164° \times 3I_{0,3} \tag{4.5}$$

$$I_{k,9} = -\frac{Z_{na,9} + Z_{nb,9} + Z_{nc,9}}{3Z_{nn,9}} \times 3I_{0,9} = 0.60\angle -175° \times 3I_{0,9} \tag{4.6}$$

The results are nearly the same with the simulation results, which means that the average neutral current in the MGN system can be calculated by the above equations at the fundamental, 3rd, and 9th order harmonic frequencies.

Based on the neutral current ratios, the influence of MGN on the induced voltage can be compared at different frequencies, as shown in Figure 4.5. The term "without MGN" means that only three phase currents induce the voltage on the

buried pipeline. On the other hand, "with MGN" indicates that the induced voltage includes the component contributed by the neutral current. It can be concluded from the results that the influence of the MGN system is more significant at a higher frequency. As a result, the MGN configuration is an important impact factor.

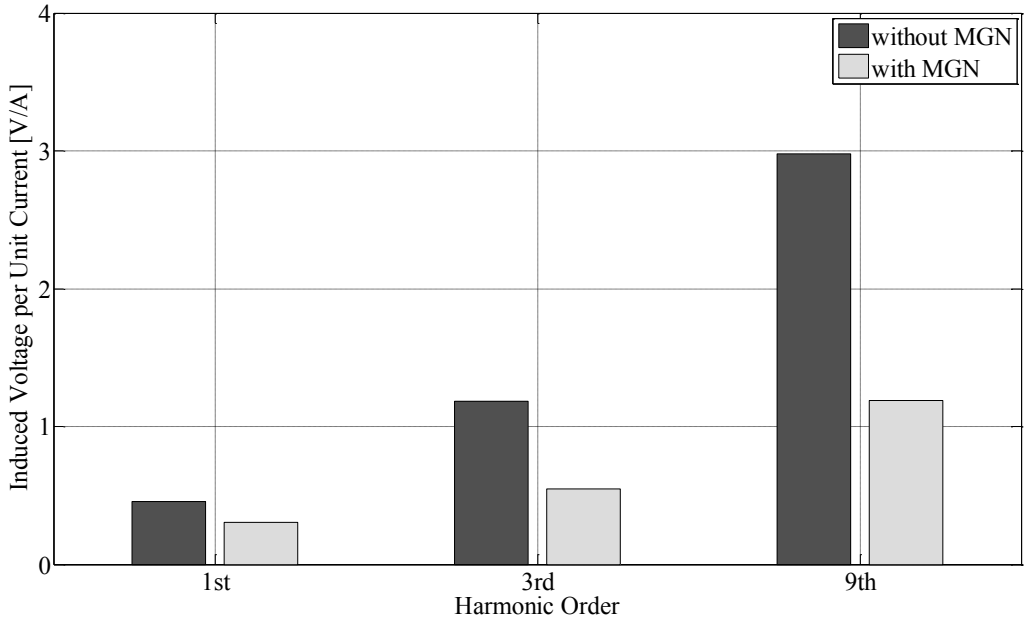

Figure 4.5: The influence of MGN system on the induced voltage.

4.2 Effect of Pipeline Parameters

The factors, soil resistivity, and coating material will influence the induced voltage by the EMF, the propagation constant γ. The soil resistivity has a complex relationship with the induced voltage because it is involved in the calculations of mutual impedance and propagation constant. The coating material mainly determines the grounding admittance that further influences the propagation constant. The parallel length will directly determine the induced voltage by the term $(1 - e^{-\gamma L})$ in the induced voltage calculation.

4.2.1 Effect of Soil Resistivity

As the soil resistivity is involved in both the mutual impedance and propagation constant, it is difficult to reveal its effect on the induced voltage by analytical study. Figure 4.6 shows the relationship between soil resistivity and induced voltage at the fundamental, 3rd and 9th order harmonics based on the simulation results. The main findings are as follows:

- the induced voltage almost stays the same with the increasing of soil resistivity at fundamental frequency;
- the induced voltage, at the 3rd order harmonic, slightly increases at lower soil resistivity and almost stays the same at higher soil resistivity;
- the induced voltage, at the 9th order harmonic, increases with higher soil resistivity but the ratio decreases with higher soil resistivity.

It can be concluded from the findings that the influence of soil resistivity can be amplified at higher frequency and this difference is more obvious with lower soil resistivity than higher soil resistivity. Therefore, the soil resistivity should be considered as one of the main impact factors.

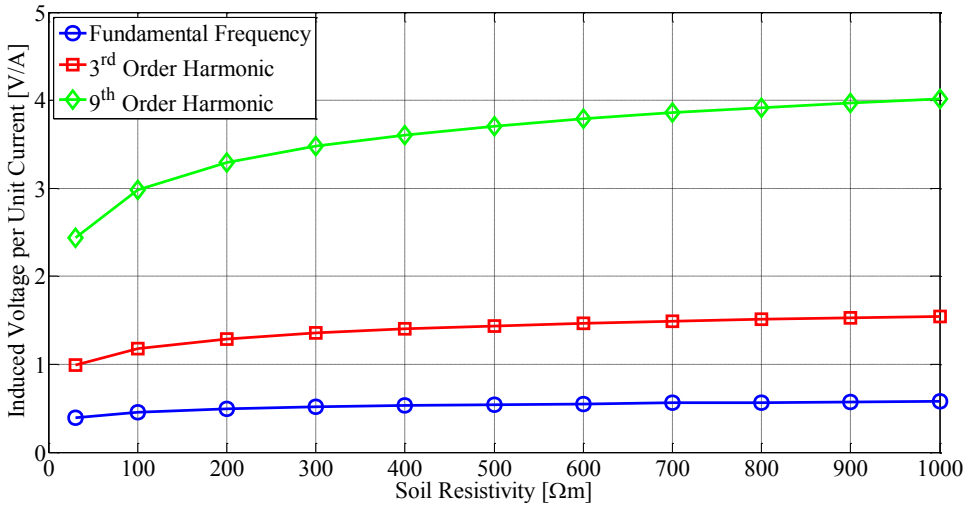

Figure 4.6: Induced voltage due to soil resistivity.

4.2.2 Effect of Coating Material

The coating material determines its coating resistance r_c, which is defined by the product of coating resistivity and coating thickness. The general resistance values of commonly used coating materials are shown in Table 4.7 [60].

Table 4.7: The general resistance values of commonly used coating materials [60].

	Polyethylene Coating	**Bituminous Coating**
Resistance r_c [Ωm^2]	$1*10^5$	$1*10^3$

The influences of the coating material on the induced voltage, compared at the fundamental, 3rd and 9th order harmonic frequencies, are shown in Figure 4.7. The induced voltage difference between polyethylene and bituminous coating is getting larger with higher frequency. The reason is explained below.

Assume that the self-impedance and self-admittance of the buried pipeline are presented as follow:

$$Z = R + jX \times h \tag{4.7}$$

$$Y = G + jB \times h \tag{4.8}$$

$$\gamma = \sqrt{ZY} = \sqrt{RG - XBh^2 + jRBh + jGXh} \tag{4.9}$$

where

γ is the propagation constant;

Z is the self-impedance;

R is the real part of the self-impedance at 60 Hz;

X is the imaginary part of self-impedance at 60 Hz;

Y is the self-admittance;

G is the real part of the self-admittance at 60 Hz;

B is the imaginary part of the self-admittance at 60 Hz;

h is the harmonic order.

The coating resistance mainly influences the real part of the self-admittance *G*. During the calculation of the propagation constant as presented in equation (4.9), the difference of *G* will be amplified by the harmonic order in the term, *jGXh*. Finally, the induced voltage, as a function of the propagation constant, changes more obviously at higher frequency. As a result, it can be concluded that the influence of the coating material is more significant at higher frequencies.

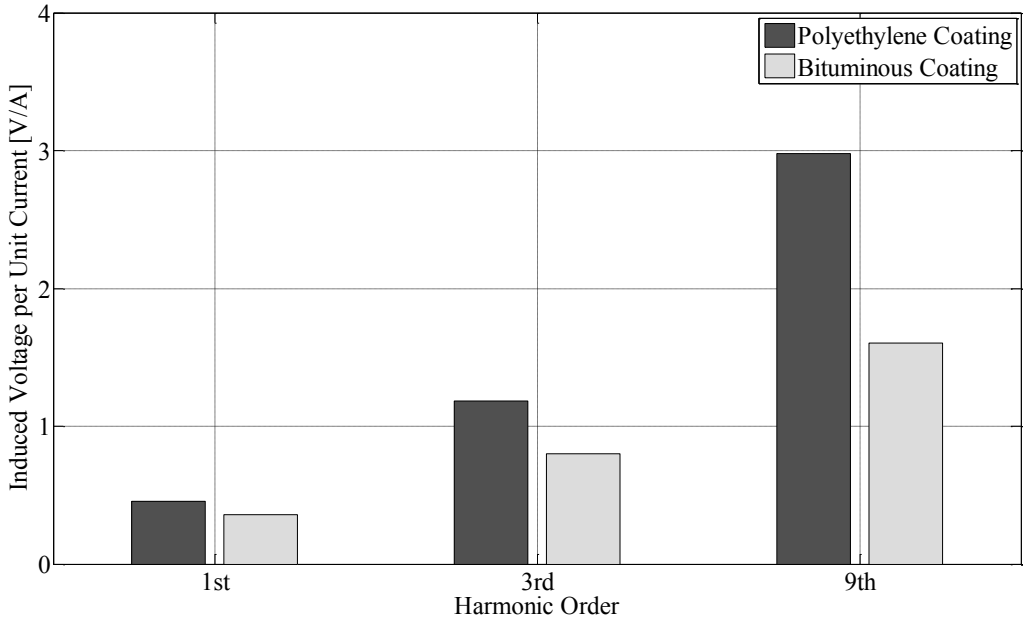

Figure 4.7: Induced voltage due to coating material.

4.2.3 Effect of Parallel Length

Figure 4.8 (a) and (b) show the influence of parallel length on the induced voltage at the fundamental, 3rd, and 9th order harmonic frequencies. There are three main findings from the simulation results:

- the induced voltage is more sensitive to the parallel length at a higher frequency;

- the induced voltage appears to have a positive linear correlation with the parallel length at each frequency when the buried pipeline is coated by the polyethylene material;

- the induced voltage has a saturation value at each frequency with the buried pipeline coated by the bituminous material.

The reasons of the above findings are explained as follows. The parallel length influences the induced voltage according to the following equation:

$$V_{induced} = \frac{E_h}{2\gamma_h}\left(1 - e^{-\gamma_h L}\right) \tag{4.10}$$

where

γ_h = propagation constant at h order harmonic;

L = total parallel length;

E_h = EMF induced on the pipeline per unit length at h order harmonic.

If the term $\gamma_h L$ is small enough, the first-order-correct approximation of the equation (4.10) becomes

$$V_{induced} = \frac{E_h}{2\gamma_h}\left(1 - e^{-\gamma_h L}\right) \approx \frac{E_h}{2\gamma_h}\left[1 - \left(1 - \gamma_h L\right)\right] = \frac{1}{2} E_h L \tag{4.11}$$

The induced voltage is then linear with the parallel length. The positive ratio, $\frac{1}{2}E_h$, increases with higher frequency. Those are the reasons that the induced voltage is linear with the parallel length and more sensitive to it at a higher frequency.

On the other hand, if the term $\gamma_h L$ is large enough, which means that $e^{-\gamma_h L}$ is almost zero, the equation (4.10) is simplified as follows:

$$V_{induced} = \frac{E_h}{2\gamma_h}\left(1 - e^{-\gamma_h L}\right) \approx \frac{E_h}{2\gamma_h} \tag{4.12}$$

At this time, the induced voltage is determined by E_h and γ_h, but independent with the parallel length. Due to the fact that the buried pipeline with the bituminous coating has a larger γ_h, the saturation phenomenon normally exists in the bituminous coating case. Based on the simulation results from Figure 4.8 (b), the saturation value still increases with higher frequency. In conclusion, the parallel length factor is significant in harmonic study.

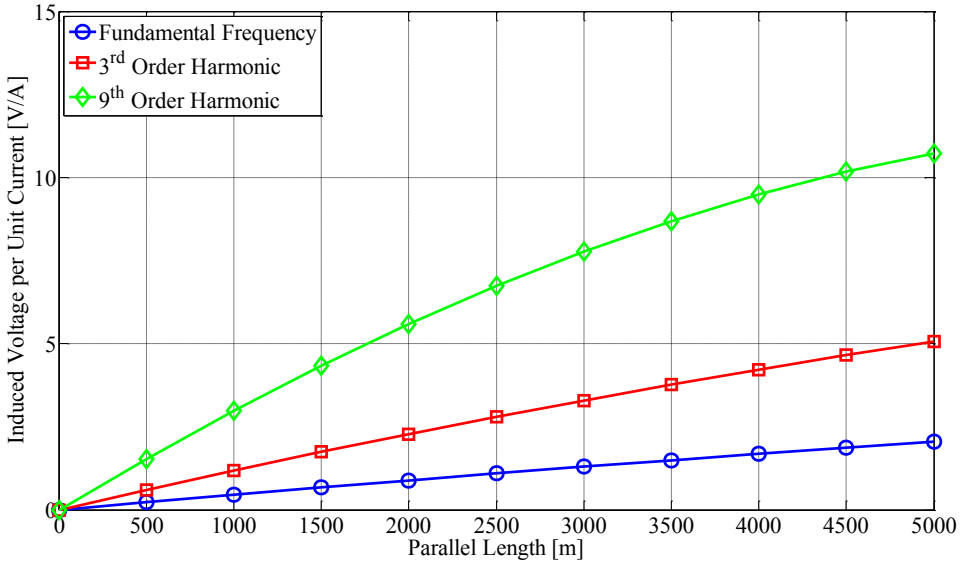

(a) Polyethylene Coating

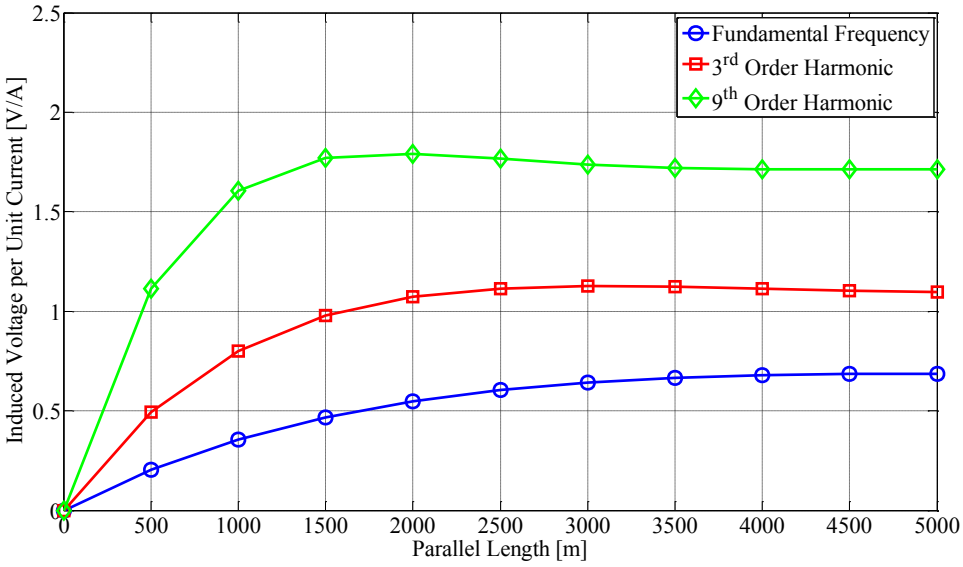

(b) Bituminous Coating

Figure 4.8: Induced voltage due to parallel length.

4.3 Main Impact Factors and Summary

Sensitivity studies have shown the effects of potential factors at the fundamental, 3rd and 9th order harmonic frequencies. It can be concluded that the MGN system, soil resistivity, coating material, and parallel length are the main impact factors. The results of the sensitivity study are summarized below:

1. Both pole height and arm size of pole structure cannot influence the induced voltage on buried pipeline significantly at the fundamental, 3rd and 9th order harmonic frequencies.

2. The neutral in the MGN system will play a significant role in reducing the induced voltage at harmonic frequencies on buried pipelines. A good estimation of the neutral current is approximated by the analytical method based on the MGN ladder network. Based on the simulation results, the reduction effect of MGN is more significant with a higher frequency.

3. The influence of soil resistivity can be amplified at a higher frequency, and this difference is more obvious with lower soil resistivity than higher soil resistivity. The induced voltage almost stays the same with the increasing of soil resistivity at the fundamental frequency, but increases at the 3rd order harmonic and more obviously at the 9th order harmonic.

4. The polyethylene coating will create a larger induced voltage because its insulating property is much better than that of the bituminous coating. This phenomenon is more obvious at the 9th order harmonic than at the 3rd order harmonic and fundamental frequency. The coating resistance mainly influences the real part of the self-admittance *G*. The difference of *G* between the polyethylene and bituminous coatings will be amplified by the harmonic order. Finally, the induced voltage, as a function of the propagation constant, changes more obviously at a higher frequency.

5. The induced voltage increases faster at a higher frequency with longer parallel length. If the production of the propagation constant and parallel length is small enough, the induced voltage is almost linear with the parallel length at each harmonic frequency. The ratio is determined by the EMF which increases with a higher frequency. On the other hand, if the production of the propagation constant and parallel length is large enough, the induced voltage has a saturation value that still increases with a higher frequency.

Chapter 5

Mitigation Methods

The published standards and guidelines have suggested a few methods to mitigate the induction problems between power lines and pipelines. The feasibility of applying these methods to mitigate induced voltages at the fundamental, 3rd, and 9th order harmonic frequencies in the distribution system is assessed in this Chapter. The mitigation targets are the terminal induced voltages, which are the maximum voltages along the pipeline. The typical parameters used in this chapter are the same as those of previous chapters. Section 5.1 will briefly review the existing mitigation methods in industry and summarize the potential useful methods. Section 5.2 to Section 5.4 will analyze each potential useful mitigation method at the fundamental, 3rd, and 9th order harmonic frequencies. The voltage reduction factor, *k*, is defined as the reduction ratio of applying the mitigation method to reveal the effectiveness of each mitigation method, as shown in equation (5.1):

$$k = \left(1 - \left|\frac{V_{mitigated}}{V_{normal}}\right|\right) \times 100\% \tag{5.1}$$

where

$V_{mitigated}$ is the induced voltage with the mitigation method;

V_{normal} is the induced voltage without the mitigation method.

5.1 Review of Mitigation Methods

The methods recommended by practical guides for mitigating inductive effects from transmission lines to pipelines are summarized as follows [59][60]:

- installation of shield wires to power lines;

- installation of mitigation wires;
- grounding of pipeline;
- installation of pipeline insulation flanges;
- use of a different sequence of the phases in case of lines with two circuits;
- utilization of equipotential grounding mat at access points.

The shield wire will reduce the inductive coupling significantly under the fault condition because the fault current will produce the current in the shield wire, thereby partially cancelling the total EMF. For the 3rd and 9th order harmonic currents in distribution lines, the neutral wire can play the role of the shield wire. The effectiveness of an islanded multi-grounded neutral (IMGN) installed in the exposed zone is analyzed in Section 5.2.

Mitigation wire is commonly made of bare conductor, which is installed parallel with and near the pipeline but not bonded to it. Their effectiveness depends on the resistance of the conductor and on the distance between the pipeline and the conductor. Similar to the IMGN method, the mitigation wire can cancel part of the total EMF at each frequency. This method is analyzed in Section 5.3.

Grounding the pipeline is the most classical method to reduce voltage due to inductive coupling. The most effective location on a buried pipeline is at terminals where the induced voltages are generally the largest. Generally, the effectiveness is based on the relationship between the grounding resistance and the characteristic impedance Z_0 of the buried pipeline. Lower grounding resistance of the grounding installation will provide better reduction of induced voltage. This grounding method will be discussed at the 3rd and 9th order harmonic frequencies in Section 5.4.

Insulating flanges are frequently used at the entry of a station to isolate the pipeline from the local grounding system. They can also be used to subdivide the pipeline into several sections inside a long exposed zone and reduce the inductive

coupling. However, the exposed length of pipeline to distribution line may be short. The method is, therefore, not practical for most distribution line cases.

When a tower carries two or more circuits, an appropriate choice of phase sequence arrangements can bring a significant reduction of the inductive coupling to the nearby pipeline at the fundamental frequency. However, at the 3rd and 9th order harmonic frequencies, this method can rarely reduce the inductive coupling due to the fact that the harmonic currents are almost in phase and their creating EMFs cannot cancel each other by the phase conductor arrangement.

An additional solution to the personnel safety concern is the equipotential grounding mats. According to the guides, the grid of equipotential grounding mats can be buried at a very low depth and should be connected to the pipeline. This method does not contribute to the reduction of induced voltages at each frequency.

In a nutshell, IMGN, mitigation wire, and grounding pipeline are potentially useful mitigation methods at the fundamental, 3rd and 9th order harmonic frequencies. The first two methods work on the reduction of EMF and the last method works on the reduction of grounding resistance.

5.2 Effectiveness of Islanded Multi-Grounded Neutral

The effectiveness of MGN on the reduction of induced voltage at the fundamental, 3rd, and 9th order harmonic frequencies has been studied and presented in Section 4.1.2. Since the pipeline is always exposed to only a portion of the distribution feeder, it is useful to determine if installing an islanded multi-grounded neutral, as shown in Figure 5.1, will reduce the inductive coupling effect.

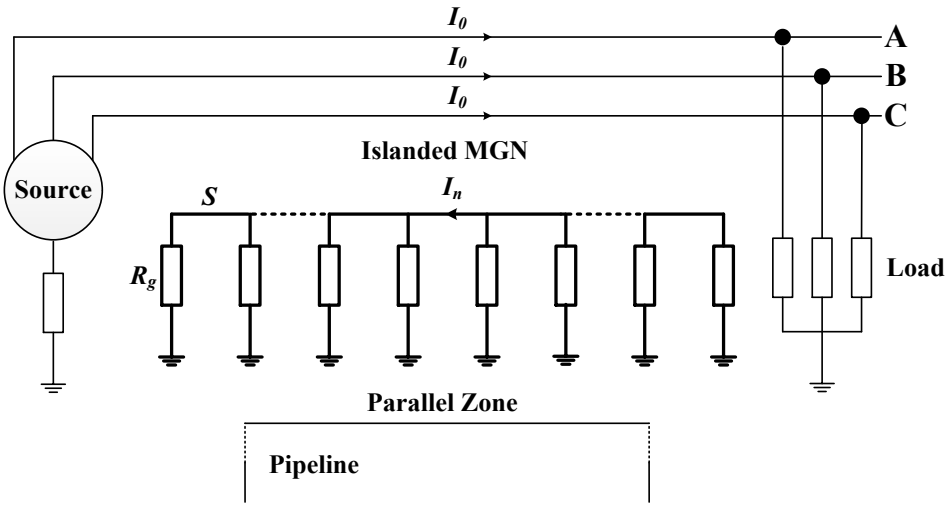

Figure 5.1: Scheme of islanded MGN parallel with buried pipeline.

The neutral current in an islanded MGN system will only contain an inductive component, so the analysis is quite similar to the discussion of inductive coupling in the MGN system. Simulation study has been conducted using MHLF software [80] to show the characteristics of the neutral current of islanded MGN at the fundamental, 3rd and 9th order harmonic frequencies. The parameters are similar to the simulation study of MGN in Table 4.5 in Section 4.1.2. The neutral current magnitude ratio, showing the relationship between neutral current and zero sequence phase current, is defined by the following equation (5.2):

$$Ratio_h = I_{n,h} / \left(3 \times I_{0,h}\right) \times 100\% \tag{5.2}$$

where

$Ratio_h$ is the neutral current magnitude ratio at h harmonic order;

$I_{n,h}$ is the neutral current at h harmonic order;

$I_{0,h}$ is the zero sequence phase current at h harmonic order.

As we can observe from the simulation results in Figure 5.2, the neutral current ratio increases with higher frequency. The neutral current ratio has a steady-state value in the middle section. The explanation is similar to that of MGN in Section 4.1.2. However, the crucial difference is that the neutral current ratio decreases

when approaching the neutral terminals. Therefore, only the middle section of the neutral, named as the effective zone in Figure 5.2, contains the steady-state neutral current to effectively reduce the induced voltage on the buried pipeline from the zero sequence phase current. As been concluded in [70], if the neutral is about 1.2~1.5 times longer than the parallel zone, an adequate shielding effect can be provided by the IMGN.

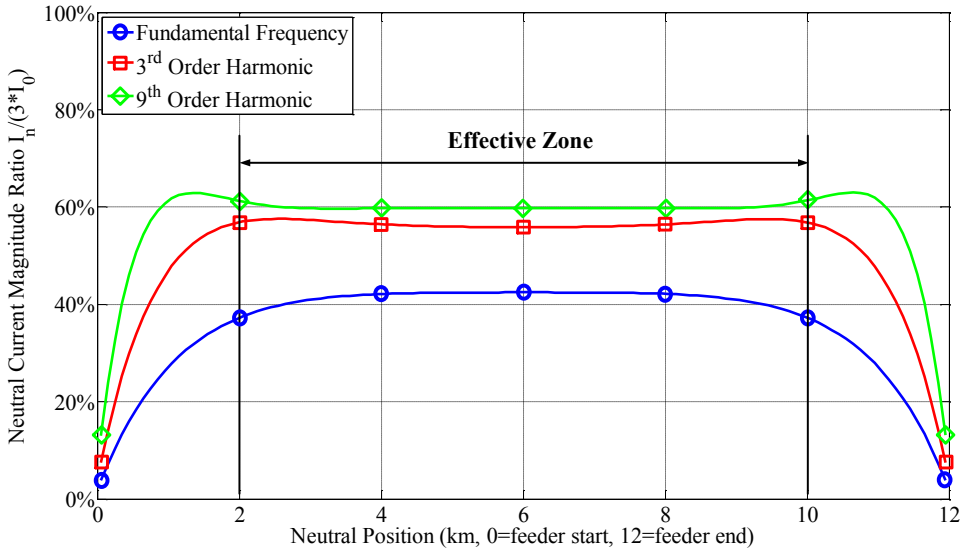

Figure 5.2: Neutral current ratios of islanded MGN system at different frequencies.

The mechanism of inductive coupling in IMGN system can be explained in Figure 5.3. The EMFs, produced by the phase currents ($e_{nk} = \sum Z_m I_0$), will create a circling current in each grounding segment. With enough segments in IMGN system, the current I_{k-1} and I_k will be nearly the same.

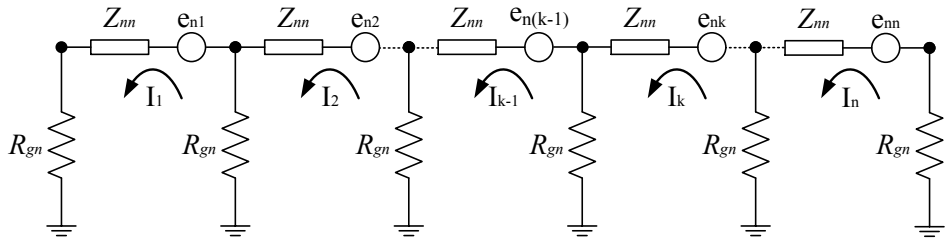

Figure 5.3: Mechanism of inductive coupling in IMGN system.

Similar to the prior MGN analysis, the relationship between the neutral current and the zero sequence phase current of the islanded MGN is shown as follows:

$$I_{n,h} = -\frac{Z_{na,h} + Z_{nb,h} + Z_{nc,h}}{3Z_{nn,h}} \times 3I_{0,h} \tag{5.3}$$

where

$Z_{na,h}$, $Z_{nb,h}$ and $Z_{nc,h}$ are the mutual impedance between neutral conductor and each phase conductor at h harmonic order;

$Z_{nn,h}$ is the self-impedance of the neutral conductor at h harmonic order;

$I_{n,h}$ is the neutral current at h harmonic order;

$I_{0,h}$ is the zero sequence phase current at h harmonic order.

Therefore, the total induced EMF on the buried pipeline from both phase and neutral conductors is

$$E_{total,h} = E_{phase,h} + E_{neutral,h} = I_{0,h}\left[\left(Z_{ap,h} + Z_{bp,h} + Z_{cp,h}\right) - \left(Z_{na,h} + Z_{nb,h} + Z_{nc,h}\right)\frac{Z_{np,h}}{Z_{nn,h}}\right] \tag{5.4}$$

where

$Z_{ap,h}$, $Z_{bp,h}$ and $Z_{cp,h}$ are the mutual impedance between the buried pipeline and each phase conductor at h harmonic order;

$E_{phase,h}$ is the total EMF of phase currents at h harmonic order;

$E_{neutral,h}$ is the EMF of neutral current at h harmonic order;

$E_{total,h}$ is the total EMF at h harmonic order.

If the geometrical distances between the buried pipeline and each conductor are much longer than the distances among each conductor, the mutual impedances between the buried pipeline and each conductor are nearly the same, so the equation (5.4) will be simplified to the following:

$$E_{total,h} \approx I_{0,h}\left(Z_{ap,h} + Z_{bp,h} + Z_{cp,h}\right)\left[1 - \frac{\left(Z_{na,h} + Z_{nb,h} + Z_{nc,h}\right)}{3Z_{nn,h}}\right] \tag{5.5}$$

Finally, the voltage reduction factor of the induced voltage on pipeline k_{IMGN}, defined in equation (5.6), can be used to assess the impact of IMGN.

$$k_{IMGN} = \left(1 - \left|\frac{V_{ind.IMGN}}{V_{ind}}\right|\right) \times 100\% = \left(1 - \left|1 - \frac{\left(Z_{na,h} + Z_{nb,h} + Z_{nc,h}\right)}{3Z_{nn,h}}\right|\right) \times 100\% \quad (5.6)$$

where $V_{ind.IMGN}$ is the induced voltage in the islanded MGN system and V_{ind} is the induced voltage without an islanded neutral.

Figure 5.4 shows the voltage reduction factor k_{IMGN} at the fundamental, 3rd and 9th order harmonic frequencies with different separation distances. The voltage reduction factor increases with higher frequency but is almost independent with the separation distance. The neutral will contain more current at a higher frequency, which leads to the increased cancellation of the total EMF. On the other hand, the distance between each phase conductor and neutral conductor is much shorter than the distance to the buried pipeline, so the total EMF can be seen as the production of one conductor from the buried pipeline perspective. Therefore, the voltage reduction factor is only related with the total EMF but independent with the separation distance. The average voltage reduction factors of IMGN at different frequencies are shown in Table 5.1. As a result, the IMGN can effectively mitigate the induced voltage at a higher frequency.

Table 5.1: Average voltage reduction factors of IMGN system at different frequencies.

	Fundamental	**3rd Order Harmonic**	**9th Order Harmonic**
k_{IMGN}	33.3%	53.2%	59.8%

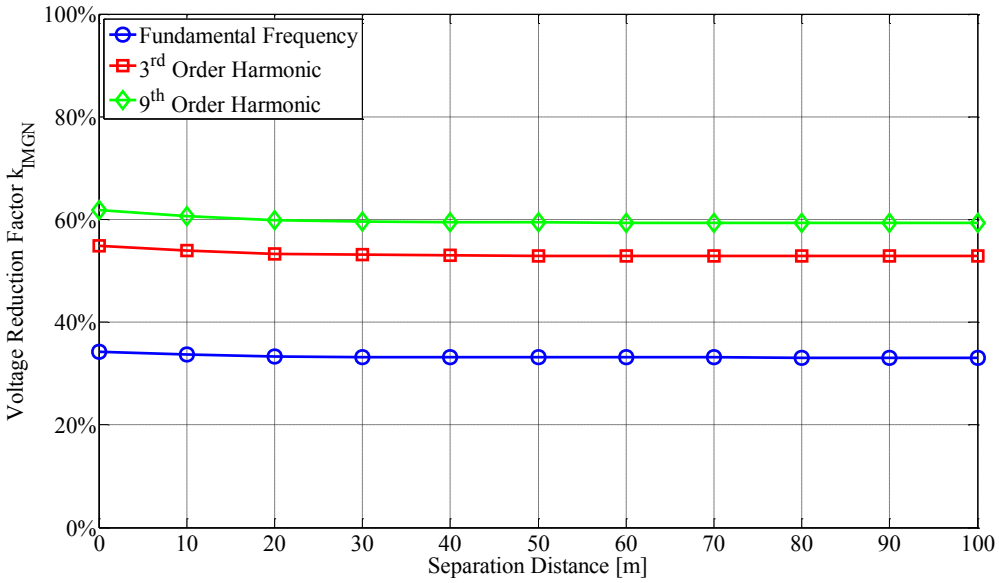

Figure 5.4: The voltage reduction of IMGN at fundamental, 3rd and 9th order harmonic frequencies.

5.3 Effectiveness of Mitigation Wire

Mitigation wire, a bare conductor buried at the same depth and closely parallel with the buried pipeline as shown in Figure 5.5, is often used to reduce the induced voltage on the pipeline. The mitigation wire can also be installed on the other side of the buried pipeline if applicable. The function of mitigation wire is to induce another EMF on the buried pipeline to reduce the total EMF from the power lines. Therefore, the mechanism of mitigation wire is similar to that of IMGN for mitigating the inductive coupling effect.

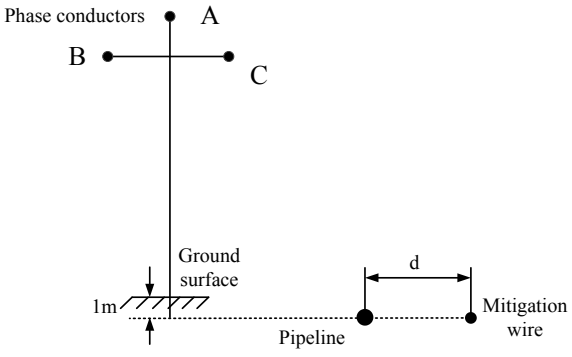

Figure 5.5: Scheme of mitigation wire parallel with buried pipeline.

The mechanism of current in the mitigation wire is explained first. As shown in Figure 5.6, the mitigation wire, buried in the soil, has a grounding resistance to the earth R_{gw} of each small segment ΔL that is similar to the analysis of the neutral current in IMGN. Furthermore, the grounding resistance is much larger than the resistance of the mitigation wire, so the current will mostly flow in the mitigation wire. Based on the assumption that the mutual impedance between the mitigation wire and each phase conductor is generally the same, the current of the mitigation wire can be calculated by the following equation:

$$I_w = -\frac{3Z_{wl}I_0}{Z_{ww}} \tag{5.7}$$

where

Z_{ww} is the self-impedance of the mitigation wire;

Z_{w1} is the mutual impedance between the mitigation wire and the phase conductor;

I_w is the current induced on the mitigation wire;

I_0 is the zero sequence phase current.

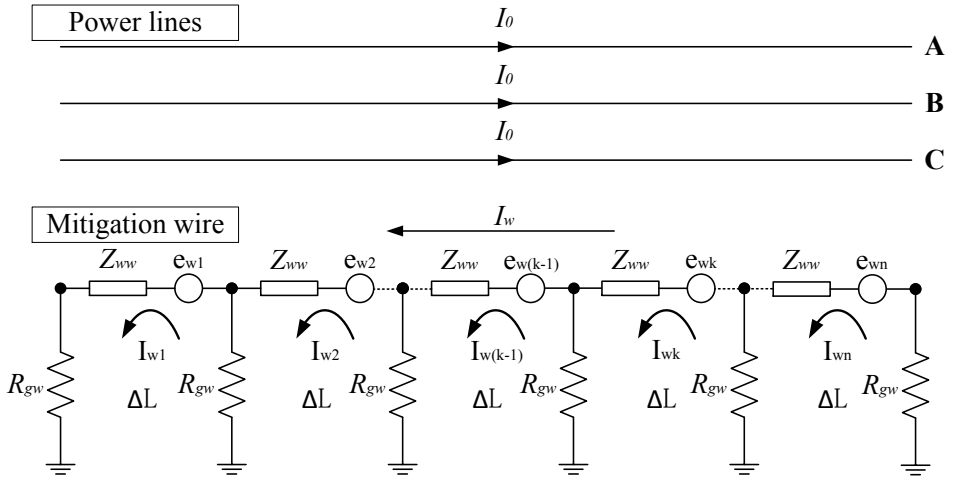

Figure 5.6: Mechanism of current flowing in the mitigation wire.

5.3.1 The Case of Fully Screened by the Mitigation Wire

Now, it is possible to discuss the effectiveness of applying mitigation wire. First, the case of pipeline fully screened by the mitigation wire is analyzed. In the absence of the mitigation wire, the EMF on the buried pipeline is

$$E_p = 3Z_{pl}I_0 \tag{5.8}$$

where

E_p is the induced EMF on the buried pipeline without mitigation wire;

Z_{pl} is the mutual impedance between the mitigation wire and the phase conductor.

With the mitigation wire, the total EMF on the buried pipeline includes two components both from the power line and the mitigation wire, so the total EMF can be calculated as

$$E_p^{'} = Z_{pw}I_w + E_p \tag{5.9}$$

where

$E_p^{'}$ is the induced EMF on the buried pipeline with mitigation wire;

Z_{pw} is the mutual impedance between the buried pipeline and the mitigation wire.

By solving the equation (5.7) (5.8) and (5.9), we obtain

$$E_p^{'} = 3Z_{p1}I_0\left(1 - \frac{Z_{pw}}{Z_{ww}}\frac{Z_{wl}}{Z_{p1}}\right) \tag{5.10}$$

As the mitigation wire is closely parallel with the buried pipeline, the mutual impedances Z_{w1} and Z_{p1} are equal. Therefore, the equation (5.9) can be simplified as the following:

$$E_p^{'} \approx E_p \left(1 - \frac{Z_{pw}}{Z_{ww}} \right) \tag{5.11}$$

Then, the voltage reduction factor k_{m} is

$$k_m = \left(1 - \left| \frac{E_p^{'}}{E_p} \right| \right) \times 100\% = \left(1 - \left| 1 - \frac{Z_{pw}}{Z_{ww}} \right| \right) \times 100\% \tag{5.12}$$

The effectiveness of this method depends on the mutual impedance, Z_{pw}, and self-impedance, Z_{ww}. The calculation of the mutual impedance between the buried pipeline and mitigation wire at the fundamental frequency is similar with that between the buried pipeline and phase conductor as discussed in the Chapter 2. The self-impedance of the bare conductor, depending on the material and the size of the bare conductor, is often provided by the data sheet at the fundamental frequency. For example, the self-impedance of 1/0 size bare copper conductor is 0.3+j0.7 Ω/km at the fundamental frequency [81].

At higher harmonic frequencies, the self and mutual impedances can be approximated by equation (5.13) and (5.14) respectively [63]:

$$Z_{ww,h} = 0.3 + j0.7 \times h \tag{5.13}$$

$$Z_{pw,h} = R_1 + jX_1 \times h \tag{5.14}$$

where

h is harmonic order;

$Z_{ww,h}$ is the self-impedance at h harmonic order;

$Z_{pw,h}$ is the mutual impedance at h harmonic order.

Then Figure 5.7 shows the voltage reduction factor of mitigation wire at each frequency. The main findings are

- the voltage reduction factor increases with higher frequency;

- the voltage reduction factor decreases with longer separation distance.

The term Z_{pw}/Z_{ww} increases with higher frequency, which is generally similar with the analysis of the IMGN mitigation method. As a result, the mitigation wire contains more current at a higher frequency. Finally, the voltage reduction factor increases with a higher frequency. On the other hand, the mutual impedance Z_{pw} decreases with a longer separation distance, so the EMF produced by the mitigation wire is smaller. However, the results in Figure 5.7 indicate that the voltage reduction factor is still effective when the separation distance is extended to 5 m. In conclusion, the mitigation wire can effectively mitigate the induced voltage at a higher frequency.

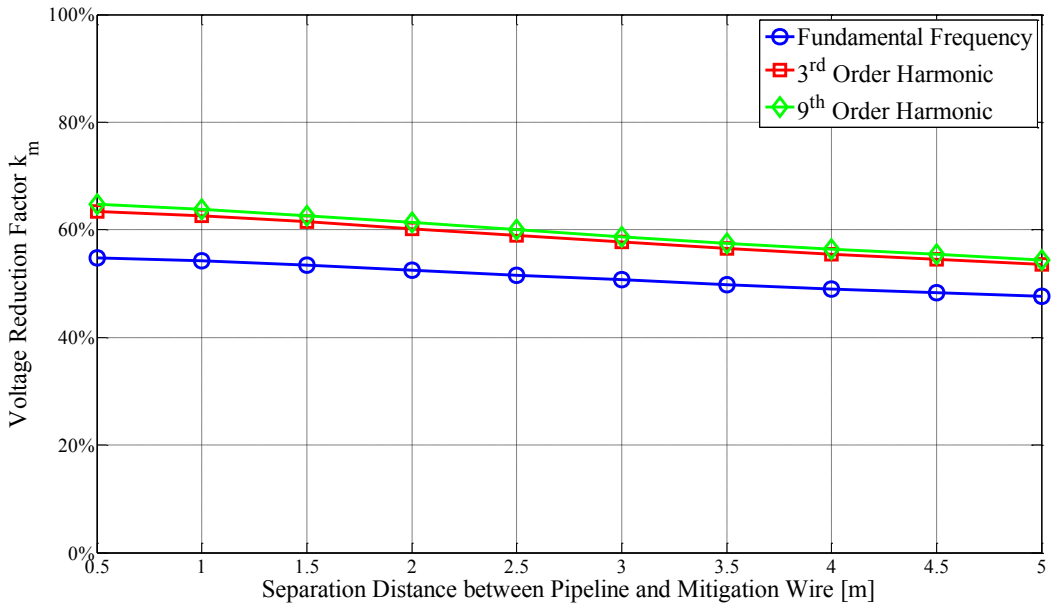

Figure 5.7: The voltage reduction of mitigation wire at fundamental, 3rd and 9th order harmonic frequencies.

If the mitigation wire is the same length as the zone of influence, the induced voltage along the entire pipeline will drop $k_{\mathrm{m}}V$. The situation of pipeline partially screened by mitigation wire will be analyzed at each frequency.

5.3.2 The Case of Partially Screened by the Mitigation Wire

As shown in Figure 5.8, a 1 km pipeline is screened by the mitigation wire of αL portion. The pipeline will be divided into two sections. There will be three extremities, A, B and C. A and B are the terminals of the buried pipeline. C is a moving point whose location changes with the different screened scales of the buried pipeline. The equivalent circuit is shown in Figure 5.9.

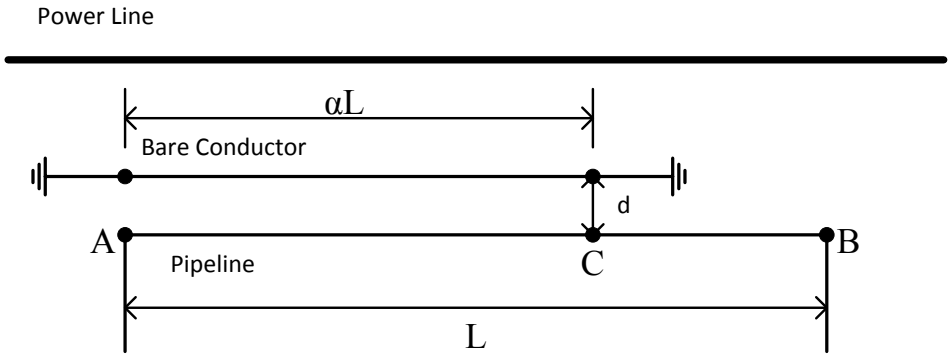

Figure 5.8: Pipeline partially screened by mitigation wire.

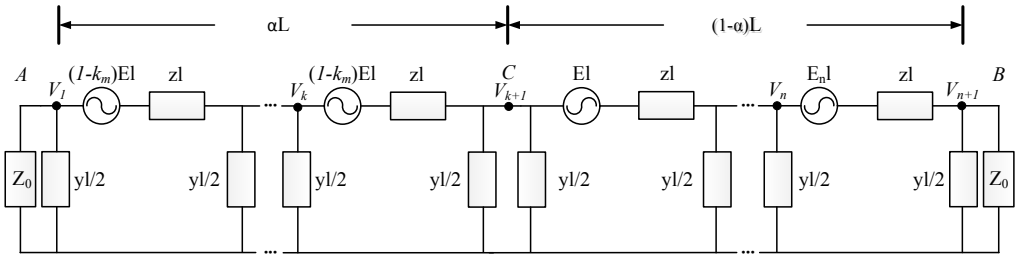

Figure 5.9: The equivalent circuit of pipeline partially screened by bare conductor.

Using the nodal admittance matrix method, the induced voltages at A, B and C can be calculated

$$\begin{bmatrix} V_1 \\ V_2 \\ \cdots \\ V_n \\ V_{n+1} \end{bmatrix} = \begin{bmatrix} Y_{11} & Y_{12} & \cdots & Y_{1n} & Y_{1,n+1} \\ Y_{21} & Y_{22} & \cdots & Y_{2n} & Y_{2,n+1} \\ \cdots & \cdots & \cdots & \cdots & \cdots \\ Y_{n1} & Y_{n2} & \cdots & Y_{nn} & Y_{n,n+1} \\ Y_{n+1,1} & Y_{n+1,2} & \cdots & Y_{n+1,n} & Y_{n+1,n+1} \end{bmatrix}^{-1} \begin{bmatrix} I_1 \\ I_2 \\ \cdots \\ I_n \\ I_{n+1} \end{bmatrix} \tag{5.15}$$

$$\begin{bmatrix} V_A \\ V_C \\ V_B \end{bmatrix} = \begin{bmatrix} V_1 \\ V_{k+1} \\ V_{n+1} \end{bmatrix} \tag{5.16}$$

where Y_{xx} is the sum of admittances connected to point X, and Y_{xy} is the negative value of admittance connecting point X and Y. $I_1 = (1 - k_m)E/z$, $I_{k+1} = (1 - k_m)\,E/z$, $I_{n+1} = -E/z$, $I_2 = \cdots = I_k = I_{k+2} = \cdots = I_n = 0$.

In the absence of mitigation wire, the maximum induced voltage is equal to $V_{\max} = \frac{E}{2\gamma}\left(1 - e^{-\gamma L}\right)$ appearing at terminal A and B, so the voltage reduction factors of induced voltage at A, B and C are

$$k_{m.A} = \left(1 - \left|\frac{V_A}{V_{\max}}\right|\right) \times 100\% \tag{5.17}$$

$$k_{m.B} = \left(1 - \left|\frac{V_B}{V_{\max}}\right|\right) \times 100\% \tag{5.18}$$

$$k_{m.C} = \left(1 - \left|\frac{V_C}{V_{\max}}\right|\right) \times 100\% \tag{5.19}$$

The voltage reduction factors at A, B and C will be compared at different frequencies with screened scale α from 0% to 100%. The separation distance *d* is assumed to be 2.5 m, which can generally reveal the average voltage reduction at each harmonic frequency. The average voltage reduction factor of 100% screened at each frequency is shown in Table 5.2.

Table 5.2: The average voltage reduction factor of mitigation wire at each frequency (d=2.5 m; α=100%).

	Fundamental	**3rd Order Harmonic**	**9th Order Harmonic**
k_m	51.6%	58.9%	60.0%

Figure 5.10 (a) (b) and (c) show the comparison of voltage reduction factors at different frequencies in the situation of a pipeline partially screened.

At terminals A and B, the difference of voltage reduction factor between each frequency is amplified with a larger screened scale of the pipeline. The explanation of this phenomenon is that, as more of the pipeline is screened, the reduced EMF resulting from the influence of the mitigation wire on the screened pipeline will become more and more dominant in the induced voltage calculation. Therefore, the difference of mitigation effects between each frequency is more obvious with the increasing of the screened scale.

At the moving point C, the voltage reduction factor increases up to almost 100% with the larger screened scale from 0% to 70% more or less, and then decreases to the average voltage reduction factor level until the point of a 100% screened scale. The voltage reduction factor first comes to 100% (the actual induced voltage is nearly zero) at the fundamental frequency, and then at the 3rd and 9th order harmonic frequencies. The reason is due to the difference of k_m at each frequency, as explained below.

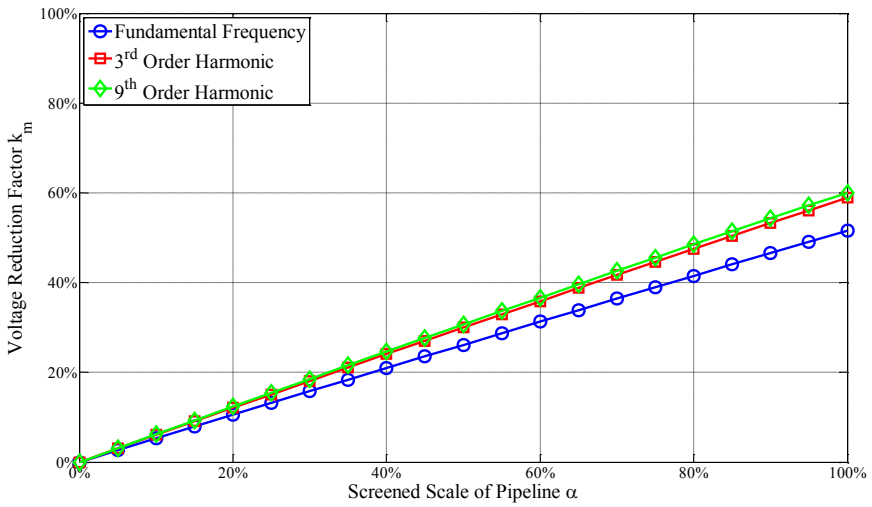

(a) Voltage reduction factor at terminal A

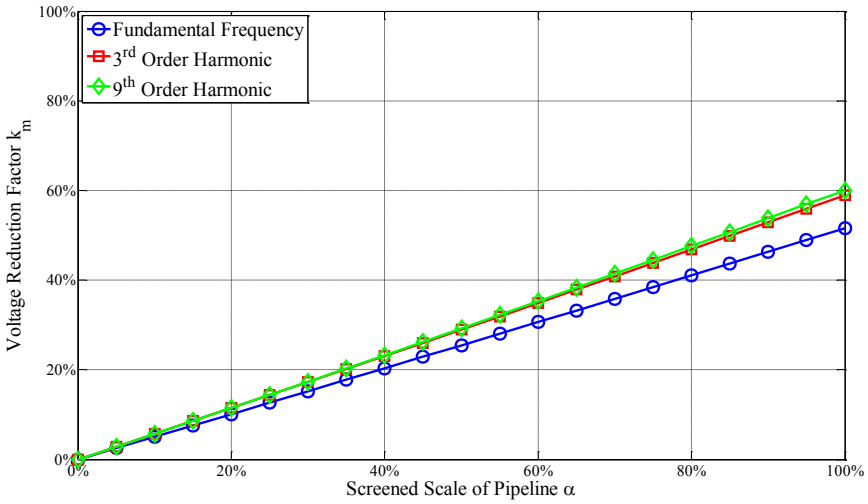

(b) Voltage reduction factor at terminal B

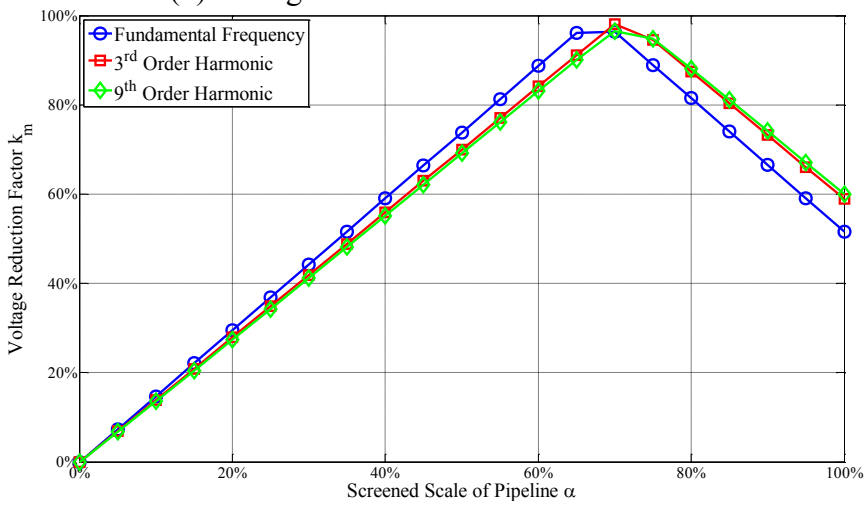

(c) Voltage reduction factor at moving point C

Figure 5.10: The comparison of voltage reduction factor at different frequencies in the situation of pipeline partially screened.

The general reason for the results in Figure 4.10 (c) is the voltage reduction factor k_m at each frequency. Figure 5.11 shows the lumped model in the situation of pipeline partially screened. The equivalent Norton circuit of the lumped model is shown in Figure 5.12.

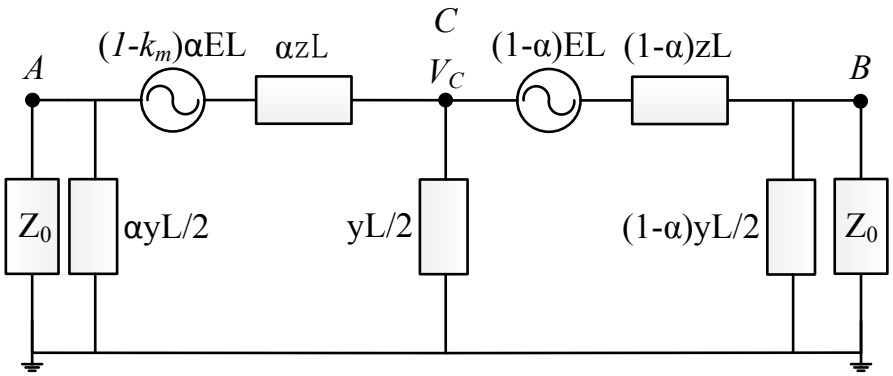

Figure 5.11: The lumped model in the situation of pipeline partially screened.

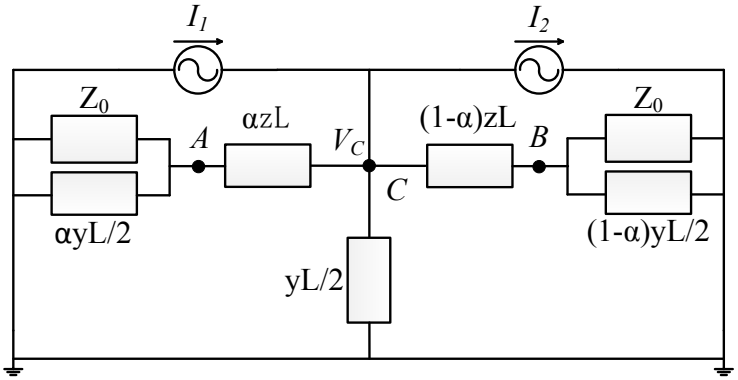

Figure 5.12: The equivalent Norton circuit of the lumped model.

The equivalent currents I_1 and I_2 are determined by the voltage sources and impedances as follows:

$$I_1 = \frac{(1-k_m)\alpha EL}{Z_0 \| \frac{2}{\alpha yL} + \alpha zL} \tag{5.20}$$

$$I_2 = \frac{(1-\alpha)EL}{Z_0 \| \frac{2}{(1-\alpha)yL} + (1-\alpha)zL} \tag{5.21}$$

If the induced voltage at point C is zero, the equivalent currents I_1 and I_2 should be equal. Therefore, the relationship between k_m and α is:

$$\frac{(1-k_m)\alpha EL}{Z_0 \| \frac{2}{\alpha yL} + \alpha zL} = \frac{(1-\alpha)EL}{Z_0 \| \frac{2}{(1-\alpha)yL} + (1-\alpha)zL} \tag{5.22}$$

Generally, the characteristic impedance Z_0 is much smaller than the grounding impedance and much larger than the series impedance of the pipeline. As a result, the equation (5.22) can be simplified as

$$\frac{(1-k_m)\alpha EL}{Z_0} = \frac{(1-\alpha)EL}{Z_0} \tag{5.23}$$

$$\alpha = \frac{1}{2-k_m} \tag{5.24}$$

So the screened scale of 100% voltage reduction at point C decreases with an increased k_m. Based on the values in Table 4.2, the screened scales are 67.4%, 70.9% and 71.4% at the fundamental, 3rd, and 9th order harmonic frequencies, further confirming the results in Figure 5.10.

The induced voltage at point C, however, is always smaller compared with the induced voltage at terminals, which means that the induced voltages at terminal A and B are the mitigation targets. Since the voltage reduction factors at terminal A and B are always increasing with higher frequencies. As a result, the mitigation wire method is more effective at a higher frequency.

5.4 Effectiveness of Pipeline Grounding

Grounding pipeline can reduce the local induced voltage. As shown in Figure 5.13, the buried pipeline is grounded by the grounding electrode in a series with a decoupler at its two terminals that are the extremities of the parallel zone. The grounding resistances at the two terminals are assumed to be the same. The decoupler is a capacitor-type of device to block DC current while allowing the flow of AC current in order to ground the pipeline without affecting the Cathodic Protection levels. The impedance of decoupler to AC current is 0.01 Ω at the

fundamental frequency, and will be even smaller at a higher frequency [82]. So in the context of the general value of grounding resistance, the decoupler will be neglected in further analysis.

The mitigation effect at the two terminals depends on the grounding resistance and the impedances of the buried pipeline seen at the terminals. The equivalent impedance outside the zone of influence is assumed to be the characteristic impedance of the buried pipeline. The equivalent impedance seen into the zone of influence depends on the parallel length. Figure 5.14 illustrates the equivalent circuit of pipeline after grounding.

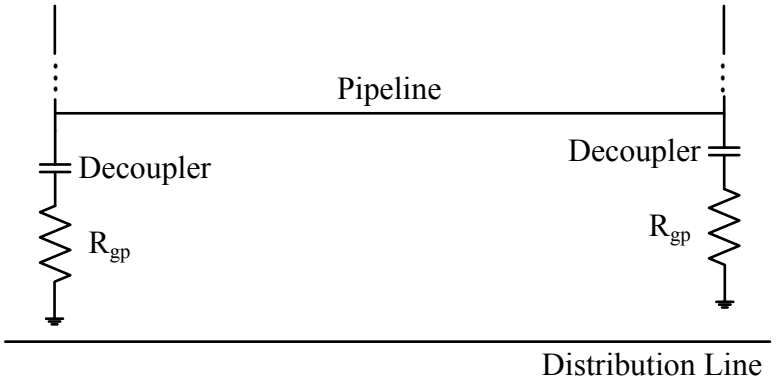

Figure 5.13: Scheme of grounding pipeline at terminals.

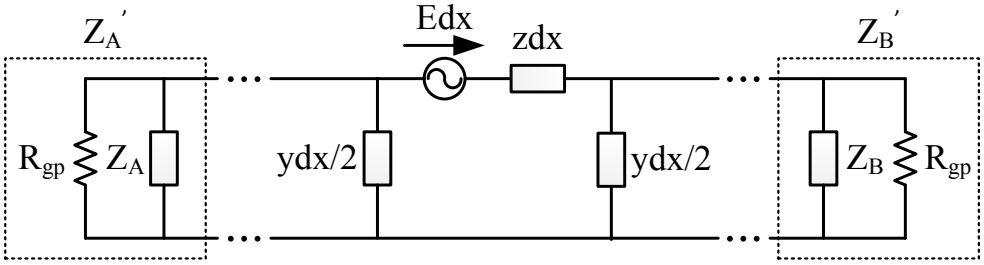

Figure 5.14: The equivalent circuit of pipeline after grounding.

The induced voltage is affected by the terminal impedance. The grounding resistance R_{gp} will change the terminal impedance to Z_A' and Z_B'. The voltage reduction factor k_g is derived in the following equations:

$$k_g = \left(1 - \left|\frac{V\left(Z_A^{'}, Z_B^{'}\right)}{V\left(Z_A, Z_B\right)}\right|\right) \times 100\% \tag{5.25}$$

$$Z_A = Z_B = Z_0 \tag{5.26}$$

$$Z_A^{'} = Z_B^{'} = Z_0 \parallel R_g = \frac{R_g}{Z_0 + R_g} Z_0 \tag{5.27}$$

where

Z_0 = characteristic impedance of pipeline;

R_{gp} = grounding resistance at pipeline terminals.

Assuming the parallel length is 1000 m, the relationship between the voltage reduction factor and pipeline grounding resistance can be achieved, as indicated in Figure 5.15. The following conclusions can be drawn:

- grounding pipeline is more effective at higher frequency;
- the difference of mitigation effectiveness between each frequency decreases with a larger grounding resistance.

The reason behind the first conclusion is that the characteristic impedance increases with a higher frequency. As parallel with the same grounding resistance, the larger impedance will be reduced more than the smaller impedance. Therefore, the voltage reduction factor k_g is larger at a higher frequency. Similarly, the differences of characteristic impedance at each frequency are reduced by the increasing of the grounding resistance. As a result, the difference of voltage reduction between each frequency is less obvious with increased grounding resistance.

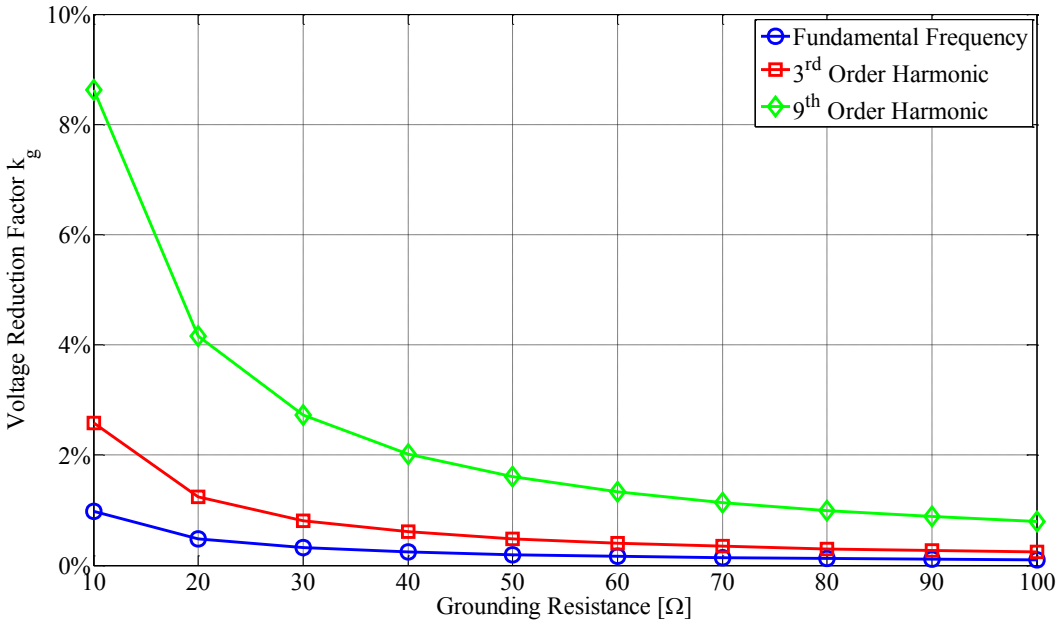

Figure 5.15: The voltage reduction of grounding pipeline at fundamental, 3rd and 9th order harmonic frequencies.

On the other hand, the parallel length also influences the effectiveness of grounding pipeline, so it is necessary to discuss this influence at different frequencies. Assuming the grounding resistance is 10 Ω, the impacts of parallel length on the voltage reduction factor at different frequencies are shown in Figure 5.16 (a) and (b). There are four main findings from the simulation results:

- the grounding mitigation method is more effective at higher frequency with longer parallel length;
- the voltage reduction factor is generally linear with the parallel length at each frequency when the buried pipeline is coated by the polyethylene material;
- the voltage reduction factor has a saturation value at each frequency with the buried pipeline coated by the bituminous material;
- the voltage reduction factor is smaller with bituminous coating than polyethylene coating at each frequency.

Due to the fact that the impedance of buried pipeline in the parallel zone increases with higher frequency and also longer parallel length, the induced voltage will drop more on the buried pipeline than the grounding resistance. This phenomenon is then reflected by the increasing of the voltage reduction factor at a higher frequency with longer parallel length.

The rationale for the second and third findings is similar to that of the sensitivity study of parallel length on the induced voltage in Section 4.2.3. If the product of the propagation constant and parallel length is small enough, the induced voltage is almost linear with the parallel length. If the production is large enough, the induced voltage is almost constant. Since the grounding resistance does not change either the propagation constant or parallel length, the voltage reduction factor has the same relationship with parallel length at each frequency, under the condition of different coating materials.

For the last finding, the impedance of buried pipeline with bituminous coating is smaller than with polyethylene coating, so the parallel section impedance is small compared to the terminal impedance. As a result, most of the voltage drop is still on the terminal impedance, and therefore the grounding resistance will less effectively reduce the voltage on buried pipeline with bituminous coating even at a higher frequency.

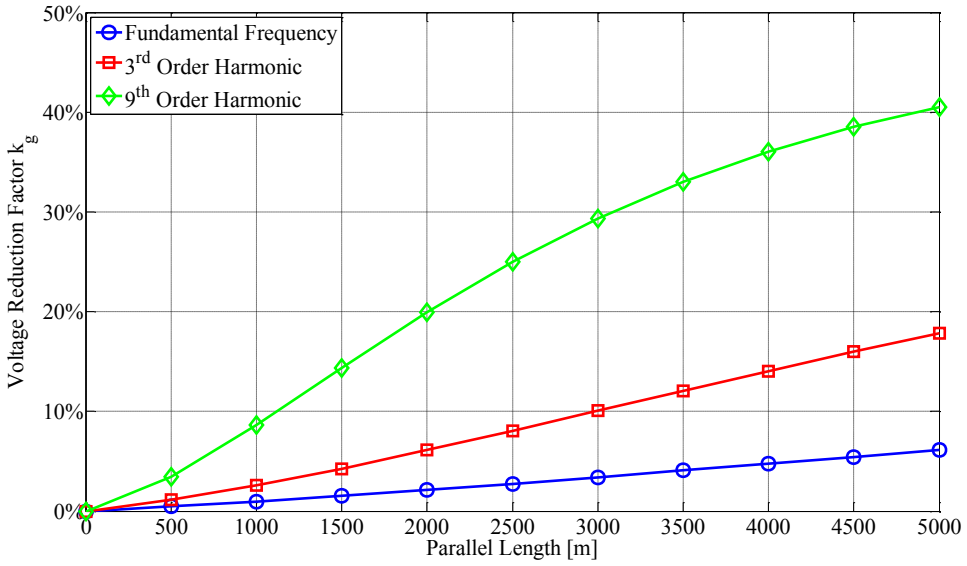

(a) Polyethylene coating

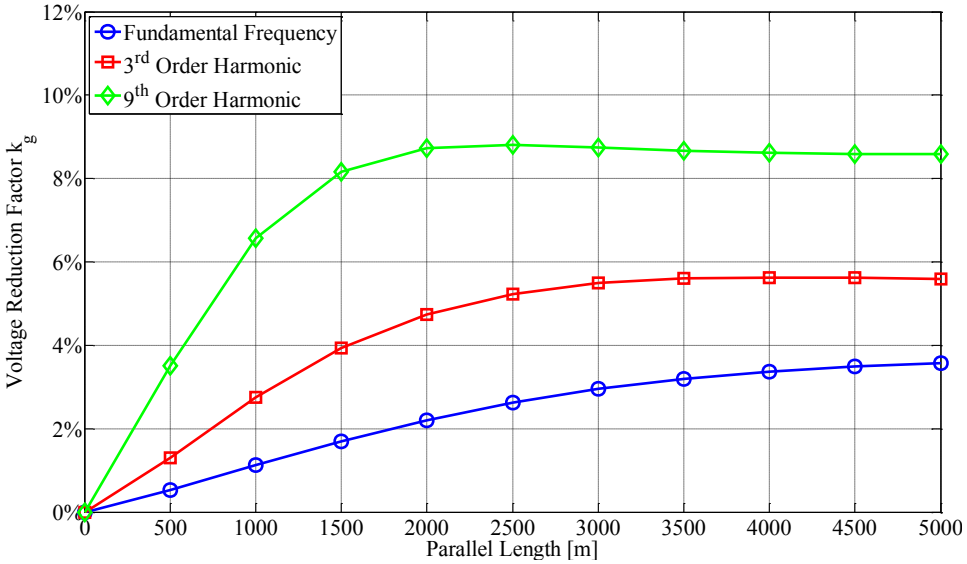

(b) Bituminous coating

Figure 5.16: The impact of parallel length on voltage reduction factor k_g.

Overall, the effectiveness of grounding pipeline increases with higher frequency but is limited by the parallel length and coating material. This mitigation method is more effective for buried pipeline with long parallel length and polyethylene coating. On the other hand, multiple grounding electrodes with low grounding resistance may be required to build a grounding structure in order to significantly reduce the grounding resistance. However, this solution is not feasible to the areas with high soil resistivity.

5.5 Summary

Based on the above analysis, the three potential methods for mitigating inductive coupling from distribution power line to pipeline at each frequency are the following:

- installation of IMGN;
- installation of mitigation wire;
- pipeline grounding.

The methods of IMGN and mitigation wire have the same mitigation mechanism. The current in the installed conductor, produced by the inductive coupling of zero

sequence phase current, can partially cancel the total EMF on the buried pipeline. As a result, the induced voltage on buried pipeline will be reduced.

The effectiveness of IMGN mainly depends on the current flowing in the neutral conductor. Based on the analysis, the neutral current is determined by the ratio of mutual impedance (between neutral conductor and each phase conductor) and self-impedance of neutral conductor. This ratio increases with higher frequency, so the IMGN mitigation method is more effective at higher frequency.

The mitigation wire, located closely to the buried pipeline, can provide better mitigation at a higher frequency. The effectiveness of mitigation wire decreases with a longer separation distance and increases with a larger pipeline screened scale. Neither the separation distance nor the pipeline screened scale changes the relationship of voltage reduction factor between each frequency. However, the difference of voltage reduction factor between each frequency is amplified with bigger pipeline screened scale while the separation distance does not influence the difference of the voltage reduction factor between each frequency.

The effectiveness of grounding pipeline increases with a higher frequency due to the fact that the impedance of buried pipeline increases with higher frequencies, but the voltage reduction factor is limited by the parallel length and coating material. This mitigation method is more effective for buried pipeline at higher frequency with long parallel length and polyethylene coating. On the other hand, the necessity of a low grounding resistance value may require multiple grounding electrodes in the field application and sometimes can hardly be met in the areas with bad soil conditions. As a result, this mitigation method is not always applicable.

Chapter 6

Conclusions and Future Work

This thesis discusses the topics related to the voltage induction on pipeline caused by the power line harmonic current. The 3^{rd} and 9^{th} order harmonic currents, which are dominant in zero sequence, will significantly influence the buried pipeline with higher induced voltages. Detailed analysis is conducted on the method of calculating induced voltage and the potential pipeline issues at harmonic frequencies. Sensitivity studies of different parameters from pipeline and distribution line perspectives reveal their impacts on the induced voltage at harmonic frequencies by the comparison with the fundamental frequency. In addition, the mitigation methods, focusing on the 3^{rd} and 9^{th} induced voltage reduction, are investigated. The major conclusions and achievement of this thesis are summarized as follows:

- An extensive survey on the inductive coordination between the power transmission line and buried pipeline at the fundamental frequency is conducted to explain the mechanism, theoretical evaluation method, and potential issues of induced voltage on buried pipeline. These findings can be applied to the distribution line cases since both transmission and distribution lines follow the same induction principle.

- The field measurements of currents in different distribution feeders are reviewed to extract the common features of the harmonic situation in the current distribution system. Current measurements in the residential feeders contain much stronger harmonics (3^{rd} ~9^{th}) in the distribution system. The values of IDD for each harmonic decrease from low order to high order harmonics.

- The analytical method of calculating induced voltage at harmonic frequencies is fully discussed. The adopted methods for the mutual and self-impedance calculation at harmonic frequencies have already been discussed and verified in many published papers through analytical study and finite-element method simulation. A simplified equation for the mutual impedance calculation is developed from Carson's formula to support the calculation up to 540 Hz and 100 m separation distance under 30 Ωm soil resistivity. The margin of the error with this equation can be controlled within 5% based on the simulation results.

- The per-unit-current induced voltage increases with higher frequency. The zero sequence current is the most significant source of induced voltage on buried pipeline rather than the positive and negative sequence currents. Considered the realistic value of each sequence current magnitude, the zero sequence induced voltage is still dominant in the total induced voltage at any frequency. The induced voltages at the 3^{rd} and 9^{th} order harmonic frequencies, based on the measurements from residential feeders, are larger than that at the fundamental frequency.

- The corrosion rate of the fundamental, 3^{rd}, and 9^{th} order harmonic frequencies are comparable, and it is slightly larger when three frequency currents combine together. As a result, the potential pipeline AC corrosion at high frequencies needs to be considered.

- Through the sensitivity study, the main factors influencing the degree of inductive coupling caused by the 3^{rd} and 9^{th} order harmonic currents in distribution line are as follows: multi-grounded neutral, soil resistivity,

coating material, and parallel length. The neutral in the MGN system will play a significant role of reducing the induced voltage on buried pipeline at harmonic frequencies. The influence of soil resistivity can be amplified at a higher frequency, and this difference is more obvious with lower soil resistivity than higher soil resistivity. The polyethylene coating will create a larger induced voltage because its insulating property is much better than that of bituminous coating. This phenomenon is more obvious at the 9^{th} order harmonic than at the 3^{rd} order harmonic and fundamental frequency. The induced voltage increases faster at a higher frequency with longer parallel length. The pole structure has limited impact on induced voltage because the differences of pole height and arm size are much smaller than the geometrical distances between phase conductors and buried pipeline.

- The three potential methods for mitigating inductive coupling from the distribution power line to the buried pipeline are IMGN, mitigation wire and pipeline grounding. The methods of IMGN and mitigation wire have the same mitigation mechanism. The effectiveness of IMGN mainly depends on the current flowing in the neutral conductor. The neutral current increases with a higher frequency, so the IMGN mitigation method is more effective at a higher frequency. Similarly, the mitigation wire, located closely to the buried pipeline, can provide better mitigation at higher frequency. The effectiveness of mitigation wire decreases with a longer separation distance and increases with a larger pipeline screened scale. The effectiveness of pipeline grounding increases with higher frequency due to the fact that the impedance of buried pipeline increases with a higher frequency, but the voltage reduction factor is limited by the parallel length and coating material. This mitigation method is more effective for buried pipeline at a higher frequency with long parallel length and polyethylene coating. Due to the uncertainty of the soil condition, however, the pipeline grounding method is not always applicable.

More work is needed to extend and modify the findings of this thesis in the future. The suggestions for future work are summarized as follows:

- This thesis only analyzes the inductive coordination between distribution line and buried pipeline. In the future, it would be desirable to investigate the impact of undergrounding cable on the buried pipeline.

- In this thesis, there are only four experiments testing the pipeline AC corrosion rate under mixed frequencies including the fundamental, 3^{rd}, and 9^{th} order harmonic components due to the long time consuming. The impact of AC induced voltage waveform on pipeline corrosion should be further investigated through more corrosion experiments. As a result of more study, the impact of the harmonic current on pipeline AC corrosion will be explained more adequately.

- The effectiveness of the pipeline grounding method is restricted by the soil conditions. IMGN and mitigation wire methods are effective but may cost a lot to build if the parallel section is too long. Thus, new mitigation methods are needed to be developed for reducing the induced harmonic voltages.

References

[1] J. Pohl, “Influence of High-Voltage Overhead Lines on Covered Pipelines”, CIGRE Paper No. 326, Paris, France, June 1966.

[2] B. Favez and J. C. Gougeuil, “Contribution to Studies on Problems Resulting from the Proximity of Overhead Lines with Underground Metal Pipe Lines”, CIGRE Paper No. 336, Paris, France, June 1966.

[3] CSA C22.3 No.6-13, “Principles and practices of electrical coordination between pipelines and electric supply lines,” 2013.

[4] NACE SP0177-2014, “Mitigation of alternating current and lightning effects on metallic structures and corrosion control systems,” 2014.

[5] IEEE, “IEEE guide for safety in AC substation grounding,” *IEEE Std 80-2000*, vol., no., pp.i,192, 2000.

[6] NACE International Task Group 327, “AC corrosion state-of-the-art: corrosion rate, mechanism, and mitigation requirements,” *NACE International*, January 2010.

[7] L. Di Biase, “Corrosion due to alternating current on metallic buried pipeline: background and perspectives,” *Committee on the Study of Pipe Corrosion and Protection*, *5th International Congress*, Bruxelles, Belgium, CEOCOR, 2000

[8] I. Ragault, “AC corrosion induced by V.H.V electrical lines on polyethylene coated steel gas pipelines,” *CORROSION/1998*, paper no. 557, Houston, TX: NACE, 1998.

[9] D. Funk, H.G. Schoeneich, “Problems with coupons when assessing the AC-corrosion risk of pipeline,” *3R International*, *Special Steel Pipeline* 41, 10-11 (2002): p. 54.

[10] W. Bruchkner, “The effects of 60 cycle alternating current on the corrosion of steels and other metals buried in soils,” University of Illinois, *Technical Bulletin* No. 470, November 1964.

[11] M. Yunovich, N.G. Thompson, “AC corrosion: corrosion rate and mitigation requirements,” *CORROSION/2004*, paper no. 206, Houston, TX: NACE, 2004.

[12] C. Goran, “Alternating current corrosion on cathodically protected steel in soil – A long term field investigation,” 5th International Congress, Bruxelles, Belgium, CEOCOR, 2000.

[13] J. Williams, “Corrosion of metals under the influence of alternating current,” *Materials Protection* 5, 2, 1966.

[14] W. Prinz, “Alternating current corrosion of cathodically protected pipelines,” *Proceedings of the 1992 International Gas Research Conference*, November 1992.

[15] S. Pookote, D. T. Chin, “Effect of alternating current on the underground corrosion of steels,” *Materials Performance* 17, 3, 1978.

[16] R. Gummow, R. Wakelin, S. Segall, "AC Corrosion-A new challenge to pipeline integrity," CORROSION/98, paper no. 566, Houston, TX: NACE, 1998.
[17] S. Goidanich, L. Lazzari, M. Ormellese, M.P. Pedeferri, "Influence of AC on carbon steel corrosion in simulated soil conditions," *16th International Corrosion Congress*, paper 04-03, Sept., 2005.
[18] G. Helm, T. Helm, H. Heinzen, W. Schwenk, "Investigation of corrosion of cathodically protected steel subjected to alternating currents," *3R International* 32, 5 (1993), p. 246.
[19] W. Prinz, "Alternating current corrosion of cathodically protected pipelines," Proceedings of the 1992 International Gas Research Conference, Nov., 1992.
[20] (D.T. Chin, T.W. Fu, "Corrosion by Alternating Current: A Sudy of the Anodic Polarization of Mild Steel in Na2SO4 Solution," *Corrosion* 35, 11 (1979): p. 514.
[21] F. Stalder, "AC corrosion of cathodically protected pipelines. Guidelines for risk assessment and mitigation measures, Annex N.5-4," Proceedings of the 4th International Congress, held 2002, (Groniue, Holland: CEOCOR).
[22] A. Pourbaix, P. Carpentiers, R. Gregoor, "Detection and Assessment of Alternating Current Corrosion," *Materials Performance* 38, 3 (2000): pp. 34-39.
[23] D. Jones, "Effect of Alternating Current on Corrosion of Low Alloy and Carbon Steels," *Corrosion* 24, 12 (1978): p. 428.
[24] L.V. Nielsen, P. Cohn, "AC corrosion in pipelines. Field experiences from a highly corrosive test site using ER corrosivity probes," Proceedings of the 6th International Congress, held 2003 (Groniue, Holland: CEOCOR).
[25] S. Goidanich, "Influence of alternating current on metals (sic) corrosion," PhD thesis, Politecnico di Milano, 2005.
[26] R.D. Floyd, "Testing and Mitigation of AC Corrosion on 8" Line: A Field Study," CORROSION/2004, paper no. 210 (Houston, TX: NACE, 2004).
[27] S.Z. Fernandes, S.G. Mehendale, S. Venkatachalam, "Influence of Frequency of Alternating Current on the Electrochemical Dissolution of Mild Steel and Nickel," *Journal of Applied Electrochemistry* 10, 5 (1980): pp. 649-654.
[28] M.L. Mateo, T. Fernandez Otero, D.J. Schiffrin, "Mechanism of Enhancement of the Corrosion of Steel by Alternating Currents and Electrocatalytic Properties of Cycled Steel Surfaces," *Journal of Applied Electrochemistry* 20, 1 (1990): pp. 26-31.
[29] M. Yunovich, N.G. Thompson, "AC corrosion: mechanism and proposed model,", Proceedings of International Pipeline Conference 2004, paper no. IPC04-0574, held October 4-8, 2004 (Materials Park, OH: ASME).
[30] A.W. Hamlin, "Alternating Current Corrosion," *Materials Performance* 25, 1 (1986): p. 55.
[31] R. Radeka, D. Zorovic, D. Barisin, "Influence of frequency of alternating current on corrosion of steel in seawater," *Anti-Corrosion Methods* 27, 4 (1980): p. 13.

[32] H. Song, Y. Kim, S. Lee, Y. Kho, Y. Park, " Competition of AC and DC Current in AC Corrosion Under Cathodic Protection," *CORROSION/2002*, paper no. 117 (Houston, TX: NACE, 2002).
[33] M. A. Pagano, S. B. Lalvani, "Corrosion of Mild Steel Subjected to Alternating Voltage in Seawater," *Corrosion Science*, vol.36, no. 1, pp 127-140, 1994.
[34] ISO International Standard 15589-1, "Petroleum and natural gas industries Cathodic protection of pipeline transportation systems Part 1: On-land pipelines," 2003.
[35] CEN/TS 15280, "Evaluation of A.C. Corrosion Likelihood of Buried Pipelines— Application to Cathodically Protected Pipelines" (London, England: BSI)
[36] Electrical Transmission and Distribution Reference Book, Fourth Edition. Westinghouse Electric Corp., 1964.
[37] Directives Concerning the Protection of Telecommunication Lines Against Harmful Effects from Electricity Lines. International Telegraph and Telephone Consultative Committee (CCITT), International Telecommunications Union, 1962.
[38] Taflove, Allen; Dabkowski, John, "Prediction Method for Buried Pipeline Voltages Due to 60 Hz AC Inductive Coupling Part I-Analysis,"*Power Apparatus and Systems, IEEE Transactions on*, vol.PAS-98, no.3, pp.780,787, May 1979.
[39] Dabkowski, John; Taflove, Allen, "Prediction Method for Buried Pipeline Voltages Due to 60 Hz AC Inductive Coupling Part II--Field test Verification,"*Power Apparatus and Systems, IEEE Transactions on*, vol.PAS-98, no.3, pp.788,794, May 1979.
[40] E. F. Vance, DNA Handbook Revision, Chapter 11, Coupling to Cables (for Dept. of the Army, Contract DAAG39-74-C-0086). Stanford Research Institute, Menlo Park, CA, December 1974.
[41] "Electromagnetic Effects of Overhead Transmission Lines- Practical Problems, Safeguards, and Methods of Calculation," by IEEE Working Group on E/M and E/S Effects of Transmission Lines, IEEE Trans. Power App. Systems, Vol. PAS-94, pp. 892-899,May/June 1974.
[42] A. W. Peabody and A. L. Verhiel, "The Effects of High Voltage Alternating Current (HVAC) Transmission Lines on Buried Pipelines," Paper No. PCI70-32 presented at IEEE/IGA Petroleum and Chemical. Industry Conference, Tul sa, Oklahoma, 15 September 1970.
[43] C. G. Siegfried, "AC Induced Interference on Pipelines," presented at Interpipe 73 Conference, Houston, Texas, 31 October 1973.
[44] C. A. Royce, "Alternating Current Problems of Pipelines," presented at A.G.A. Operating Section Transmission Conference, Houston, Texas, 18 May 1971.
[45] E. C. Paver, Sr., "The Effects of Induced Current on a Pipeline," Paper No. 54 presented at NACE 26th Annual Conference, Philadelphia, Pa., 2-6 March 1970.

[46] M. A. Puschel, "Power Lines and Pipelines in Close Proximity During Construction and Operation," Material Performance Vol. 12, pp. 28-32, December 1973.
[47] D. N. Gideon et al., Final Report on Project Sanguine Parametric Study of Costs for Interference Mitigation in Pipelines (to IIT Research Institute). Battel le Col umbus Laboratories, Columbus, Ohio, 30 September 1971.
[48] J. R. Sherbundy, "The Effects of High Voltage Overhead Transmission Lines on Underground Pipelines", MSc Thesis, Department of Electrical Engineering, Ohio State University, 1975.
[49] Reilly, J.P., "Electric Field Induction of Long Objects - a Methodology for Transmission Line Impact Studies," *Power Apparatus and Systems, IEEE Transactions on*, vol.PAS-98, no.6, pp.1841,1852, Nov. 1979
[50] Jaffa, Kent C.; Stewart, J.B., "Magnetic Field Induction From Overhead Transmission and Distribution Power Lines on Buried Irrigation Pipelines," *Power Apparatus and Systems, IEEE Transactions on*, vol.PAS-100, no.3, pp.990,1000, March 1981
[51] Subcommittee, G.S., "Electromagnetic Effects of Overhead Transmission Lines Practical Problems, Safeguards, and Methods of Calculation," *Power Apparatus and Systems, IEEE Transactions on*, vol.PAS-93, no.3, pp.892,904, May 1974.
[52] H.W. Dommel, J.H. Sawada "Report on the Calculation of Induced Voltages and Currents on Pipelines Adjacent to AC Power Lines," CEA Contract No. 75-02, 1976.
[53] F. P. Dawalibi, R.D. Southey, J. Ma, and Y. Li, "On the Mechanisms of Electromagnetic Interference between Electrical Power Systems and Neighboring Pipelines", *NACE 2000 T10B Symposium on DC & AC Interference*, Orlando, March 26-31, 2000.
[54] CDEGS Software Package Safe Engineering Services & Technologies Brochures, available online at http://www.sestech.com/products/Brochures/SES-CDEGS.pdf
[55] Wang, H., "Harmonic Impact of Modern Residential Loads on Distribution Power System and Mitigation Solutions," M.Sc. dissertation, University of Alberta, fall 2011.
[56] W. Xu, J. Yong, "Harmonic characteristics in distribution systems supplying residential loads," *APIC Project* 2015.
[57] D. H. Boteler, "Measurements of Higher Harmonics in AC Interference on Pipelines," *CORROSION 2010 Conference&Expo*, paper no. 10107, 2010.
[58] D. H. Boteler, K. Malmborn, H. E. Edwal, "AC Interference on Ppelines in Southern Sweden," *CEOCOR*, paper no. 17, 2013.
[59] EPRI Document EL-904, "Mutual design considerations for overhead AC transmission lines and gas transmission pipelines," 1978.
[60] CIGRE Working Group 36.02 Guide, "Guide on the influence of high voltage AC power systems on metallic pipelines," 1995.
[61] F. Pollaczek, "Uber das feld einer unendlich langen wechselstrom durchlossenen einfachleitung," E.N.T., vol. 3, no. 9, pp. 339–359, 1926.
[62] J. R. Carson, "Wave propagation in overhead wires with ground return, Bell

Syst. Tech. J., vol. 5, pp. 539–554, 1926.
[63] H.W. Dommel, “EMTP Theory Book Second Edition” May, 1992.
[64] Ametani, A.; Miyamoto, Y.; Baba, Y.; Nagaoka, N., "Wave Propagation on an Overhead Multiconductor in a High-Frequency Region," *Electromagnetic Compatibility, IEEE Transactions on*, vol.56, no.6, pp.1638,1648, Dec. 2014.
[65] W. H. Wise, “Potential coefficients for ground return circuits,” Bell Syst. Tech. J., vol. 27, pp. 365–371, 1948.
[66] H. Kikuchi, “Wave propagation on the ground return circuit in high frequency regions,” J. IEEE Jpn., vol. 75, no. 805, pp. 1176–1187, 1955.
[67] M. Nakagawa, A. Ametani, and K. Iwamoto, “Further studies on wave propagation in overhead lines with earth return: Impedance of stratified earth,” Proc. IEEE, vol. 120, no. 12, pp. 1521–1528, 1973.
[68] A. Ametani, “Stratified earth effects on wave propagation − frequency dependent parameters −,” IEEE Trans. Power App. Syst., vol. 93, no. 5, pp. 1233–1239, Sep. 1974.
[69] Lucca, G., "Mutual impedance between an overhead and a buried line with earth return," *Electromagnetic Compatibility, 1994., Ninth International Conference on*, vol., no., pp.80,86, 5-7 Sep 1994.
[70] Y. Wang, J. Acharya, W. Xu, “Shielding effect of multi-grounded neutral wire in the distribution system,” *Euro. Trans. Electr. Power* 2011; 21:624-634, 2011.
[71] E. D. Sunde, Earth Conduction Effects in Transmission Systems, New York: Dover Publications, 1968, pp. 14-16 and pp. 146-149.
[72] Theethayi, N.; Thottappillil, R.; Paolone, M.; Nucci, C.A.; Rachidi, F., "External impedance and admittance of buried horizontal wires for transient studies using transmission line analysis," *Dielectrics and Electrical Insulation, IEEE Transactions on*, vol.14, no.3, pp.751,761, June 2007.
[73] EPRI Progress Report, “Engineering the Multiple Use of the Right of Way”, 2006.
[74] IEC/TS, “Effect of current on human beings and livestock – part 1: general aspects,” *IEC/TS 60479-1-2005*, 2005.
[75] P. N. Saveskie, “Earth Constants,” *TAI Inc Consuletter International*, Vol. 6, No. 5, 2000.
[76] Papagiannis, G.K.; Triantafyllidis, D.G.; Labridis, D.P., "A one-step finite element formulation for the modeling of single and double-circuit transmission lines," *Power Systems, IEEE Transactions on* , vol.15, no.1, pp.33,38, Feb 2000.
[77] Tsiamitros, D.A.; Papagiannis, G.K.; Labridis, D.P.; Dokopoulos, P.S., "Earth return path impedances of underground cables for the two-layer earth case," *Power Delivery, IEEE Transactions on* , vol.20, no.3, pp.2174,2181, July 2005.
[78] Tsiamitros, D.A.; Christoforidis, G.C.; Papagiannis, G.K.; Labridis, D.P.; Dokopoulos, P.S., "Earth conduction effects in systems of overhead and underground conductors in multilayered soils," *Generation, Transmission and Distribution, IEE Proceedings-* , vol.153, no.3, pp.291,299, 11 May 2006.
[79] Distribution Pole Structure Data Sheet, provided by utility companies.

[80] W. Xu, “MHLF Reference Manual: Documentation in Support of the Multiphase Harmonic Load Flow Program,” 1991.
[81] Bare Copper Ground Wire Conductor Data, available online at http://www.generalcable.com/NR/rdonlyres/813CFAE6-B133-4E76-87A6-D1D499DFD95C/0/BrCpprCondGrndSS.pdf
[82] Henry Tachick, “Decoupler Applications in Cathodically Protected Systems,” Calgary 2013.
[83] ASME B36.19M-2004, “Stainless Steel Pipe,” 2004.

Appendix A.

Neutral Current of Multi-grounded Neutral

This appendix provides study results for neutral current of MGN system at fundamental frequency in normal condition. The current distributions along the neutral of full neutral configuration are simulated by the EMTP-based multiphase harmonic load flow (MHLF) program.

The neutral current is the combination of the conducted and induced neutral currents. Sensitivity studies of different grounding resistances, grounding spans and load types (branch number and load span) show that the neutral current $I_{neutral}$ settles to a steady-state value, which is about 30% of $3I_0$ at about 4 km from the load neutral point. Table A.1 summarizes the distribution system parameters used in the simulation and Figure A.1 shows the current distribution along the neutral.

Table A.1: Distribution system parameters for Full MGN simulation.

Voltage level	25 kV
Feeder length	12 km
Substation grounding resistance	0.15 Ω
Unbalanced lumped load	5, 5.5, 4.5 MVA
Distributed load span	100, 200, 300, 400, 500m
Neutral grounding resistance	7, 15, 30 Ω
Neutral grounding span	50, 100, 250, 500 m

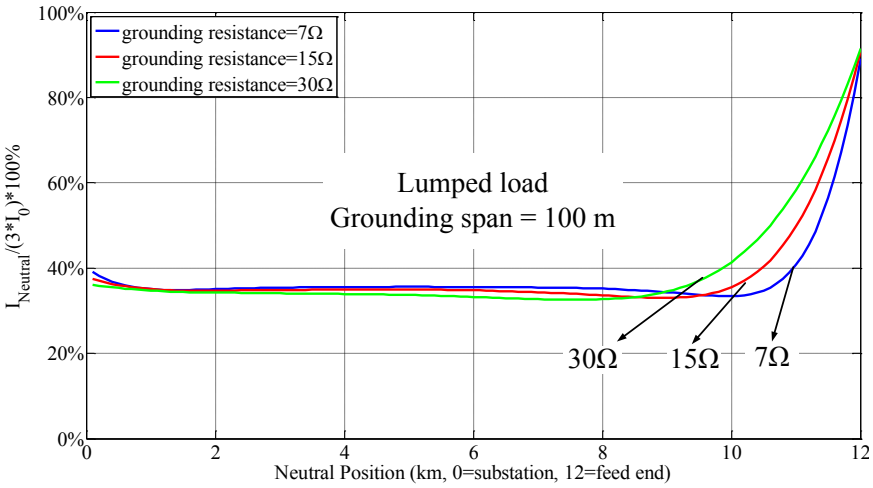

(a) Effect of neutral grounding resistance

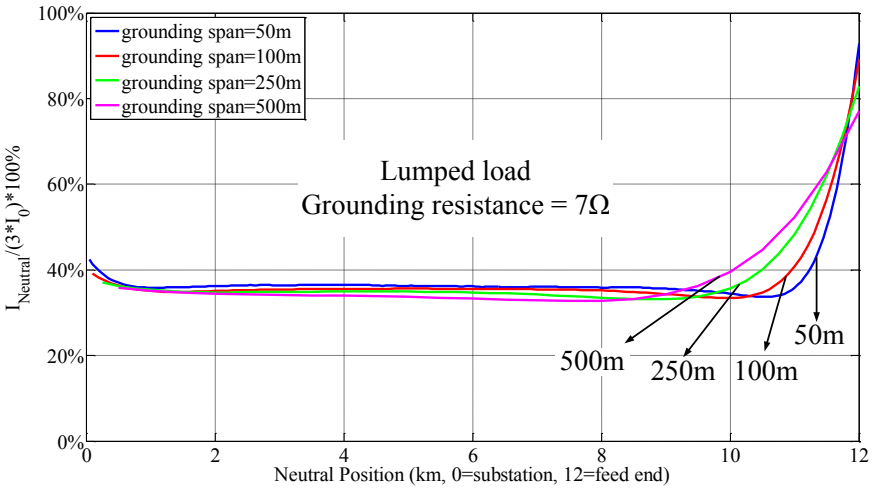

(b) Effect of neutral grounding span

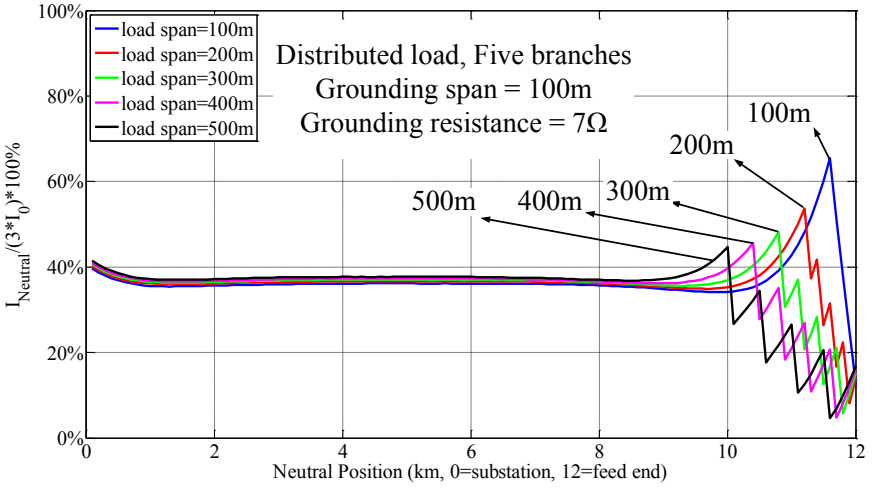

(c) Effect of distributed load span

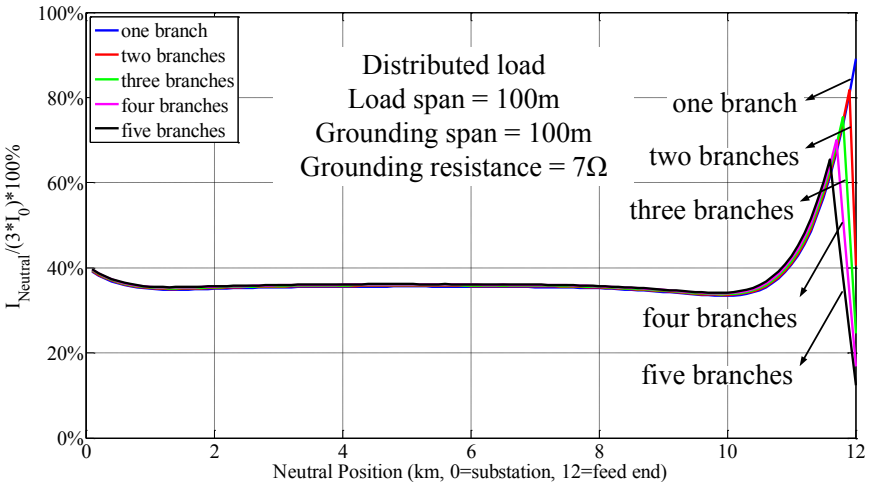

(d) Effect of distributed load branch

Figure A.1: Sensitivity study of currents distribution along the neutral in normal condition.

Appendix B.

Typical Values of Pipeline Parameters at Fundamental and Harmonic Frequency

This appendix documents the typical values of pipeline parameters at fundamental and harmonic frequencies such as:

- Self-impedance z (Ω/km);
- Self-admittance y (Ω^{-1}/km);
- Propagation constant $\gamma = \sqrt{zy}$ (km^{-1});
- Characteristic impedance $Z_c = \sqrt{z/y}$ (Ω);
- Pipeline wavelength $\lambda = 1/\omega\sqrt{LC}$ (km);
- Pipeline effective length L_e (km).

The typical values of pipeline parameters with polyethylene coating are shown in Table B.1. The typical values of pipeline parameters with bituminous coating are shown in Table B.2. The results are calculated based on the following assumptions to produce conservative and reasonable results:

- The depth of pipeline is 1 m;
- The radius of the pipeline is 0.3 m;
- The coating thickness is 0.004 m;
- The coating resistance is $1*10^5$ Ωm^2 for polyethylene coating and $1*10^3$ Ωm^2 for bituminous coating.

The extending length of pipeline outside the parallel section determines the pipeline equivalent impedance Z_{eq}, which finally influences the induced voltages at the terminals of pipeline parallel section. The pipeline equivalent impedance Z_{eq} can be presented by the exact PI model as shown in Figure B.1.

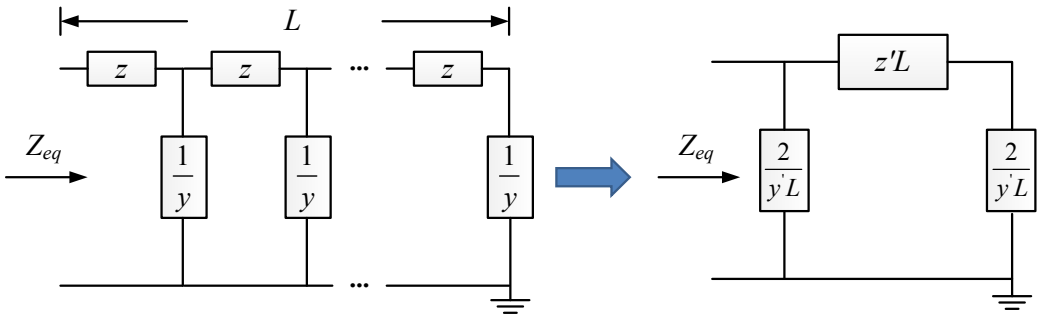

Figure B.1: The equivalent circuit of pipeline outside of parallel section.

Therefore, the pipeline equivalent impedance Z_{eq}, as a function of extending length L, is calculated by the following equations:

$$Z_{eq} = \left(z'L + \frac{2}{y'L} \right) \frac{2}{y'L} \Bigg/ \left[\left(z'L + \frac{2}{y'L} \right) + \frac{2}{y'L} \right] \tag{B.1}$$

$$z' = z \frac{\sinh(\gamma L)}{\gamma L} \tag{B.2}$$

$$y' = y \frac{\tanh\left(\frac{\gamma L}{2}\right)}{\frac{\gamma L}{2}} \tag{B.3}$$

Where

z= pipeline self-impedance;

y = pipeline self-admittance;

γ = pipeline propagation constant;

L = pipeline extending length.

The relationship between equivalent impedance Z_{eq} of polyethylene coating pipeline and extending length L is shown in Figure B.2. The pipeline equivalent impedance will eventually stay at the value of pipeline characteristic impedance Z_c when the extending length is long enough.

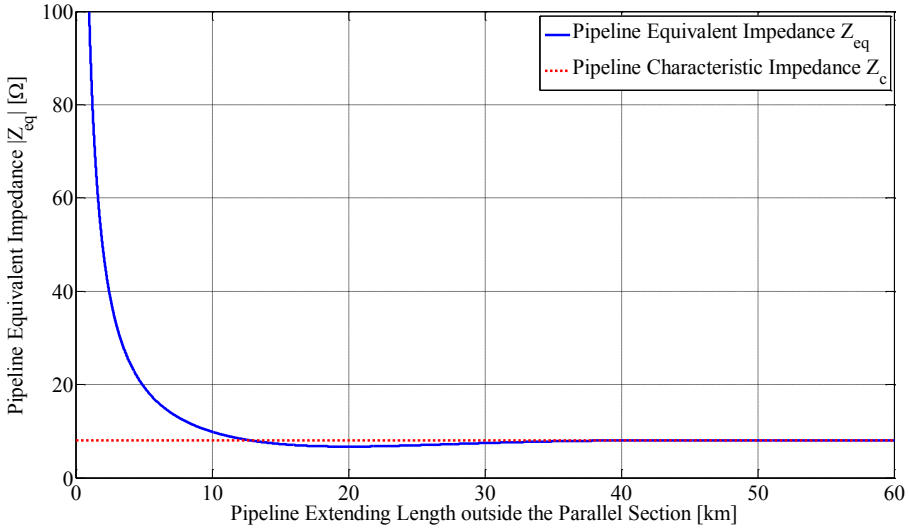

Figure B.2: The relationship between pipeline equivalent impedance Z_{eq} and pipeline extending length L.

The relationship between induced voltages at the terminals of parallel section V_{ind} and the pipeline extending length L can be achieved based on the above pipeline equivalent impedance. Voltage variation factor F_v is defined as the ratio of the terminal induced voltage V_{ind} as percentage of V_{max}, which equals to $\frac{E}{2\gamma}(1-e^{-\gamma L})$ when the extending length is long enough:

$$F_v = V_{ind} / V_{\max} * 100\% \tag{B.4}$$

Assuming the pipeline extending length is from 0 to 60 km at the terminal x=L and the other terminal pipeline extends long enough, the relationship between R_v and L is shown in Figure B.3. The parallel section is assumed to be 1 km.

As we can see from the Figure, the voltage variation factor F_v at x=L decreases into the range between 90% to 110% when the extending length is longer than 11 km. On the other hand, the voltage variation factor F_v at x=0 increases into the range between 90% to 110% when the extending length is longer than 9 km. In order to represent the effective extending length on the induced voltage, the factor L_e is defined as follow:

$$\left|F_v\left(L_e\right)\right| = 10\% \tag{B.5}$$

This equation means that if the pipeline extending length is longer than L_e, the impact of pipeline extending length on the induced voltages at terminal is less than 10%, which can be neglected. The typical values of effective extending length L_e are shown in Table B.1 and Table B.2. Unlike the L_e of bituminous coating pipeline decreasing with higher harmonic frequency in Table B.1, the L_e of polyethylene coating pipeline at either 3rd or 9th order harmonic frequency is larger than that at fundamental frequency due to the effective oscillation caused by inductance and capacitance.

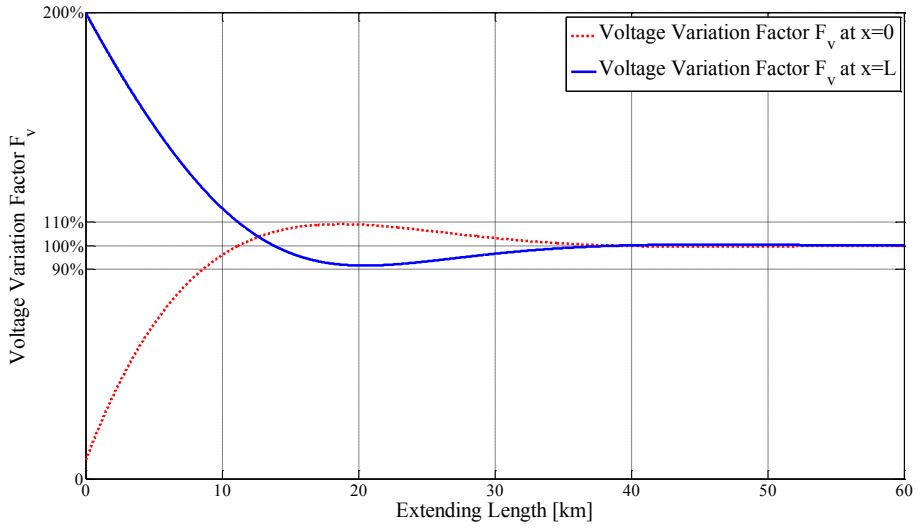

Figure B.3: The relationship between Voltage variation factor F_v and pipeline extending length L.

Table B.1: The typical values of pipeline parameters with polyethylene coating.

Harmonic Order	z [Ω/km]	$y*10^{-3}$ [Ω^{-1}/km]	γ [km^{-1}]	Z_c [Ω]	λ [km]	L_e [km]
1st	0.176+j0.569	9.40+j3.91	0.053+j0.058	6.94+j3.26	21.1	11.7
3rd	0.380+j1.45	9.43+j11.7	0.068+j0.134	9.75+j2.08	7.7	14.4
9th	0.884+j3.71	9.70+j35.2	0.093+j0.361	10.2+j0.175	2.8	10

Table B.2: The typical values of pipeline parameters with bituminous coating.

Harmonic Order	z [Ω/km]	y [Ω^{-1}/km]	γ [km^{-1}]	Z_c [Ω]	λ [km]	L_e [km]
1st	0.175+j0.569	0.784+j0.015	0.546+j0.412	0.706+j0.511	10.7	1.42
3rd	0.378+j1.44	0.793+j0.022	0.851+j0.675	1.10+j0.821	5.65	0.89
9th	0.879+j3.69	0.802+j0.040	1.34+j1.12	1.74+j1.30	2.61	0.55

The typical values of voltage variation factor F_v, with respect of pipeline extending length from 0 to 20 km, are shown in Table B.3. The F_v of bituminous coating pipeline is not included due to the fact that the L_e of bituminous coating pipeline is much shorter than that of polyethylene coating pipeline.

Table B.3: The typical values of voltage variation factor F_v (Polyethylene Coating).

Harmonic Order		**Pipeline Extending Length [km]**				
		2	**4**	**6**	**8**	**10**
1st	F_v (x=L)	179.60%	161.24%	144.78%	130.41%	118.32%
	F_v (x=0)	34.27%	55.47%	72.01%	84.59%	93.86%
3rd	F_v (x=L)	170.20%	137.77%	107.96%	86.47%	77.69%
	F_v (x=0)	62.47%	95.26%	114.61%	122.97%	123.15%
9th	F_v (x=L)	128.42%	55.12%	93.07%	120.40%	109.94%
	F_v (x=0)	130.00%	143.26%	104.84%	79.56%	97.22%
Harmonic Order		**Pipeline Extending Length [km]**				
		12	**14**	**16**	**18**	**20**
1st	F_v (x=L)	108.63%	101.37%	96.39%	93.41%	92.03%
	F_v (x=0)	100.40%	104.73%	107.31%	108.54%	108.78%
3rd	F_v (x=L)	80.31%	88.07%	95.85%	101.38%	104.21%
	F_v (x=0)	118.12%	110.77%	103.58%	98.31%	95.66%
9th	F_v (x=L)	92.40%	94.37%	102.86%	103.23%	99.26%
	Fv (x=0)	109.18%	103.54%	96.28%	97.77%	101.42%

Appendix C.

Field Measurements of Harmonic Currents in Power Distribution Systems

This appendix provides field measurements of harmonic currents in power distribution systems. Currents of 10 distribution feeders supplying residential area at different substations for more than one week for each feeder in Nov. ~ Dec. 2008, July 2009, Oct. ~ Nov. 2008 and April 2011, separately. The resolutions of DAQs for different measurements are shown in Table C.1.

Table C.1: Resolutions of Measurements.

Feeder number	Samples per cycle	Cycles per snapshot	Snapshot per minute	Results
Feeder 1	256	6	20	Average of the first 6 cycle waveforms per 1 minute
Feeder 2, 3, 4	256	12	5	
Feeder 5, 6	256	6	60	
Feeder 7, 9	256	6	5	
Feeder 8,10	128	6	10	

Due to the large amount of data, only sample measurements are presented. The harmonic characteristics of phase current are presented in the following figures.

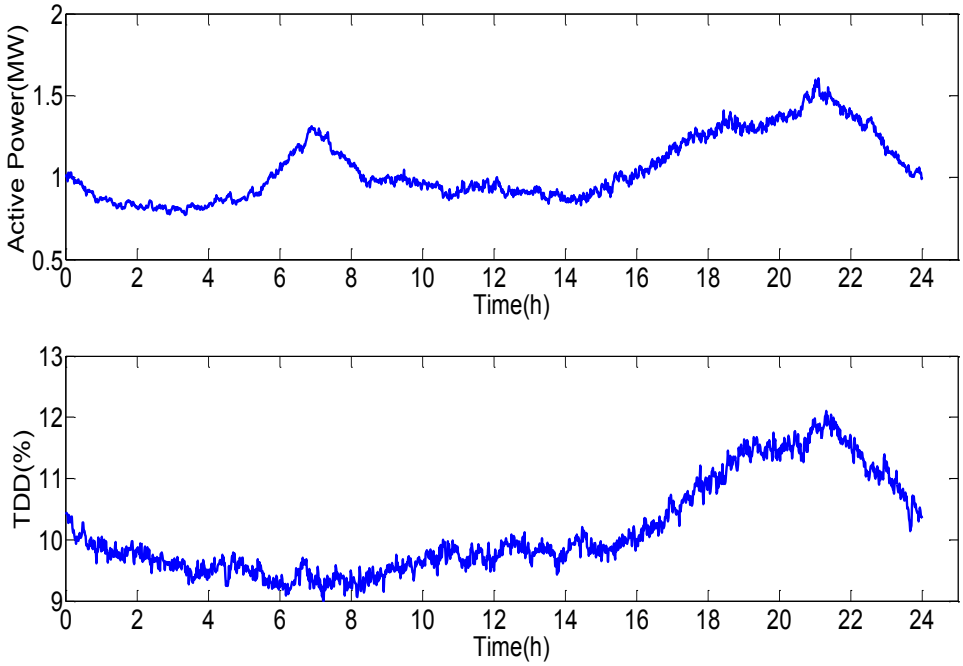

Figure C. 1: 24-hour pattern of the active power and TDD (weekday).

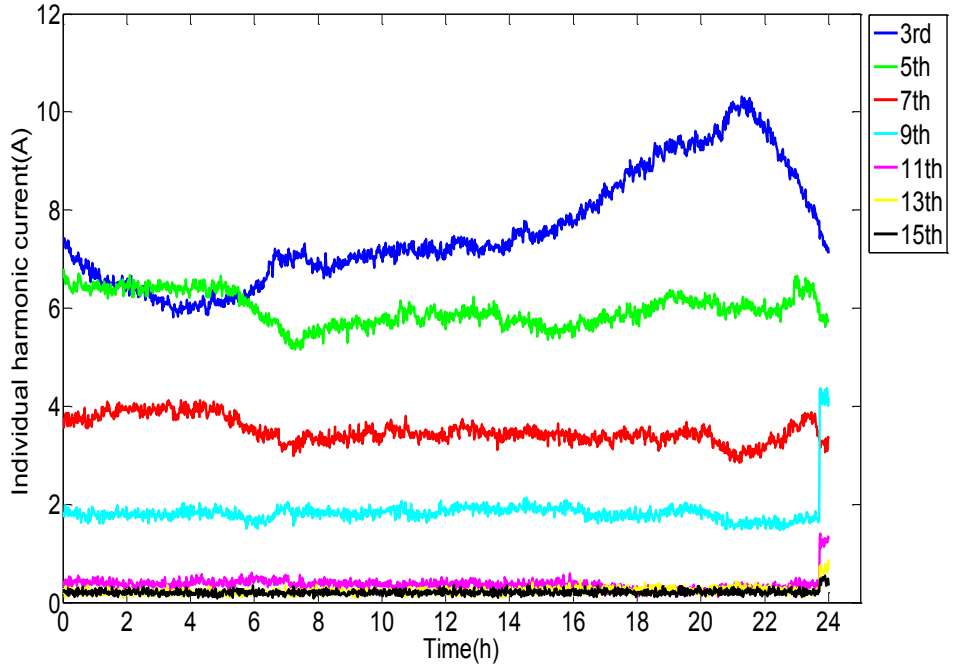

Figure C. 2: 24-hour Pattern of each individual harmonic current (weekday).

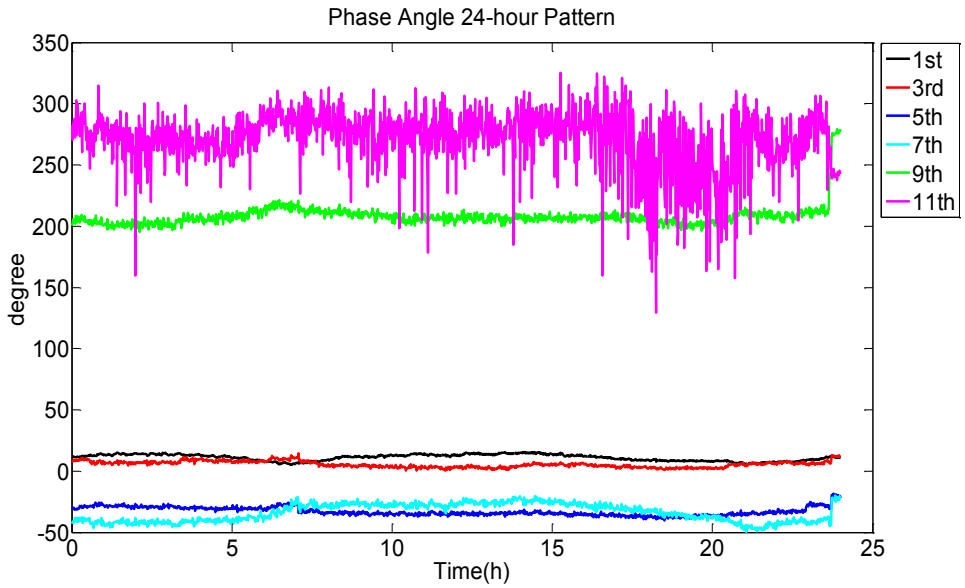

Figure C.3: 24-hour Pattern of each individual harmonic current phase angle (weekday).

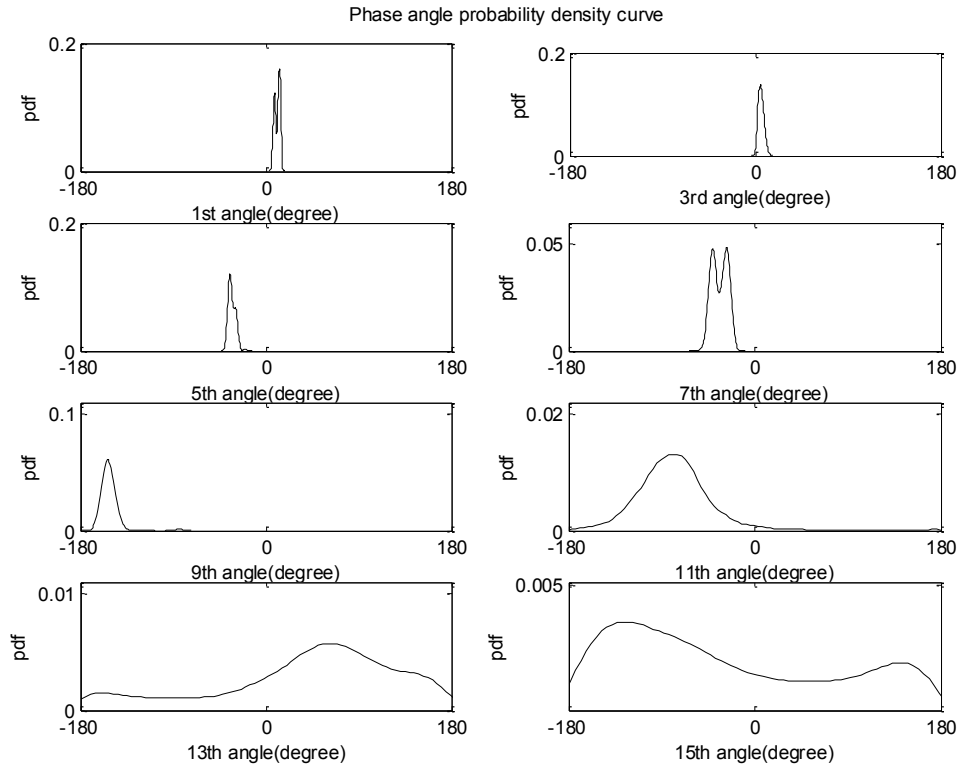

Figure C.4: Harmonic current phase angle probability density curve (weekday).

Appendix D.

Setup of Pipeline AC Corrosion Experiment

D.1 Devices

1) Two programmable power generators
2) Two sets of corrosion test devices provided by CME, Parameters:
    - Solution resistivity: 4730 Ω.cm;
    - 7 samples connected in parallel in each test device;
    - Exposed surface of each coupon: 1.96 cm^2;
    - Density of each coupon: 7.87 g/cm^3.

D.2 Test Setup

1) The first round
    - Test duration: 724.25 hours;
    - Setup date: Dec. 9th 2014;
    - Disassembled date: Jan. 8^{th} 2015;
    - Device 1: Vrms=6.6V with 60Hz frequency to achieve 1mA current;
    - Device 2: Vrms=11.8V with 180Hz frequency to achieve 1mA current.

Note: The parameters of two test devices are not identical.

2) The second round
    - Test duration: 716.7 hours;

- Setup date: Jan. 29th 2015;
- Disassembled date: Feb. 28th 2015;
- Device 1: Vrms=4.3V with 540Hz frequency to achieve 1mA current (rms);
- Device 2: multiple frequency voltage as follows to achieve 1mA current (rms):

  Vrms_1=1.3V, 60Hz, 0 degree (phase angle);

  Vrms_3=3.9V, 180Hz, 80 degree (phase angle);

  Vrms_9=0.6V, 540Hz, 130 degrees (phase angle).

Note: The test device 1 is the same as device 1 in the first round test. The test device 2 is not the same as device 2 in the first round test.

D.3 Raw Data

1) First test round-Device 1

Table D. 1: Corrosion rate at 60Hz.

Sample location	Initial weight (g)	Final weight (g)	Weight loss (g)	Corrosion rate (mm/h)	mil/year
top	5.9803	5.97365	0.00665	5.95E-06	2.05
	6.1781	6.17337	0.00473	4.23E-06	1.46
	6.0682	6.06407	0.00413	3.70E-06	1.28
	6.0995	6.09585	0.00365	3.27E-06	1.13
	5.9916	5.98810	0.00350	3.13E-06	1.08
	6.1256	6.12246	0.00314	2.81E-06	0.97
bottom	6.0867	6.08204	0.00466	4.17E-06	1.44

2) First test round-Device 2

Table D. 2: Corrosion rate at 180Hz.

Sample location	Initial weight (g)	Final weight (g)	Weight loss (g)	Corrosion rate (mm/h)	mil/year
top	6.0380	6.03496	0.00304	2.72E-06	0.94
	5.5803	5.57801	0.00229	2.05E-06	0.71
	5.8968	5.89309	0.00371	3.32E-06	1.15
	5.9892	5.98602	0.00318	2.85E-06	0.98
	5.9889	5.98553	0.00337	3.02E-06	1.04
	5.7984	5.79455	0.00385	3.45E-06	1.19
bottom	5.4623	5.46017	0.00213	1.91E-06	0.66

3) Second test round-Device 1

Table D. 3: Corrosion rate at 540Hz.

Sample location	Initial weight (g)	Final weight (g)	Weight loss (g)	Corrosion rate (mm/h)	mil/year
top	6.02091	6.01693	0.00398	3.60E-06	1.24
	6.09026	6.08706	0.0032	2.89E-06	1.00
	6.13219	6.12791	0.00428	3.87E-06	1.34
	6.08519	6.08129	0.0039	3.53E-06	1.22
	6.10373	6.09953	0.00420	3.80E-06	1.31
	6.08781	6.08360	0.00421	3.81E-06	1.31
bottom	5.90117	5.89707	0.0041	3.71E-06	1.28

4) Second test round-Device 2

Table D. 4: Corrosion rate at 60, 180 and 540Hz combined.

Sample location	Initial weight (g)	Final weight (g)	Weight loss (g)	Corrosion rate (mm/h)	mil/year
top	6.13042	6.11875	0.01167	1.06E-05	3.64
	6.08007	6.07375	0.00632	5.72E-06	1.97
	6.08943	6.08258	0.00685	6.20E-06	2.14
	6.11011	6.10298	0.00713	6.45E-06	2.23
	6.07036	6.06250	0.00786	7.11E-06	2.45
	5.99150	5.98454	0.00696	6.30E-06	2.17
bottom	5.97306	5.96638	0.00668	6.04E-06	2.09

Note: mil/year--Mils penetration per year is a unit of measurement equal to one thousandth of an inch. It is used to gauge a coupon's corrosion rate. This unit is typically applied in industries like manufacturing and engineering to measure coating thickness or tolerance.

Appendix E.

Pipeline AC Corrosion Issue Caused by Transmission Line Harmonic Induction

This appendix provides the analysis of transmission line current induction on pipeline AC corrosion issue in order to demonstrate the inductive interference transmission lines on pipelines at harmonic frequencies.

Table E.1 shows the parameters of studied 144kV transmission line tower structure. Table E.2 shows the transmission line harmonic current data based on the field measurements. Table E.3 shows the parameters of buried pipeline and its surrounding soil condition. The mechanism of induced current in the shield wire is similar to that of neutral current in MGN system which is already presented in Section 4.1.2, so the current in the shield wire is calculated by the following equation:

$$I_{s,h} = -\frac{Z_{as,h}I_{a,h} + Z_{bs,h}I_{b,h} + Z_{cs,h}I_{c,h}}{Z_{ss,h}} \quad \text{(E.1)}$$

where

$I_{s,h}$ is the shield wire current at h order harmonic frequency;

$I_{a,h}$ is the phase A current at h order harmonic frequency;

$I_{b,h}$ is the phase B current at h order harmonic frequency;

$I_{c,h}$ is the phase C current at h order harmonic frequency;

$Z_{as,h}$, $Z_{bs,h}$, $Z_{cs,h}$ are the mutual impedances between each phase conductor and shield wire at h order harmonic frequency;

$Z_{ss,h}$ is the self-impedance of shield wire at h order harmonic frequency.

Table E.1: Parameters of 144 kV transmission line tower structure.

Phase	Horizontal Position (m)	Height (m)		
		At Tower	At Mid-Span	Average Position
A	-1.97	14.24	7.45	9.71
B	1.93	12.75	5.96	8.22
C	-2.34	11.57	4.78	7.04
S(shield wire)	0.00	17.22	10.43	12.69

Table E.2: Transmission line harmonic current data.

	Harmonic Current Magnitude [A]						
	1st	3rd	5th	7th	9th	11th	13th
Phase A	405.66	1.33	14.76	4.02	0.45	1.31	1.03
Phase B	374.80	1.66	13.68	4.15	0.28	1.19	0.95
Phase C	361.96	0.71	14.28	3.94	0.31	1.49	1.29
Shield Wire	18.76	0.27	0.67	0.15	0.46	0.14	0.09
	Harmonic Current Phase Angle [°]						
	1st	3rd	5th	7th	9th	11th	13th
Phase A	0	-44	63	47	129	-48	105
Phase B	-123	124	-179	-74	150	55	13
Phase C	123	-40	-62	167	133	-173	-121
Shield Wire	163	179	-79	176	-43	133	-90

Table E.3: Parameters of pipeline and its surrounding soil condition.

Parameter	Value
Pipeline Diameter [m]	0.3
Pipeline Buried Depth [m]	1
Coating Type	Polyethylene
Soil Resistivity [Ωm]	100

Assuming the parallel length is 3 km, Figure E.1 demonstrates the induced voltage on pipeline at each harmonic frequency. It can be seen that the fundamental currents produce significant induced voltage on pipeline, whereas the harmonic currents induce much smaller voltages on pipeline. As a result, the total induced voltage, rms value of fundamental and each harmonic induced voltage, is contributed by the fundamental induced voltage mostly. Similar to the analysis of

distribution line, the clearance distance between transmission line and pipeline is calculated as shown in Figure E.1. The clearance distances for both fundamental and total induced voltage are generally the same, which is 17 m.

In conclusion, the harmonic currents in transmission system do not have a significant impact on pipeline AC corrosion issue.

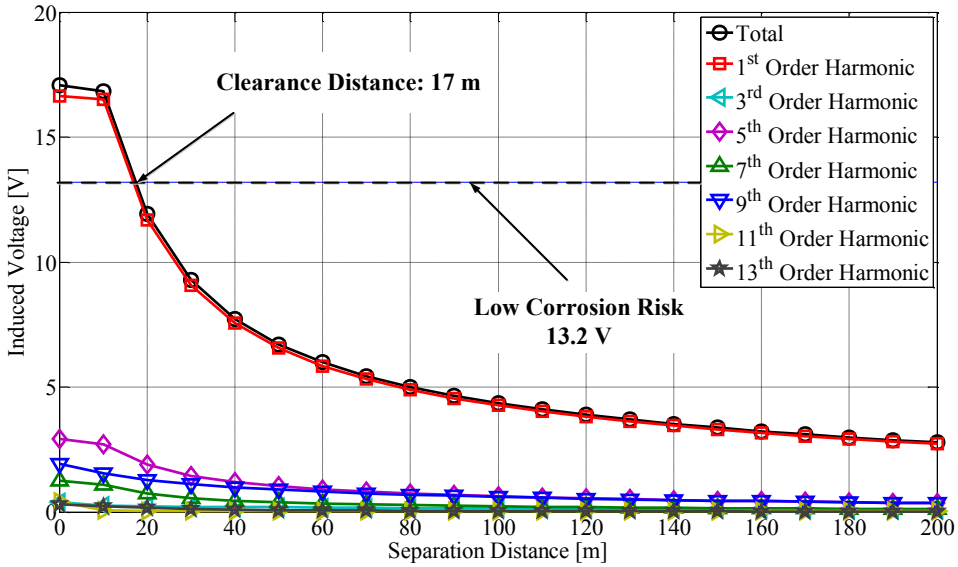

Figure E.1: The clearance distances between transmission line and pipeline to avoid low corrosion risk at different frequencies.

Appendix F.

Sensitivity Study of Pipeline Diameter on Induced Voltage

This appendix discusses the sensitivity study of pipeline diameter on induced voltage at fundamental and harmonic frequencies. The typical parameters are the same with other sensitivity studies as shown in Table 4.3.

As provided by ASME standard, the typical pipeline diameter is from 10 mm to 762 mm [83]. Based on these parameters, a sensitivity study of pipeline diameter is conducted from 10 mm to 1000 mm. The results are shown in Figure F.1. From the results we can conclude that the pipeline diameter does not significantly influence the induced voltages at fundamental and harmonic frequencies.

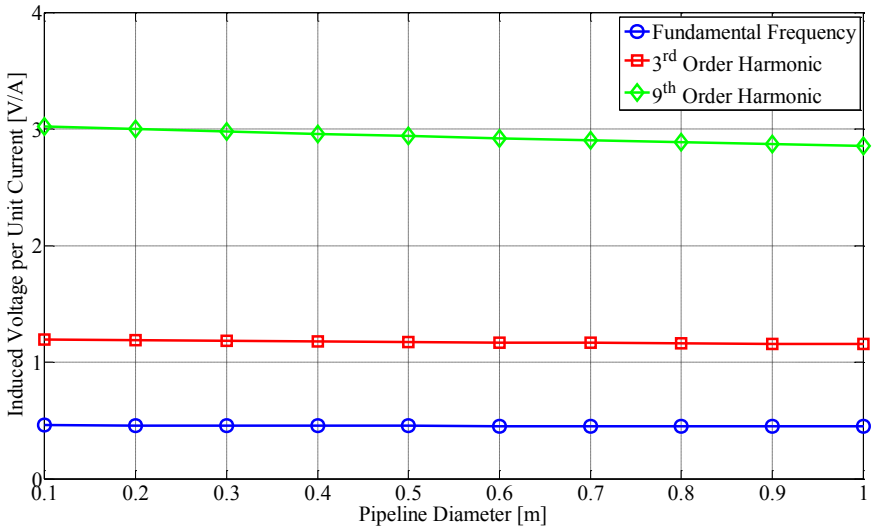

Figure F.1: The influence of pipeline diameter on the induced voltage.